2018

EVALUATING POLICY AND CLIMATE IMPACTS ON WATER RESOURCES SYSTEMS USING COUPLED HUMAN-NATURAL MODELS

HASSAAN FURQAN KHAN

**EVALUATING POLICY AND CLIMATE IMPACTS ON WATER RESOURCES
SYSTEMS USING COUPLED HUMAN-NATURAL MODELS**

A Dissertation Presented

by

HASSAAN FURQAN KHAN

Submitted to the Graduate School of the
University of Massachusetts Amherst in partial fulfillment
of the requirements for the degree of

DOCTOR OF PHILOSOPHY

SEPTEMBER 2018

Department of Civil and Environmental Engineering
Environmental and Water Resources Engineering

EVALUATING POLICY AND CLIMATE IMPACTS ON WATER RESOURCES SYSTEMS USING COUPLED HUMAN-NATURAL MODELS

A Dissertation Presented

by

HASSAAN FURQAN KHAN

Approved as to style and content by:

_____
Casey Brown, Chair

_____
David Ahlfeld, Member

_____
Bernard Morzuch, Member

_____
Yi-Chen E. Yang, Member

                          _____
                          Richard Palmer, Department Head
                          Department of Civil and Environmental Engineering

DEDICATION

To my parents, for decades of hard work and sacrifices that made all of this possible

ACKNOWLEDGMENTS

The following is not an exhaustive list of people who have contributed towards this work, for that is simply not possible in this short space. I wish to emphasize that had it not been for the numerous generous people Allah placed in my life, I would have never been able to complete my PhD. Having established that…….

I am grateful to my advisor Casey Brown for his guidance throughout my graduate education. I would like to thank Ethan Yang for going out of his way to mentor me, and for always being available and willing to help me navigate the challenges that came up during my time at UMass. I owe a huge debt of gratitude to Ethan for his extraordinary dedication to helping me grow as a scholar. Bernie Morzuch, for showing me what a great teacher looks like, and for his (unexplainable) belief in me. I would also like to thank Dr. Ahlfed for his helpful comments and insights. I extend thanks to the various organizations (IFPRI, WAPDA, PMD, SFPUC) that supported the work presented in this dissertation.

I would like to make a special mention of the role my colleagues, especially the Hydrosystems Research Group, played in my development as a scholar. I am extremely grateful to Sungwook, Patrick, Katherine, Umit and every member of the HRG for the stimulating discussions, tutelage and collaborations throughout my time here. To say they helped me in my work would be an understatement.

To my friends who made the years in Amherst the most memorable of my life: from the bottom of my heart, thank you. From skiing trips to the potluck dinners to the intramural soccer tournaments, these friendships and bonds were invaluable in keeping me sane and energized. I have to mention the fabulous housemates I had the privilege of

living with: Mark, Joe, Amro, Chinedum and Ho-Zhen. Thank you for being my anchors in turbulent waters. In particular, I want to acknowledge the hugely influential role Mark Hagemann played during my PhD. Along with showing me the ropes of adult life when I moved to Amherst, Mark is the sole reason why I successfully learnt how to code.

Finally, none of this would be possible without the countless sacrifices my parents made in allowing me to pursue a high quality education. I am forever grateful to them and to my large and loving family whose support and belief helped me get through to the finishing line.

ABSTRACT

**EVALUATING POLICY AND CLIMATE IMPACTS ON WATER RESOURCES
SYSTEMS USING COUPLED HUMAN-NATURAL MODELS**

SEPTEMBER 2018

HASSAAN FURQAN KHAN,

B.S., LAFAYETTE COLLEGE

M.S., UNIVERSITY OF MASSACHUSETTS AMHERST

Ph.D., UNIVERSITY OF MASSACHUSETTS AMHERST

Directed by: Professor Casey M. Brown

Extensive human intervention in the terrestrial hydrosphere means that virtually every river basin globally reflects the interaction between human and natural hydrologic processes. Thus, sustainable watershed management needs to not only account for the diverse ways humans benefit from the environment but also incorporate the impact of human actions on the natural system. Informed policy making to address our water challenges requires a comprehensive understanding of these feedbacks and how they might be affected by future changes in climate. This work develops coupled human-natural models for improved surface water and groundwater management in water-scarce regions under future changes in climate. An agent-based water use model is coupled with a physically-based groundwater model in an agricultural setting to compare groundwater management policies under varying climatic conditions. Shifting spatial scales to a watershed level, we couple a process-based distributed hydrologic model with an agent-based model to simulate the impacts of water management decisions on the food-water-

energy-environment nexus in transboundary river basins. A stochastic weather generator is developed to produce a wide ensemble of future climate, changes in which can vary spatially and temporally, while incorporating low-frequency variability. The primary goal of this work is to advance modeling approaches that effectively represent heterogeneity within a water system, capture the linkage between society and hydrology, and account for future changes in climate.

TABLE OF CONTENTS

LIST OF TABLES

LIST OF FIGURES

CHAPTER 1

INTRODUCTION

Water scarcity is recognized as the one of the most serious challenges facing societies globally [*World Economic Forum*, 2016]. Expected increases in population and living standards, especially high in the most water stressed countries, will further exacerbate water shortages and their impact on food and energy production. It is increasingly clear that sustainably addressing the water challenges of the 21st century requires approaches that move beyond individually applying engineering, hydrology, management, sociology, or economics: successful resolution of water challenges can come only from the synergy of the above understandings of water.

Extensive human intervention in the terrestrial hydrosphere means that virtually every river basin globally reflects the interaction between human and natural hydrologic processes. Maintaining a healthy ecosystem can be mutually beneficial to both human society and ecological systems and a failure to do so may result in compromising human benefits for future generations [*Baron et al.*, 2004]. There is therefore a growing recognition among water resources managers that sustainable watershed management needs to not only account for the diverse ways humans benefit from the environment but also incorporate the impact of human actions on the natural system [*Vogel et al.*, 2015]. This is perhaps most prominently advocated in the emerging science of 'socio-hydrology', which calls for an understanding of the two-way interactions and co-evolution of coupled human-water systems [*Sivapalan et al.*, 2012]. Thus, informed policy making to address our water challenges requires a comprehensive understanding of the feedbacks between societal water use and the environment.

Discounting freshwater available in the polar ice caps, groundwater constitutes almost 90% of global freshwater, thus making groundwater resource management one of the most important

and critical natural resource management frontiers [*Koundouri*, 2004; *Gorelick and Zheng*, 2015]. With the rapid depletion of surface waters, groundwater is also increasingly becoming the primary buffer against droughts [*Taylor et al.*, 2013]. However, in recent years, harmful impacts of unmanaged groundwater extraction have emerged. A recent analysis shows that storage in 21 of the 37 largest aquifers in the world has decreased over the past decade, with over a third severely depleted, threatening regional water availability [*Richey et al.*, 2015].

The Indus River Basin (IRB) in Pakistan is home to one of these over depleted aquifers. Over the past few decades, groundwater has become an integral part of Pakistan's irrigation system. Since the 1970s, cropping intensities have doubled [*Mirza and Latif*, 2012] despite an overall decrease in available surface water supplies due to sedimentation in existing reservoirs. This increase has been achieved primarily through expansion of groundwater abstraction bringing about huge increases in crop production, resulting in significant economic gains and ensuring food security for millions. However, this exponential increase in unmanaged groundwater usage has led to a variety of both water quality and quantity issues. Despite the critical role of groundwater in achieving food security and supporting economic growth, groundwater governance is practically non-existent in the Indus River Basin (IRB). An inadequate understanding of groundwater dynamics on a provincial level is a primary reason for the absence of effective groundwater management policy in Pakistan [*Khair et al.*, 2014]. The first chapter of this dissertation seeks to fill this research gap by developing a physically-based province wide groundwater model for the Indus Basin and performing various sensitivity analyses to simulate groundwater conditions under different policy and climate scenarios.

Increased groundwater stress calls for improved groundwater management. In recent years, economic incentive-based policies, such as groundwater markets, have become increasingly

popular as an alternative to the command and control approach. Nebraska [*Aladjem and Sunding*, 2015], Texas [*Johnson et al.*, 2009] and Australia [*Wheeler et al.*, 2013] are examples of regions where permit trading programs have been adopted for groundwater management. Groundwater management policies cannot be meaningfully evaluated if the models used do not realistically simulate hydrogeologic conditions and capture the impacts of varied human water use decisions. To represent the spatial and temporal heterogeneity in groundwater conditions and incorporate impact of human use, models for groundwater markets need to be coupled with physically-based hydrogeologic models [*Mulligan et al.*, 2014].

In addition to the need to address spatial variation, possible temporal variation caused by future changes in climate on a groundwater system needs to be incorporated. Climate variability and change can impact groundwater directly, mainly through changes in temperature and precipitation, and indirectly, through change in irrigation-water demand due to reduced surface water availability. Analysis of performance of groundwater markets, with the explicit intent of addressing distributional impacts while accounting for climate change, has been rare [*Skurray et al.*, 2012]. The second chapter of this dissertation addresses this research need by coupling an agent-based model representing farmers' water use with a physically-based groundwater model to compare the performances of different groundwater management policies and quantify resulting distributional impacts, using the Republican River Basin in the US as a case study.

Coupled models of human and natural systems can also be useful in the context of surface water management. A review of the existing literature shows most coupled models of the natural and human systems in the context of surface-water management are only loosely linked and thus do not fully capture the impact of human actions on hydrology [*Yang et al.*, 2012; *Giacomoni et al.*, 2013]. The two-way coupling between society and hydrology needs to be integrated into

computational tools used to aid watershed management. Furthermore, traditional watershed modeling does not effectively capture system heterogeneity limiting its ability to effectively represent the two-way interaction between human and natural systems. Often, human actions and societal dynamics are represented using static assumptions rarely based on empirical data.

In the third chapter, we present a modeling framework that can effectively address both system heterogeneity and the linkage between human society and hydrology that influences water cycling in the watershed. We do so by differentiating key stakeholders of ecosystem services as active agents based on their characteristics such as location and water use preferences; we then tightly couple the human system with a process-based watershed model that simulates the stock and flow of environmental variables needed by the stakeholders. We apply this modeling framework to two transboundary basins where ecological needs are competing with growing human demands on water resources: the Mekong River Basin in Southeast Asia and the Niger River Basin in West Africa.

Changes in climate will affect natural systems and society as well as the feedbacks between the two. Long-term water resources planning needs to include and account for uncertainty in future climate. Bottom-up or decision-centric approaches to addressing climate change are increasingly being adopted where water system performance is evaluated under a wide variety of changes in future climate [*Brown et al.*, 2012]. Traditionally, system vulnerability to climate has been evaluated by applying simple change factors to climatic variables. However, literature suggests that future changes in climate could include, in addition to mean shifts in climate, shifts in intraannual climate, long-term low frequency variability in precipitation, extreme daily precipitation or high-order statistics. Future changes in climate that go beyond just applying mean shifts can be explored using stochastic weather generators. Weather generators can be used to test

system vulnerability to possible future climate with differences in nuanced climate characteristics [*Steinschneider and Brown*, 2013]. The fourth chapter of this dissertation addresses the need for a comprehensive treatment of climate change in a water scarce region exhibiting high climate variability. We develop a stochastic weather generator to aid a long-term vulnerability assessment for the San Francisco water utility. The weather generator is developed to enable application of differential changes in climate, both spatially and temporally and account for low frequency variability for which a physical basis has been determined.

CHAPTER 2

**GUIDING GROUNDWATER POLICY IN THE INDUS BASIN OF PAKISTAN USING
A PHYSICALLY BASED GROUNDWATER MODEL**

2.1 Introduction

Over the past few decades, groundwater has become an integral part of Pakistan's irrigation system. Since the 1970's, cropping intensities have doubled [*Mirza and Latif*, 2012], despite an overall decrease in available surface water supplies due to sedimentation in existing reservoirs. This increase has been achieved primarily through expansion of groundwater abstraction bringing about huge increases in crop production, resulting in significant economic gains and ensuring food security for millions. However, this exponential increase in unmanaged groundwater usage has led to a variety of both water quality and quantity issues. Despite the critical role of groundwater in achieving food security and supporting economic growth, groundwater governance is practically non-existent in the Indus River Basin (IRB). An inadequate understanding of groundwater dynamics on a provincial level is a primary reason for the absence of effective groundwater management policy in Pakistan [*Khair et al.*, 2014]. In this analysis, the first physically-based groundwater model for the entire Indus Plain aquifer underlying Punjab province is developed, which accounts for 90% of total groundwater pumping in Pakistan, and simulate future conditions under various policy and climate scenarios.

The Indus Basin Irrigation System (IBIS), with an irrigated area of approximately 17 million ha, supports 90% of food production in Pakistan. The IBIS is operated based on a continuous water supply system independent of actual crop water requirements. Each farmer is provided surface water from the canals once in seven days, for a time period in proportion to his land holding, in a fixed rotation schedule called "*warabandi*" [*Bandaragoda and Rehman*, 1995].

Since this schedule was developed decades ago, water distribution is not tailored to present-day land holdings and cropping patterns. In areas where the surface water supply does not meet the demand, farmers turned to installing tubewells to pump groundwater to fulfil their irrigation requirements. Over 70% of land in Pakistan is irrigated using groundwater in conjunction with surface water supplies [*Qureshi et al.*, 2010].

2.2 Existing Literature

While significant literature exists on surface water hydrology and water resource management in the Indus Basin, this work often fails to meaningfully incorporate the integral surface water-groundwater interaction [*Yu et al.*, 2012]. A few studies on groundwater usage based on a water-balance approach can be found in the literature. *O'Mara and Duloy* [1984] studied the joint effects of canal water allocations and subsidy policies for groundwater use on overall system efficiency. *Hassan and Bhutta* [1996] developed a water-balance model for Rechna *doab* (alluvial land between two converging rivers) and determined that the major inputs into the hydrologic system are rainfall and canal water supply. *Cheema et al.*, [2014] performed a study to quantify total groundwater abstractions in the IRB in Pakistan and India. Results from their model showed basin-wide usage of 68 km^3 and 113 km^3 for groundwater and surface water respectively. While basin-wide groundwater studies based on a water-balance approach are useful for a macro-level understanding of groundwater in the IRB, they are not physically-based and thus cannot provide insight regarding groundwater dynamics.

Existing physically-based models of groundwater usage in the Indus Basin in Pakistan have been developed on a smaller spatial scale [*Garg and Ali*, 2000]. *Chandio et al.*, [2012] used a three-dimensional finite element model (3D FEM) to investigate the extent of waterlogging under

different hydraulic conditions in Khairpur district in the lower Indus Basin. Similarly, *Ahmad et al.*, [2011] used Felflow (3D FEM) and developed GIS techniques to study groundwater fluctuations in the Upper Chaj *doab* in Punjab. They developed different groundwater recharge and abstraction scenarios to evaluate the impact of climate extremes on the water table. Regional groundwater modeling studies have also focused on aquifer depletion in large cities. Using GIS tools, *Mahmood et al.*, [2013] tracked changes in the groundwater table across Lahore and found the presence of a depression zone, moving eastwards since 2007. While useful for identifying groundwater issues in specific regions, these small-scale groundwater models are unable to reflect the significant spatio-temporal variation in groundwater quality and quantity across Punjab [*Basharat and Tariq*, 2015] and thus cannot be used to guide large scale policy reforms.

Given the rapid increase in use of groundwater in the past few decades, and the problems associated with a supply-based canal system, there is an increased need for integrated management of water resources in Punjab. Comprehensive system wide policy reform can ensure sustainable use of groundwater in the future. However, a better understanding of the hydraulically connected underground water balance is necessary to make informed policy choices on a provincial level. This study seeks to augment the current literature by developing and calibrating the first physically-based groundwater model for the entire Punjab province. The calibrated province-wide model is then used to perform simulations representing different scenarios to evaluate groundwater dynamics in the future. The following sections contain a summary of the collected groundwater data and their sources, a discussion on model development and calibration, an outline of future scenarios, followed by results of the scenario analysis and a discussion of those results.

2.2.1 The Indus Aquifer in Punjab

Five major rivers including the Indus, Jhelum, Chenab, Ravi and Sutlej flow through Punjab into Sind on their way to the Arabian Sea. Much of the Indus Plain, lying to the south of Pothwar Plateu and extending across Punjab can be classified as a flat terrain with a mild slope towards the south-west Punjab. Administratively, Punjab is divided into 36 *districts* across 9 *divisions*. There are 25 major canal command areas that fall completely within the province, through which an average of 65 billion cubic meter (BCM) of surface water is supplied for irrigation [*WAPDA*, 2013]. Figure 1 shows the spatial breakdown of districts in Punjab. Three major population centers including Lahore, Faisalabad and Multan are also shown in the figure.

Climate across most of Punjab can be classified as semi-arid to arid, with the aridity increasing towards the south. The annual average rainfall varies from around 800 mm in northern Punjab decreasing down to around 100 mm in Bahawalpur division in the south. The Indus River and its tributaries flowing through Punjab contribute to the groundwater in the province, especially during the high flow periods from June through September. Flows in the river remain relatively low during the rest of the year.

Before the construction of the canal irrigation system, groundwater in the IRB was saline due to the marine origin of the underlying geologic formation [*Asghar et al.*, 2002]. Deep percolation from the extensive surface water supply system and intensive irrigation during the past century resulted in development of relatively fresh groundwater lenses overlying the native salty groundwater. The hydraulic head in the aquifer generally decreases towards the south. Existing literature suggests that the geographic divide between the Indus plain and the Pothwar Plateau (across districts 3, 9, 10 and 11) has a parallel in the groundwater system between the two regions [*van Steenbergen and Oliemans*, 1996]. The aquifers underlying these two regions are not believed

9

to be connected. In addition, the Sulaiman Range straddles the border between south-west Punjab and Balochistan (across districts 30 and 33). This topographic divide is also observed in the aquifer underneath. Hence districts which lie partly or wholly outside the Indus Plain are excluded from this analysis.
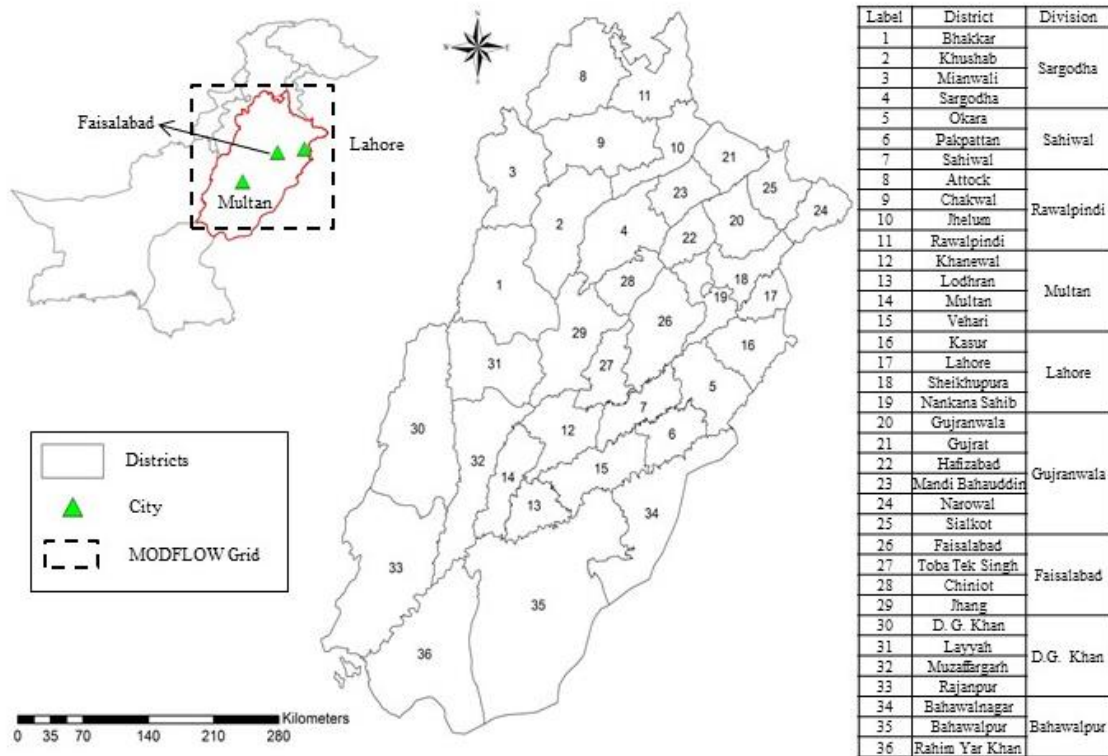
Figure 1. Map illustrating study area showing the boundary of Punjab province, the extent of the grid developed in MOFLOW for the model and the major cities in Punjab

2.3 Methods

2.3.1 Model Development

In this study, MODFLOW [*Harbaugh*, 2005] was used to develop a physically-based groundwater model for the Indus Plain aquifer underlying Punjab province in Pakistan. The

hydrogeologic conceptualization of the model is based on findings from joint field surveys conducted by Water and Power Development Authority (WAPDA) and USGS [*Bennett et al.*, 1967; *Swarzenski*, 1968]. These references describe most of Punjab as being underlain by an unconsolidated alluvium aquifer and state that "studies have shown that virtually the entire Punjab is underlain to depths of 1,000 feet or more". Thus, the thickness of this unconfined layer is assumed to be 300 m across the entire model domain. These studies characterize this aquifer as unconfined and connected hydrologically across Punjab [*Swarzenski*, 1968]. Thus, a single layer unconfined aquifer model is developed where the land surface is assigned as the top of the aquifer.

A gridded model of the aquifer with a cell size of 1 km^2 is developed. In total, there are 194000 active cells in the model. Towards the northwestern, western and southeastern boundary of Punjab, the Indus aquifer is not believed to be connected hydraulically to any other aquifer Therefore, grid cells in these regions are modeled as 'inactive', in effect acting as a no flow boundary. Towards the northeastern and southern boundary of Punjab, the aquifer is thought to extend beyond Punjab. However, no hydrogeological study that quantifies the direction and magnitude of lateral flow across these political boundaries exists to the authors' knowledge. The matter is further complicated by insufficient data regarding aquifer characteristics and groundwater level measurements in Sind (south) and India (northeast) to adequately include these regions in this groundwater model. Given these limitations, the boundary condition for this region is modeled by designating a buffer zone extending beyond the boundary of the aquifer and treating these cells as active cells. Beyond the buffer zone, no-flow boundary was specified along the edge of the modeled domain. This technique of establishing an artificial boundary condition far away from the area of interest, suggested by *Reilly and Harbaugh* [2004] prevents the boundary conditions from significantly affecting heads in the area of interest.

The *River* stress package in MODFLOW is used to model the interaction between the rivers and the aquifer that provides another hydrologic boundary condition for the aquifer. Groundwater depth-to-water-table (DTW) measurements from observation wells across Punjab, obtained from the SCARP Monitoring Organization (SMO) division of WAPDA, were used to assign starting head. The two cropping seasons in the basin, Kharif (April-September) and Rabi (October-March), are chosen as the stress periods. The *Recharge* and *Well* stress packages were used to provide the inputs for the aquifer. Both canal recharge and the groundwater abstractions were modeled using the *Well* package.

Groundwater abstraction forms the biggest flux out of the aquifer, but there exists significant uncertainty in both total abstraction and the spatial variation in groundwater pumping across Punjab. Total groundwater abstraction across Punjab for the calibration period was estimated based on a province-wide survey performed for the cropping year (CY) 2001-2002 [*Qureshi et al.*, 2003]. The survey reported utilization factors of tubewells for Kharif and Rabi seasons and further disaggregated the pumping from diesel and electric tubewells. According to the survey, total groundwater abstraction across Punjab in CY 2001-2002 is approximately 43.4 BCM. Using this estimate for groundwater abstraction, the total agricultural water usage for CY 2001-2002 (canal water used in addition to groundwater abstracted) is then determined. Using the ratio between total water usage and total crop production for CY 2001-2002, total water use from 1998-2002 is estimated based on the crop production in those years. Then the groundwater use from 1998-2002 is estimated taking into account the available canal water in those years. Due to the uncertainty associated with this approach, the calibration is limited to a four-year period.

To estimate the spatial variation in abstractions, the district level tubewell density provided in the Punjab Statistical Handbook [*Government of Punjab*, 2012] is used. The dataset provides a

time-series of the number of tubewells in each district and the type of tubewell (diesel and electric). The number of tubewells within each district was employed as a proxy for the amount of pumping that takes place in that district. For each of the 36 districts in Punjab, the ratio of total pumping from diesel and electric tubewells in Kharif and Rabi seasons is then estimated using the utilization factors provided in *Qureshi et al.*, [2003].

An extensive data acquisition process was undertaken to prepare the input data for the model. Accessibility of existing data needed for building a physically-based groundwater model (aquifer characteristics, groundwater observations) for Punjab is extremely limited. In many cases, significant pre-processing of the data had to be performed using *R* Statistical Software. Time-series data was collected and processed to obtain depth-to-water-table (DTW) measurements, province-wide precipitation and evapotranspiration and parameters to simulate river and canal recharge. An expanded discussion of data sources and processing may be found in Appendix A.

Using the described model settings and the data collected, specific yield and hydraulic conductivity of the underlying aquifer were calibrated on the district level. The choice of spatial scale for the calibration was made as a compromise between calibrating on a fine spatial scale but also one that is computationally feasible. This calibration at district scale setting also provides meaningful information for policy makers. The genetic algorithm (GA) [*Wang*, 1991] is used to calibrate the groundwater model, where the objective function minimizes the mean absolute error (MAE) between the observed and simulated heads across Punjab for each stress period in the calibration period. For the GA routine, the parameter population size of 120 is set for each generation and the parameters are calibrated over 50 generations. The model is developed using a linkage between *R* statistical software and MODFLOW, where *R* was used to generate the input files needed for MODFLOW and read output from the model to feed into the GA calibration

routine. The calibrated hydraulic conductivity and specific yield for the districts varied from 2-100 meters per day and 0.08 to 0.20 respectively. A comparison of the calibrated aquifer parameters with field observations across Punjab is shown in Figures S4 and S5 in Appendix A. Overall, a good agreement between the observed and calibrated aquifer parameters was observed. Recent groundwater modeling studies have used the Gravity and Climate Experiment (GRACE) data for model calibration [*Sun et al.*, 2012; *Xie et al.*, 2012], but since GRACE data is not available for the chosen calibration period of this study, it cannot be used to inform the calibration results.
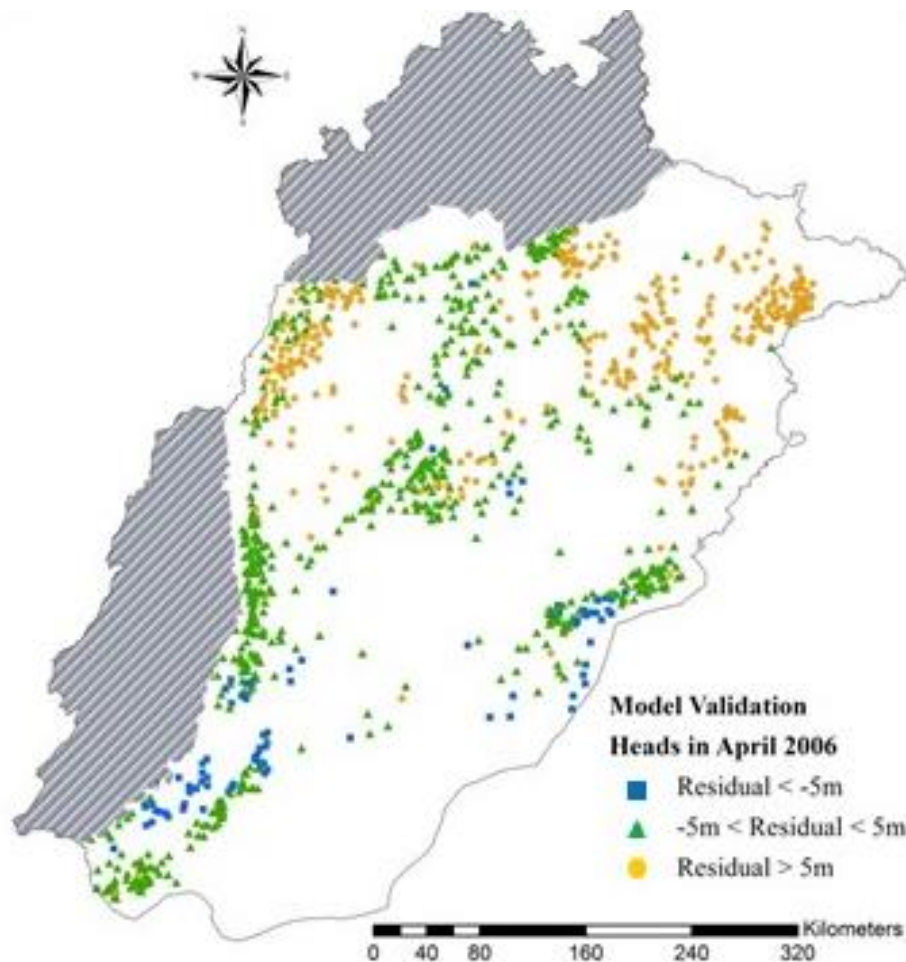
Figure 2. Residuals, observed minus heads obtained at the end of the validation period, at over 1200 wells across Punjab.

A model validation run over eight stress periods was then performed for the calibrated model. Head conditions in April 2002 were used as the starting heads. Figure 2 shows the residuals between the observed and modeled heads at the end of the validation period in April 2006 which represent the "worst" model performance if systematic errors exist. A negative residual suggests overestimation of groundwater head. The figure shows that the model performs best in regions in central and southern Punjab. Overall, model performance is lower in northeast Punjab, mainly due to the high uncertainty in groundwater abstraction data available for this area. Figure 3 shows how the observed heads compare with the modeled heads at the end of the validation period. In addition, Figure S6 through Figure S12, in Appendix A, show time series plots for observed groundwater heads compared to modeled heads from locations across the model domain.
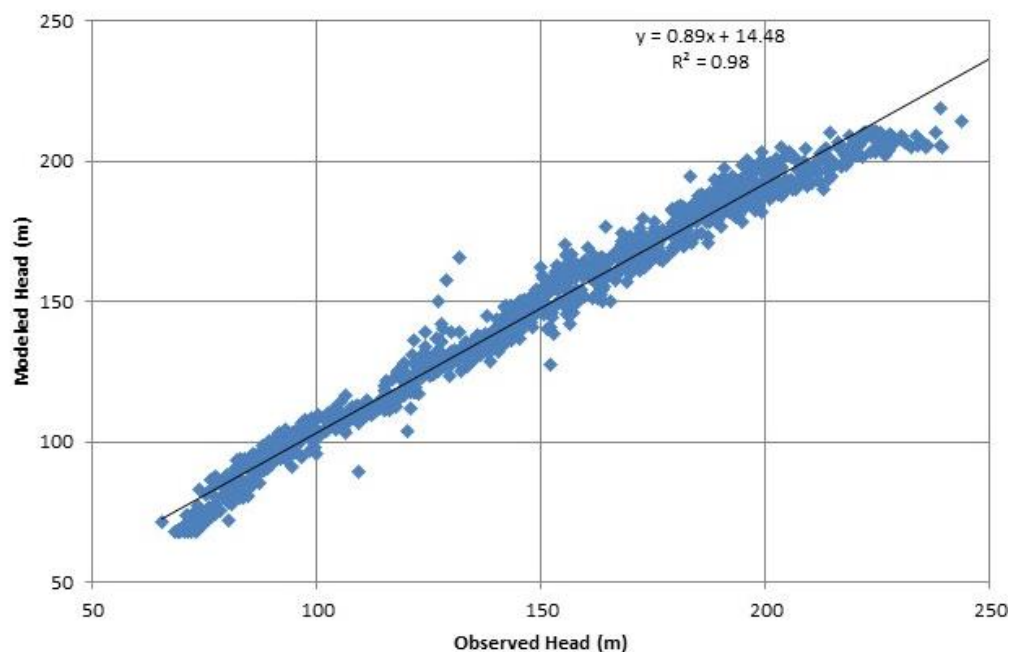
Figure 3. Heads (in meters) obtained at the end of model validation period (April 2006) compared to observed heads measured at over 1200 wells across Punjab

2.4 Scenarios

With the calibrated model, various simulations were run to project how groundwater dynamics would vary in the future. The simulation was performed over 46 seasons (23 years), starting from initial head conditions observed in October 2011. The spatial distribution of pumping was updated based on the density of installed tubewells in each district in 2011 [*GOP*, 2014]. Total groundwater abstraction in the province at the beginning of the simulation was estimated at 60 BCM [*Yang et al.*, 2013]. A set of simulations was performed using the historic time-series of the climatic input data to examine groundwater dynamics under status quo conditions. These results would be the 'status quo' case relative to which all the other scenario results would be compared.

Previous studies of groundwater across Punjab have identified recharge from the canal irrigation system and precipitation as the major components of groundwater flux [*O'Mara and Duloy*, 1984; *Hassan and Bhutta*, 1996; *Basharat and Tariq*, 2015]. In this study, three main components of the groundwater flux are varied in a sensitivity analysis. The selection of components to vary is based on possible future conditions that have been suggested or forecasted to take place [*Yu et al.*, 2012]. These future conditions comprise of possible groundwater control measures, infrastructure improvements in the canal irrigation system and changing climate conditions. Simulation specifications for these different scenario analyses are provided below. An expanded discussion on the bounds for the scenario analysis can be found in Appendix A.

2.4.1 Groundwater Control

Current groundwater abstraction across Punjab is estimated to be approximately equal to or slightly more than total groundwater recharge [*Yu et al.*, 2012; *Basharat et al.*, 2014]. Many policy instruments for addressing overuse of groundwater have been documented in the literature,

including water use quotas, pricing of groundwater and establishing water markets [*Koundouri*, 2004]. This analysis does not compare which of the groundwater control measures are more suitable for Punjab. Instead, the impact of change in pumping is evaluated as a response to various policies, on groundwater heads across Punjab. In this analysis the pumping rate is varied linearly, across the province, from a minimum of 70% (*PumpMin*) to a maximum of 130% (*PumpMax*) of status quo pumping rate by the end of the simulation period of 23 years. The *PumpMin* scenario represents the future where various policy instruments are successful in reducing pumping rates, while the *PumpMax* scenario represents a continuation of the increasing trend in groundwater abstraction leading to groundwater mining. The upper bound for this scenario is based on the observed historical annual increase in crop production. For the lower bound, estimates for the increase in surface water availability through improved canal system efficiency vary significantly, so a symmetric reduction is assumed.

2.4.2 Canal Infrastructure

Seepage from the irrigation canals across Punjab has been identified as a major component of the total recharge into the aquifer. Currently, it is estimated that approximately 50% of surface water is lost through seepage into the aquifer due to conveyance and application losses in canals and watercourses and fields [*Sultan et al.*, 2014]. While this high surface water seepage is often cited as a sign of inefficiencies across the irrigation system [*Kugelman and Hathaway*, 2009], it is the reason behind the high groundwater heads across much of Punjab. Canal lining and more efficient irrigation practices have been introduced performed over the past few years across Punjab to improve the efficiency of the irrigation system, reduce waterlogging and provide farmers with more reliable surface water supply. However, to the authors' knowledge, the impact of this

increased efficiency on the water table and associated pumping costs has not been quantified at the provincial level previously. In this set of simulations, the seepage from the canals is varied uniformly across Punjab from 30% (*CanRechMin*) to 70% (*CanRechMax*) of canal water supply by the end of the simulation period. Significant improvement in the irrigation infrastructure efficiency would reduce the proportion of surface water seeping into the aquifer. This is represented through the *CanRechMin* scenario. *CanRechMax* represents the future where the canal infrastructure deteriorates further due to a lack of maintenance, leading to an increase in seepage of canal water supplies into the aquifer. The range of variability in seepage from existing canal systems [*PPSGDP*, 1998] is used to inform the scenario bounds.

2.4.3 Precipitation change

In a water-balance analysis of groundwater across the Rechna doab, *Hassan and Bhutta* [1996] showed that rainfall is one of the most important components for groundwater recharge. There exists a lot of uncertainty and concern regarding the impact of climate change on groundwater. Effects of changing precipitation across Pakistan, especially in the summer monsoon, have already started surfacing and are projected to worsen in the near future [*Treydte et al.*, 2006]. Increasing temperatures and evapotranspiration rates will necessarily place an added burden on groundwater resources in the water-stressed regions [*Green et al.*, 2011]. A lack of province-wide data meant that these temperature effects of climate change across Punjab were not included in this analysis. In these simulations, the total volume of precipitation that falls in Punjab is varied while keeping the spatial distribution constant. Upper and lower bounds on precipitation change were determined using forecasts for precipitation change in the existing literature, which range from a 5-25% decrease [*Ragab and Prudhomme*, 2002] to a 20-24% increase in annual

average precipitation [*Kripalani et al.*, 2007]. Precipitation recharge is varied from 75% (*PrecMin*)

to 125% (*PrecMax*) of historic levels. Results from these simulations will highlight the specific

regions where the precipitation recharge is most important.

2.5 Results and Discussion

This section discusses results from different simulations. Results of status quo conditions

are presented first and compared with simulations of the future scenarios.
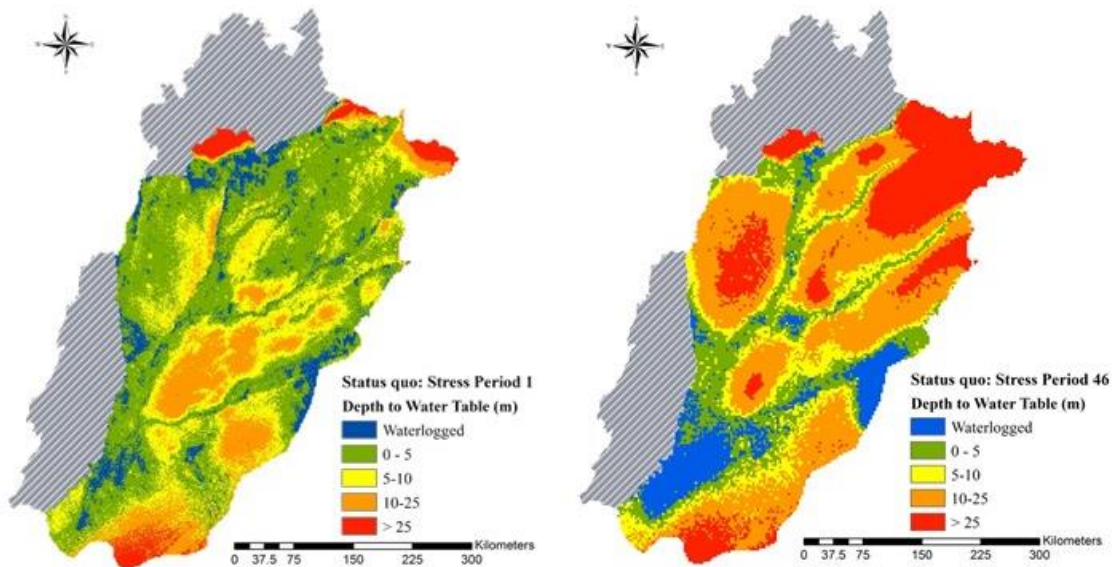
Figure 4. Simulation results across Punjab showing changes in groundwater depth-to-water table
(DTW) under status quo conditions at the end of the 23 year simulation period

Figure 4 shows the DTW across Punjab under the status quo conditions in the first and last

time steps of the simulations. Figure 4a shows that under initial conditions in 2011, DTW across

most of Punjab is less than 10 m. However, by the end of the simulation period of 23 years under

status quo conditions, DTW distribution changes drastically across the province. In northern and

central Punjab, DTW is greater than 10 m, with some areas with a DTW over 25 m. The most

significant decreases in head take place in northeastern Punjab in Lahore division. The DTW is

lower along the major rivers (Jhelum, Chenab and Ravi) due to river recharge into the aquifer.

Figure 4b also shows that most of the waterlogging occurs in southern Punjab with higher rates of waterlogging in D.G.Khan and Bahawalpur Divisions. Most of the districts in north and central Punjab experience little to no waterlogging under status quo conditions.
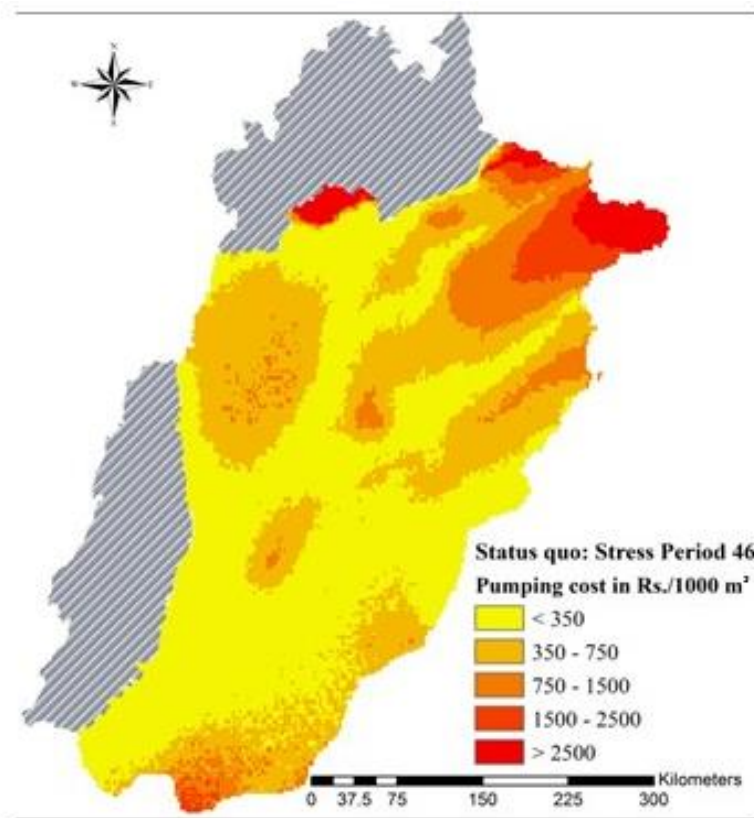
Figure 5. Pumping cost (in Rs./1000 m^3) across Punjab under status quo conditions at the end of the 23 year simulation period

Pumping cost in Pakistani Rupees (Rs) /1000 m^3 across Punjab under status quo conditions at the end of the 23-year simulation period is shown in Figure 5. The cost of groundwater pumping is determined based on the drawdown output from MODFLOW. This drawdown is converted into a depth to water table, which is then used to calculate the energy required to pump 1000m^3 of water. This energy is then converted into the cost of pumping based taking into account the approximate efficiency of a typical tubewell [*Qureshi et al.*, 2003] and the price of slow-speed diesel fuel (Rs 61/L) in Pakistan. The simulation results show that, under status quo conditions,

average province-wide pumping costs increase from Rs. 480/1000 m^3 in 2011 to Rs. 1320/1000 m^3 at the end of the 23-year simulation, an increase of 270%. For comparison, farmers currently pay approximately Rs 40/1000 m^3 for surface water supplies. The figure shows that the highest pumping costs are in northeastern Punjab due to huge decreases in groundwater head resulting from higher estimated pumping. A lower pumping cost in areas near the major rivers is observed, due to recharge from surface water into the underlying aquifer. The lowest pumping costs are observed in Bahawalpur division in southern Punjab.
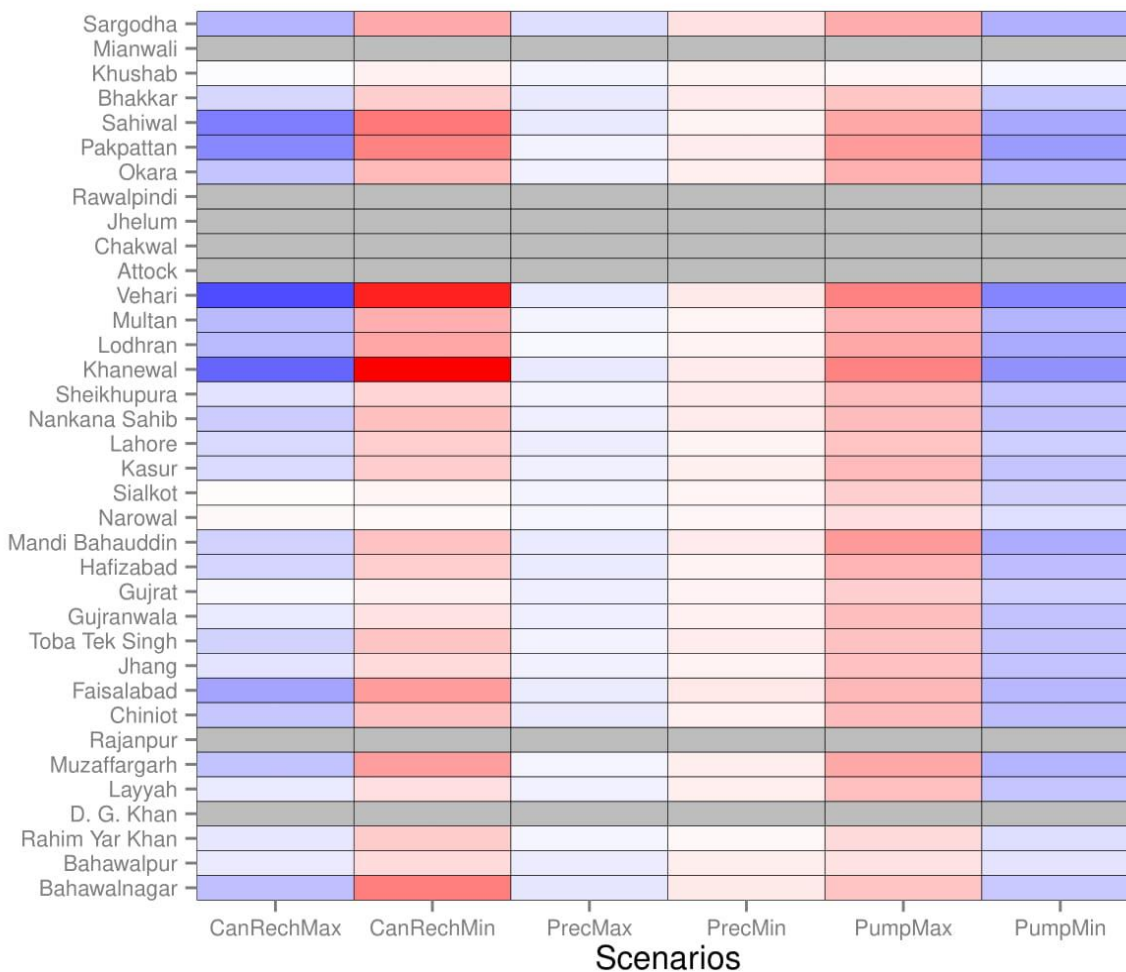
Figure 6. Heatmap of % changes in average pumping cost in each district under the different scenarios relative to status quo conditions at the end of the 23 year simulation period

Figure 6 shows a heat map illustrating the percentage change in average pumping costs relative to the status quo conditions on a district level across Punjab for the different scenarios. Pumping costs in some districts seem to be affected under all scenarios whereas costs in certain districts are relatively insensitive to all scenarios. This suggests that the sensitivity of pumping costs in some regions is independent of the future scenario, and is a function primarily of the location of the district itself. The heatmap shows that while recharge from canals into the aquifer results in the highest pumping cost changes in certain districts, across all districts changes in groundwater abstraction have a bigger impact. Under the *CanRechMin* scenario, where there is a reduction in canal recharge (seepage of only 30% of surface flows across all the canals), pumping costs are seen to increase significantly. In particular, districts in Sahiwal and Multan divisions in central Punjab are shown to have the highest percentage increase in pumping costs, suggesting that canal recharge provides significant contribution to groundwater in these areas. A similar, but less striking, pattern is observed for the pumping scenarios as well. For both the precipitation extremes, there is relatively little change in pumping costs across all districts, suggesting that direct precipitation impacts on groundwater dynamics are relatively small, compared to the impacts of changes in groundwater pumping and canal recharge.

Figure 7 shows the time series of simulated groundwater heads under the different simulation extremes in three major cities in Punjab: Lahore, Faisalabad and Multan. These major urban centers are spread across Punjab, as shown in Figure 1, and provide a good representation of aquifer conditions across the province. These plots show the 'best case' and 'worst case' results with respect to groundwater head levels. In the 'best case' heads, results for the *PumpMin*, *CanRechMax* and *PrecMax* simulations are plotted. For the 'worst case' heads, *PumpMax*, *CanRechMin* and *PrecMin* are shown. For each city, the status quo scenario is also plotted to

provide a reference point for the impact of different scenarios on groundwater head. The graphs show observed heads from 1999-2011 where a decreasing trend can be seen in Lahore and Faisalabad. Changes in the canal recharge scenario (*CanRechMax*) have the highest impact on heads in terms of deviation from the status quo scenario for all three cities. Impact of the precipitation extremes is the lowest of all scenarios and the resulting heads are very similar to the status quo scenario in all three cities. Simulated groundwater heads at Faisalabad decrease significantly under all three 'worst-case' scenarios and two of the three 'best-case' scenarios. Multan is generally the least-sensitive to changes in terms of percentage head change relative to the status quo scenario among three cities.
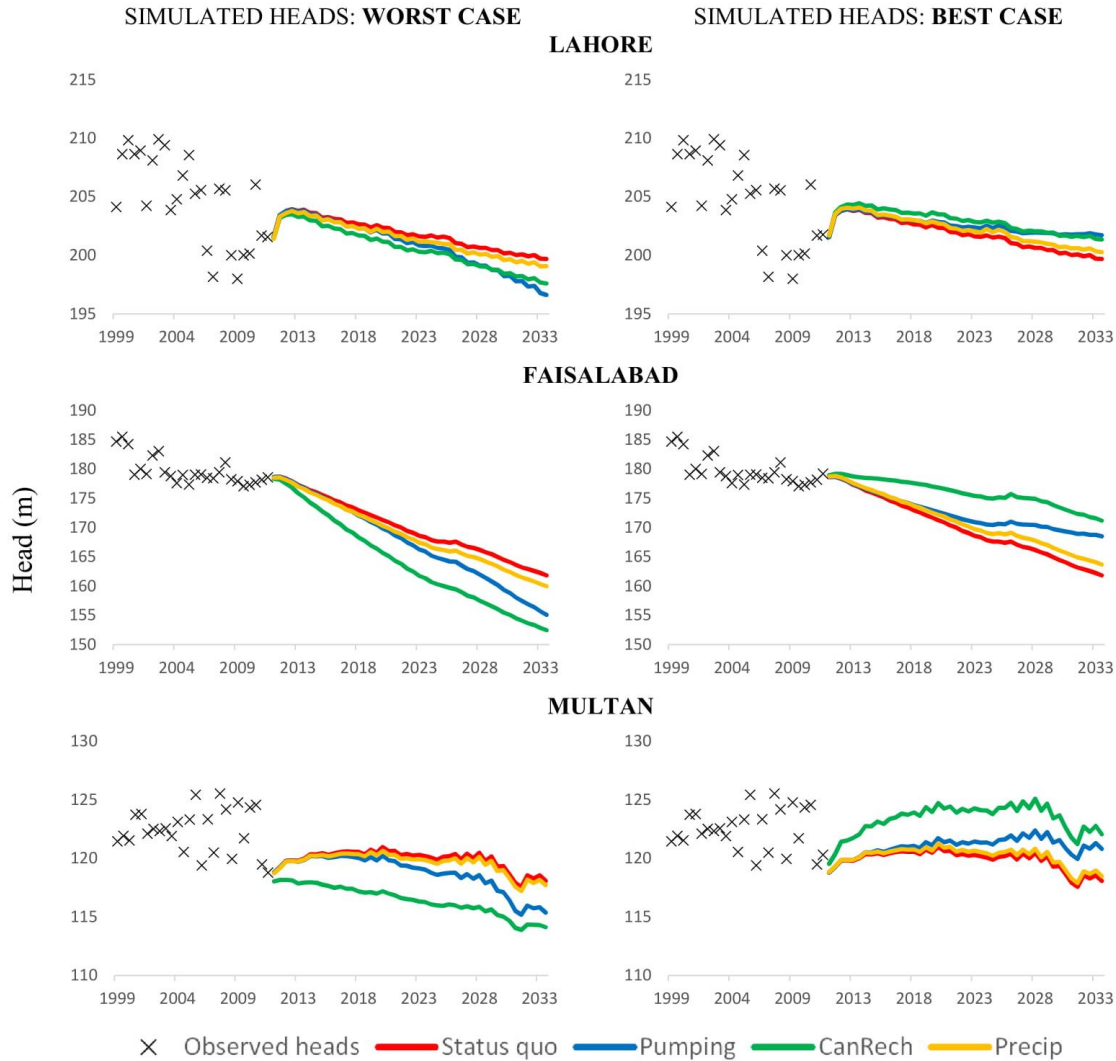
Figure 7. Observed and Simulated heads in 3 major cities across Punjab under the different scenarios

2.5.1 Groundwater Policy Implementation

The simulation results show quantitatively that seepage from canals into the aquifer in certain districts is the most significant component, while direct precipitation is a relatively small component in the overall groundwater flux for the aquifer underlying Punjab. Thus, an important policy action that the results of this analysis support is re-evaluation of the canal water allocation schedule. This reallocation of canal supplies while considering groundwater dynamics has been suggested in several other studies [*O'Mara and Duloy*, 1984; *Ahmad and Kutcher*, 1992; *van*

24

Steenbergen and Oliemans, 1996; *Basharat and Tariq*, 2015]. A study of the Bari doab by *Basharat and Tariq* [2015] highlighted the inequities in pumping costs caused by the existing canal water allocations. They found that farmers at the tail-end of the canal system were paying more than twice in pumping costs compared to head-end users. In addition to this inequity, the current surface water allocation schedule also contributes to the growing waterlogging and salinity problems in southern Punjab [*Chandio et al.*, 2012].

For regions with high levels of waterlogging, reducing the seepage into the aquifer through canal lining efforts could prove beneficial. While the relatively low efficiency of the canal irrigation system is often cited as one of the biggest drawbacks to improving agricultural productivity in the IRB [*Ahmad and Kutcher*, 1992], this study's results quantitatively show that an improvement in efficiency of the canal system would also result in reduced recharge into the aquifer and lead to much more rapid decline in groundwater tables in certain districts. However, it is also important to remember that these simulations do not take into account the possible changes in groundwater abstraction that would accompany an improved surface water delivery system.

If groundwater pumping continues at current rates of abstraction, the energy requirement associated with such pumping is projected to increase almost three-folds by 2035. The simulation results for the groundwater heads in major cities across Punjab also show that under almost all but one of the future scenarios (i.e. *best-case scenario for Multan*), groundwater head decreases steadily. Given the existing problems facing Pakistan with meeting its energy needs, the increasing energy requirements for pumping associated with falling groundwater levels could present significant problems. Increasing energy costs for groundwater pumping have been shown to adversely affect small-scale farmers globally [*Zhu et al.*, 2007]. The results emphasize the need to manage pumping in areas with high groundwater declines. Policy measures that can be taken to

curb groundwater mining in these areas would need to start with regular measurement and monitoring of groundwater heads.

2.5.2 Limitations and future development

One of the biggest sources of uncertainty in building this province-wide groundwater model was estimation of groundwater pumping in Punjab that has considerable variation, both spatially and temporally. While using the number of installed tubewells can provide a rough estimation of agricultural groundwater usage, this method does not adequately address domestic and industrial usage, where utilization factors are generally much higher and tubewells run on electricity. Thus, there exists considerable uncertainty in estimation of groundwater abstraction in major urban centers, such as Lahore, where groundwater usage is high. In addition to better data on urban usage, availability of a comprehensive dataset of agricultural groundwater usage on a district or canal command level based on field survey data, would undoubtedly improve this analysis.

It should also be noted that the model is unable to capture some of the historic variability in groundwater levels. This is primarily because the temporal resolution of this model is at the seasonal scale, based on data availability. Thus, the model effectively "averages" groundwater conditions at the seasonal level and is unable to replicate fluctuations in the groundwater level on a finer time scale. While seasonal fluctuation in the groundwater table is important to know, the key message and findings in this study focus on longer term trends in the groundwater table under different scenarios. Improved data availability would allow modeling at a finer temporal resolution but probably not substantially affect the broader policy recommendations that this study advances. In addition, the calibrated parameters are influenced significantly by the input data. This is

especially true for the northeast region of this model, where a combination of uncertain boundary conditions and input data negatively impact model calibration.

Due to a lack of time-series data on groundwater quality, this analysis focuses exclusively on groundwater quantity issues without a groundwater quality component. However, groundwater quality concerns need to be taken into account when drafting groundwater management policy. This study is unable to account for the impact of direct runoff and its relationship with surface water bodies due to a lack of reliable time-series data for river stage and overland runoff coefficients across the model domain. Given that for much of the modeled area precipitation is relatively low, this assumption will not significantly affect the major findings from the system-wide results. Data limitations in this region make groundwater modeling at this scale challenging, especially with regards to development of the boundary conditions (river, canal, recharge and well). However, this study presents a useful first step in generating an informed scientific discussion regarding groundwater management in Pakistan.

In the sensitivity analysis for future scenarios, the model is unable to capture the secondary impact of behavioral change on groundwater abstraction (e.g., increase surface water availability due to cannel lining might reduce groundwater pumping). A valuable avenue of future work extending this study would be the linkage between this physically-based groundwater model and an Agent-Based Model (ABM) to capture the impact of farmers' behavior in different scenarios, on groundwater across Punjab. The ABM approach coupled with a physically-based groundwater model has been used to assess the effectiveness of various policy instruments (Hu et al. 2015; Mulligan et al. 2014). The ABM can quantify farmers' behavior based on surveys and provide insight into farmers' behavior in response to changing policy. A linked ABM-MODFLOW model

would show a more complete picture of change in groundwater dynamics in response to changing policy.

2.6 Conclusion

The analysis presented in this paper was conducted to develop a better understanding of current groundwater dynamics across Punjab. A physically-based groundwater model for the Indus Plain aquifer underlying Punjab was built and calibrated for the first time. While the calibrated model was validated and found to perform satisfactorily, there is room for improvement in the model development, especially in the development of better boundary conditions, as more detailed and reliable datasets for the study region emerge. The model was then used to project groundwater conditions in the future under different scenarios. The fine spatial resolution of 1 km^2 allows the model to capture the various components of groundwater flux including pumping, canal recharge, river recharge, precipitation and evapotranspiration. Results of this study present issues of groundwater depletion, increasing energy costs for abstraction, and water logging. The findings emphasize the heterogeneity in groundwater conditions across Punjab and highlight the need for region-specific management of groundwater resources.

Economic growth and food security are very closely tied with groundwater use in Pakistan. It is vital that policy measures be drafted and implemented to ensure sustainable groundwater use before the problems highlighted in this analysis are exacerbated. This study highlights the need for developing water resources management policies for groundwater in conjunction with surface water due to the strong linkage between the two. An important policy measure in the Indus River Basin has to be reevaluation of existing water supply schedules both within and between the canal command areas. A reallocation of the water supplies would be useful in not only mitigating

groundwater depletion and waterlogging, but also reducing the inequities that exist within the system. What is clear is that the federal and provincial governments need to urgently play a more active role in drafting and implementation of groundwater management policies.

CHAPTER 3

A COUPLED MODELING FRAMEWORK FOR SUSTAINABLE WATERSHED MANAGEMENT IN TRANSBOUNDARY RIVER BASINS

3.1 Introduction

Comprehensive watershed management is a challenging task that requires multidisciplinary knowledge. An emerging research area highlights the importance of using watershed management to sustain various ecosystem services for human society [*Jewitt*, 2002; *Lundy and Wade*, 2011]. While the various services provided by a river are primarily viewed through the prism of human benefits, maintaining a healthy ecosystem can be mutually beneficial to both human society and ecological systems. A failure to maintain adequate levels of riverine ecosystem health may result in compromising human benefits for future generations [*Baron et al.*, 2004]. There is therefore a growing recognition among water resources managers that sustainable watershed management needs to not only account for the diverse ways humans benefit from the environment, but also incorporate the impact of human actions on the natural system [*Vogel et al.*, 2015]. This is perhaps most prominently advocated in the emerging science of 'socio-hydrology', which calls for an understanding of the two-way interactions and co-evolution of coupled human-water systems [*Sivapalan et al.*, 2012]. This two-way coupling, then, needs to be integrated into computational tools used to aid watershed management.

A coupled human natural systems modeling approach, where the stochastic interactions between agents are represented, also facilitates stakeholder involvement. It can be used as a communication tool to organize information between hydrologists, systems analysts, policy makers and other stakeholders to inform the model and provide meaning to its results. The process of involving stakeholders in the modeling process allows them to observe how their actions affect

other agents and observe the system-wide trends that emerge based on low-level agent interactions [*Lund and Palmer*, 1997].

Traditional watershed modeling does not effectively capture system heterogeneity limiting its ability to effectively represent the two-way interaction between human and natural systems. Conventional models of water resources systems developed for assisting decision-making treat human benefits as a single objective using a centralized optimization approach, which ignores the heterogeneity among water users and uses (e.g., priority of different water uses along a river system based on socioeconomic differences) [*Yang et al.*, 2009]. The decision-maker is usually assumed to possess perfect information with respect to demand and supply of water and other resources in the watershed. If they are considered at all, most ecological functions are considered as constraints in the system, often for numerical convenience and frequently leading to oversimplification [*Stone-Jovicich*, 2015].

In this paper, we develop a modeling framework that can effectively address both system heterogeneity and the linkage between human society and hydrology that influences water cycling in the watershed. We do so by differentiating key stakeholders of ecosystem services as active agents based on their characteristics such as location and water use preferences, and tightly couple the human system with a process-based watershed model that simulates the stock and flow of environmental variables needed by the stakeholders.

In this two-way coupled natural-human systems modeling framework, the human system is modeled as a decentralized water systems model and is linked to a process based, semi-distributed hydrologic model. Empirical data obtained from surveys of water practitioners are used to develop behavior rules for water use, providing a realistic representation of human behaviors in water resources modeling. In addition to incorporating indirect interaction between the agents

through the environment, i.e. surface water flows, a novel advancement offered in this framework is the ability of agents to *directly* interact by requesting assistance from other agents based on their level of cooperation. A web-based user interface for this coupled model has been developed which enables non-technical stakeholders to use this modeling platform online. The online portal allows for role-play and participatory modeling. We apply this modeling framework to two different transboundary basins where ecological needs are competing with growing human demands on the water resources: the Mekong River Basin in Southeast Asia and the Niger River Basin in West Africa.

3.2 Previous studies of coupled natural-human system modeling

Coupled natural-human system modeling through explicit modeling of both natural processes (e.g. rainfall-runoff for water supply) and human behavior (e.g., services that humans derive from natural systems, such as water resources) helps reveal the reciprocal interactions and coevolution of the natural and human systems. Modeling efforts coupling the natural and human systems have increased in recent years [*Liu et al.*, 2007], evolving from an approach that focused mostly on understanding the natural processes and treated human actions as fixed boundary conditions [*Sivakumar et al.*, 2005]. The human system coupled with the natural system can be simulation (descriptive) or optimization (prescriptive) based depending on the modeling objective [*Giuliani et al.*, 2016].

A watershed is a self-organizing system characterized by distributed, albeit interactive decision processes. If a coordination mechanism exists, it will guide the interactions among individual decision processes. The agent-based modeling (ABM) framework provides such a mechanism for integrating knowledge and understanding across diverse domains [*Yang et al.*,

2009; *Berglund*, 2015]. In an ABM, individual actors are represented as unique and autonomous "agents" with their own interests. Agents follow certain behavioral rules and interact with each other in a shared environment allowing for a natural representation of real world, "bottom-up" watershed management processes. A (semi-)distributed hydrological model that can simulate the environment, which provides ecosystem services, can then be linked with the agent-based model that represents decentralized decision-making processes. This linkage allows us to utilize the strength from both models and better represent watershed as a coupled natural-human complex system.

Distributed process-based hydrologic models are well suited for linkage with ABMs. Compared to statistical or data driven models, process-based models are more robust for extrapolation or in simulating conditions under changing management practices. Distributed and semi-distributed models have the capacity of reflecting the spatial heterogeneity of hydrologic and water quality processes within a river basin. This capacity also facilitates the evaluation of spatially variable user demands for ecosystem services. Open-source hydrologic models, where it is possible for third-party users to incorporate region-specific knowledge into the models to improve performance or extend model capability, are especially suitable for coupling with decentralized water system models. The spatial structure of the hydrologic model and its consistency with the model structure of the ABM it is being coupled to are additional important considerations.

SWAT (Soil and Water Assessment Tool) is one such hydrologic modeling platform with many of the features described above that has been used previously to explore effects of human intervention on basin water resources. It provides built-in functions to simulate reservoir operations, irrigation and a variety of best management practices (BMPs) for nutrient pollution control [*Bracmort et al.*, 2006; *Strauch et al.*, 2013]. Its open-source nature allows users to

33

incorporate locale-specific knowledge into the model to improve model performance or extend model's capabilities. SWAT conducts simulations at the level of sub-watershed, or hydrological response unit. When the modeling domain of an agent-based model is delineated following the boundaries of sub-watershed, it has the advantage of spatial unit consistency with agent-based models. Furthermore, it has been coupled with (non-ABM) decision modeling tools to identify cost-effective solutions to basin water resources management challenges [*Karamouz et al.*, 2010; *Ciou et al.*, 2012]. We therefore choose SWAT as the hydrologic model for this study.

A fully coupled modeling framework involves continuous information exchange between the agent-based and the hydrologic model such that the two models are solved simultaneously or iteratively in each time step. A review of the existing literature shows that most coupled natural-human systems models, especially in the context of surface-water management, are only loosely linked and thus do not fully capture the impact of human actions on hydrology [*Berger et al.*, 2007; *Ng et al.*, 2011; *Yang et al.*, 2012; *Giacomoni et al.*, 2013]. "Fully coupled" models can be found for groundwater analysis (e.g. *Reeves and Zellner* [2010]). This is because the common outputs from groundwater models are "stock variables" such as groundwater head and it is relatively easy to restart the simulation model from the previous step. Surface hydrologic model, on the other hand, usually output flux (i.e. streamflow) and not stock variables (e.g. lake storage and soil moisture). To be "fully coupled" with an agent-based model, a modification of the programming code of the watershed model is usually necessary to output state variables and allow the agent-based model to interact with the watershed model at monthly or daily time step [*Mishra*, 2013].

The methodology proposed here is designed primarily to help improve stakeholder understanding of a complex system as well as recognition of various, alternative development pathways for the basin in question. A linkage between an agent-based model and a process-based

watershed model, incorporating direct interactions between agents, is a promising method to accurately represent complex coupled natural-human systems as well as to appropriately involve non-technical stakeholders into the assessment.

3.3 Methodology

The generalized framework for the two-way coupling between an agent-based model and a process-based watershed model is described here in greater detail. In this framework, the river basin is divided into politically and hydrologically similar sub-regions, where water management is primarily carried under the ambit of a single administrative unit, which represents an autonomous agent. This approach to delineating regions is also found in other studies, e.g. the Food Production Unit in the International Model for Policy Analysis of Agricultural Commodities and Trade [*Robinson et al.*, 2015].

In this framework, agents follow prescribed rules based on which their benefits are calculated. Agents make water management decisions, on an annual time step, for agricultural production, hydropower generation and ecological management based on targets set using long-term historical data. They update their actions every year based on their experience from previous years; this behavior can be classified as a hybrid between reactive and deliberative approaches [*Akhbari and Grigg*, 2013]. In this modeling framework, agents can interact both directly and indirectly. Agents interact indirectly through their water usage for agriculture, and changes in streamflow in response to hydropower production. For direct communication between agents, we include a level of cooperation (LOC) parameter that signifies the willingness of an agent to alter their own water management actions to benefit a downstream agent. This setting allows for the incorporation of stochasticity in the agent decision-making process.

Figure 8 shows the higher-level coupled modeling framework. First, user-defined preferences and level of cooperation are defined based on stakeholder input. These input parameters can either be defined by individual users according to specific scenarios of interest, or be determined based on directly eliciting the information from the various water using stakeholders, for example, through surveys. As part of this project, we conducted comprehensive surveys across three transboundary river basins (Indus, Mekong and Niger) to identify water use preferences [*Khan et al.*, 2017]. The surveys were developed to elicit the perceived importance of various ecosystem services across each basin under a variety of economic and hydrologic future conditions. The survey sample size ranged from 75-85 for each of the basins. One of the questions in the survey asked respondents to rank different ecosystem services in order of importance for each agent. These responses were then averaged across all the respondents for each agent to obtain a ranking of the importance of the different ecosystem services. These rankings were used in the decision algorithm for the case study models developed and presented in this paper. Second, other initial input parameters are incorporated into the ABM framework. These include reservoir characteristics, such as storage, release capacity, efficiency and operational rules for each reservoir. The geographic linkages between subbasins, ecosystem hot spots and agents across the entire river basin are defined in the ABM as well. For each subbasin, agricultural parameters are defined including the type of land cover, total cropped area and type of crop produced. For each agent, targets are defined for each of the three water uses based on historical flow conditions. These targets form the basis relative to which the agents make their water management decisions.
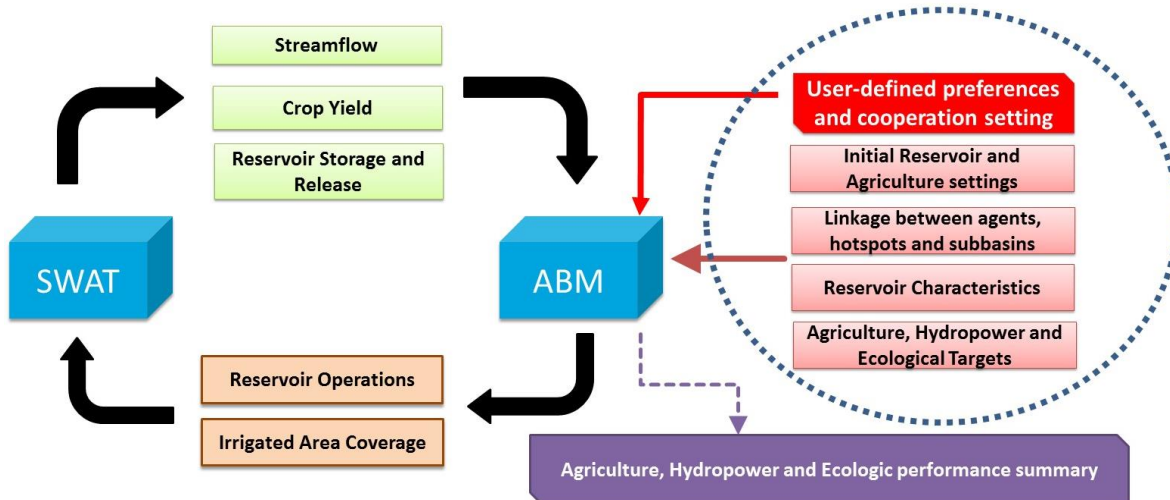
Figure 8: Overview of the modeling framework coupling ABM with SWAT

The ABM, built using *R* statistical language, reports agent decisions concerning reservoir operation and irrigated area that are then used as input for the calibrated SWAT model that simulates the hydrology for the next time step. The crop production and reservoir modules in the SWAT model are driven using water management decisions from the ABM and hydroclimatologic conditions. Upon completion, the SWAT model generates three primary output files that are used as input for the agent-based model. These files include:

- Proportion of cropped area and crop yield for each hydrologic-response unit (HRU) in each subbasin in each agent.

- Daily storage volume and releases from each reservoir

- Daily streamflow at the outlet of each of the subbasins across the basin.

The output from the SWAT model is then fed back into the ABM based on which the agents make water management decisions for the next time step. In the last time step of the modeling run, the ABM provides a summary file summarizing the performances for each of the three water uses: agriculture, hydropower and ecology.

Figure 9 shows the algorithm through which the ABM and the hydrologic model interact, and the process through which various agents make their water management decisions, in two distinct parts. In the first part, the agent's water management decision is made based on its preferences of water use, while in the second part the decisions are made based on its willingness to cooperate. In the first part, the algorithm uses the water use preferences for each agent, and compares the target value with the output from the SWAT model for each of the water uses to make the water management decision for each agent. Under the current setting, the agent is allowed to only make one water management decision every year. However, this can be modified in future studies to allow multiple decisions to be made in a year. Additional information from stakeholders (such as rules of tiebreak) would be needed for this.

For instance, consider an agent that ranks agricultural production higher than other water uses. In this case, the ABM checks to see whether crop production meets the target crop production. If crop production is significantly lower than the target crop production, then the agent decides to increase the irrigated area. If crop production meets the target production, then the ABM checks to see if hydropower generation for the current time step meets the hydropower generation target. If the hydropower generation target is not met, the agent decides to decrease the number of days actual storage needs to meet the target storage. This allows for greater releases and increased hydropower generation. If the hydropower generation target has also been satisfied, then the ABM moves to the second part of the decision-making algorithm.

An important input to the ABM is the identification of ecosystem hotspots. Ecosystem hotspots are specific regions in the river basin that are especially critical to or indicative of the health of the ecosystem in the entire basin. Ecosystem hotspots can be identified in a variety of ways including through a literature review of critical ecological concerns in a basin and/or input

from local ecological experts. For this analysis, for each ecosystem hotspot, relevant Indicators of Hydrologic Alteration (IHA) and Environmental Flow Component (EFC) parameters are selected based on expert opinion to measure ecosystem health [*Richter et al.*, 1996, 1997]. Baseline values for relevant IHA and EFC parameters, which are streamflow based indicators, are calculated from daily streamflow of the calibrated SWAT model. The IHA and EFC parameters included for the case study applications described in Sect. 3.4 include monthly median flows, 7-day annual maximum flow, small and large flood event duration, timing and duration of extreme low flows etc. We use ± 10 % from the baseline value as a decision threshold in the ABM as recommended by research consortium partner WorldFish. This means the modeled IHA and EFC values deviating from the baseline value by more than 10% would require an agent to take action.

Water management to satisfy ecological targets depends on the specific hydro-ecology of the ecosystem hotspot. For example, a river reach may need low flows during the breeding season while a downstream wetland may need higher flows to avoid eutrophic conditions. Satisfying multiple ecologic needs, as is often the case in large river basins, can require contrasting interventions and add tremendous complexity to the water management decision-making process. In the case study applications for this modeling framework, we find that the information needed to fully incorporate ecosystem hotspot management into the ABM-SWAT framework is limited. The link between management actions (e.g. reservoir operations; crop land management) and ecological concerns is not well understood and requires further investigation that is beyond the scope of this work.
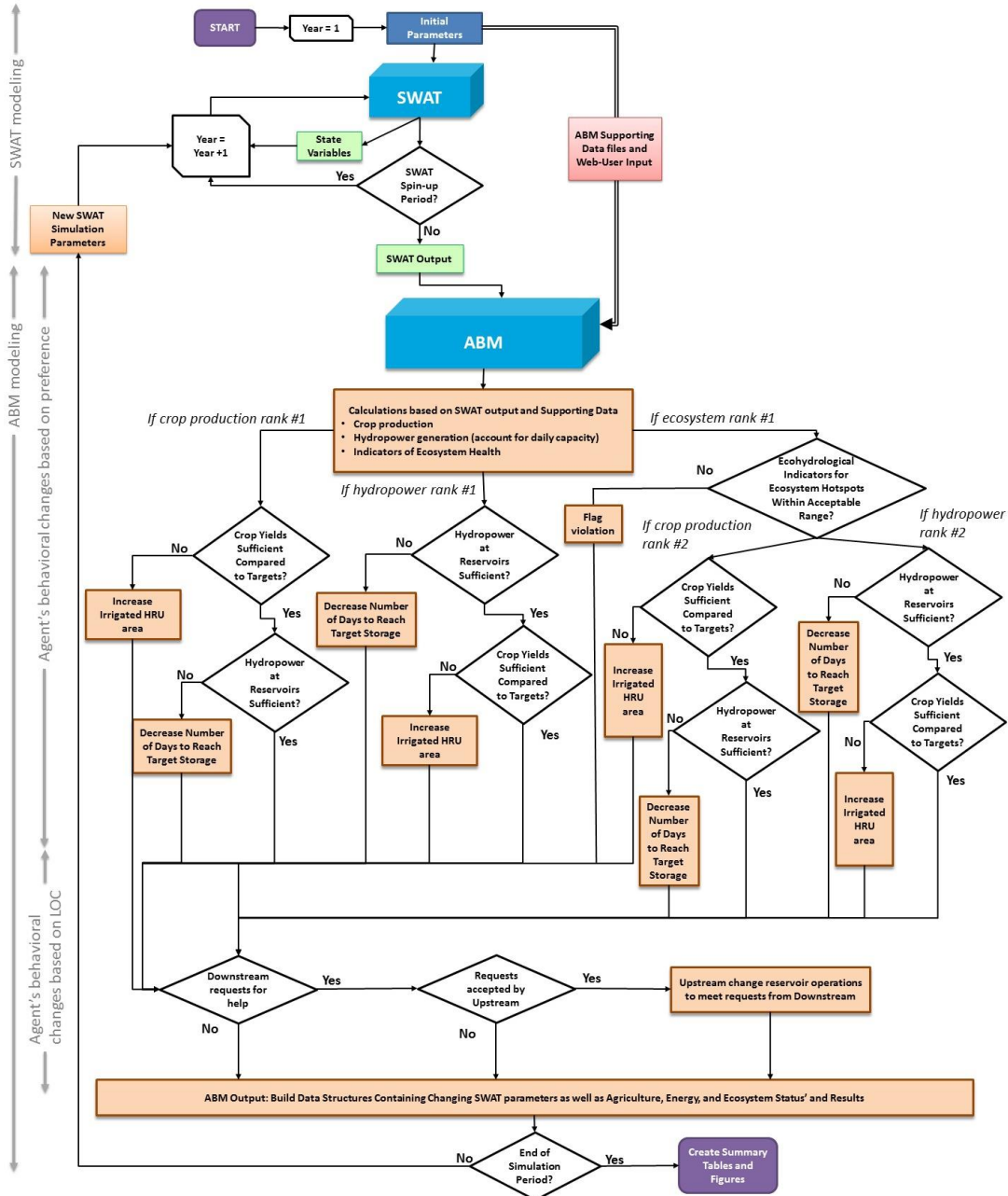
Figure 9: Modelling workflow including the two-part algorithm through which agents make water management decisions

In the absence of detailed information on ecological needs, we incorporate ecosystem hotspot management in the model by creating a "flag" when the timing and magnitude of relevant IHA and EFC deviates from the target values in each hotspot. Thus, while the agents do not actively consider ecosystem hotspots in their decisions, they recognize when violations (deviation

40

from target values) occur. We use these violations to constrain the agent's decision, so that if any of the ecologic targets have been violated and ecologic needs are ranked highest, no action can be undertaken for agricultural production or hydropower generation. This current setting mimics most real world policies about ecosystem conservation that do not have an active reaction toward environmental issues, especially in developing countries. Of course, this algorithm is flexible and allows for a more proactive decision-making process for ecologic management if more information regarding stakeholder perceptions is available.

In the second part of the decision-making algorithm, agents decide whether to alter their water management actions based on requests from downstream agents. This feature aims to represent the possibility of cooperative water management in a transboundary river basin. For instance in March 2016, China released additional water from its Jinghong Reservoir, in response to a request from Vietnam, to help alleviate water shortages in downstream countries in the Mekong River Basin [*Tiezzi*, 2016]. In the current framework, a downstream agent can request an upstream agent to change its reservoir operations to alleviate prolonged water scarcity (at least two time steps). For instance, if a downstream agent has been unable to meet its agricultural production target for two years, then it can request an upstream agent to increase releases. Wherever available, one upstream reservoir is identified for each agent.

Once a request is made by a downstream agent, the upstream agent first checks to see if it has surplus storage, after accounting for its own needs, to consider releasing additional water. If the available storage is not sufficiently higher than the target storage, then the upstream agent declines the request and does not change its reservoir operations. If the upstream reservoir has sufficient storage, then it decides whether to respond favorably to the downstream request based on its willingness to cooperate. In this modeling framework, the LOC represents the probability

(from 0 to 1) of the agent to respond favorably to a downstream request and incorporates human decision making uncertainty, making the second part of the decision-making algorithm stochastic to mimic human decision uncertainty. In any given time step, an upstream reservoir can only respond to one request. Once the second part of the algorithm is executed, the water management decisions are made and relevant information is then fed back to the SWAT model as inputs for the next time step.

This modeling framework is generalizable, tackling the challenge of paucity of transparency and reusability often associated with ABM development [*O'Sullivan et al.*, 2016]. The framework design means that the ABM can be adapted to different watersheds by simply preparing a different set of input files without having to modify the structure of the model.

3.4 Application of the Modeling Framework

In this section, we show the application of this generalized coupled modeling framework to two transboundary river basins: the Mekong and Niger River Basins. We describe the development of the ABM and hydrology model for each of the basins, and then show model outputs illustrating the impacts of agent behavior on agent-specific and basin wide outcomes. We use the Mekong River Basin as an example to show how agents' preferences impact different water uses, while the Niger River Basin is used as a case study to demonstrate how interactions between different agents and their willingness to cooperate influences basin wide outcomes.

3.4.1 Impact of Agent Preferences – Mekong Demonstration

We apply the generalized ABM framework described in Sect. 3.3 to the Mekong River Basin. The Mekong River, with an annual average discharge of 450 km^3, drains the sixth largest

river basin in the world in terms of runoff [*Kite*, 2001]. It is a transboundary river originating in China and flows through or borders Myanmar, Thailand, Laos and Cambodia before finally draining in the Mekong Delta in Vietnam. Flow in the upper Mekong in China is mainly comprised of snowmelt, while precipitation from the two monsoon systems provide the bulk of the flow in the lower Mekong [*Ringler*, 2001]. Around 70 million people depend upon the Mekong River for food, water and economic sustenance, and the basin is home to several diverse and productive ecosystems. The Tonle Sap lake, among the most productive ecosystems in the world [*Bakker*, 1999], is an example of the unique ecology and biodiversity in the basin. Agriculture accounts for about 80-90% of total freshwater consumption in the Mekong [*MRC*, 2002], with rice being the most widely grown crop. The Mekong Delta is another hot spot of economic activity and produces approximately half of Vietnam's annual rice harvest and over half of Vietnam's fish exports [*Kite*, 2001]. The Mekong is currently in a phase of rapid infrastructure development (storage and hydropower) raising concerns regarding the downstream ecological impact [*Urban et al.*, 2013].

The Mekong was spatially delineated into 12 distinct hydrologically similar agents who make water management decisions to satisfy their own targets. Figure 10 shows the distribution of the agents across the basin and the locations of major existing and planned water infrastructure facilities, and important ecological hotspots identified by local ecological experts. In total, there are 19 major dams (7 existing and 12 planned) and 23 ecological hotspots identified by local ecological experts using existing literature. To allow for a more intuitive interpretation of results, here we only model crop production for irrigated rice, but the modeling framework allows for incorporation of any number of crop types. The modeling structure allows for simulations under either existing water infrastructure or future conditions that also include under construction dams. For demonstration purpose, we present results under future water infrastructure.

A SWAT hydrology model was developed, calibrated and validated with streamflow data from 1978 to 2007. Details on model setup and calibration and validation results for the hydrology model are provided in Appendix B. In addition, Fig. 63 in Appendix B shows simulated average hydropower generation under historic streamflow conditions and compares it with the observed hydropower generation for five existing reservoirs during the period of comparison as validation for the ABM.
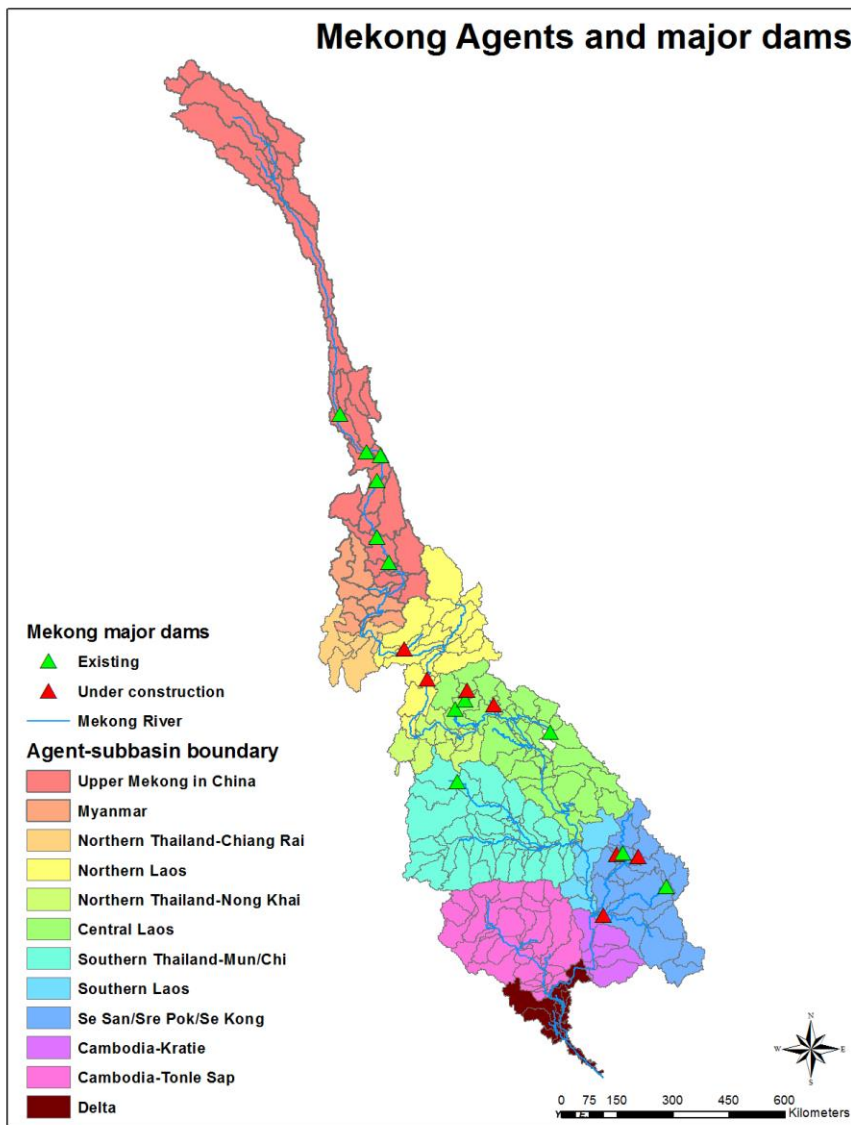
Figure 10: Basin map for the Mekong River Basin showing agent boundaries and major dams included in the model

Figure 11 shows an example of how total crop production (of irrigated rice) changes over the simulation period with different assigned priority (lowest vs highest) for agriculture for the agent representing Southern Laos. Both these simulated crop production time series are run with the same hydrologic time series, so the differences between the levels of crop production are caused by different water management actions. Over the simulation period of 25 years, there is a significant cumulative difference in agricultural production largely because of the compounding effect of increasing irrigated area whenever the crop production target is not met. When agriculture is assigned a lower priority, the agent prioritizes either hydropower generation or ecosystem health and is less likely to make decisions to increase agricultural production.
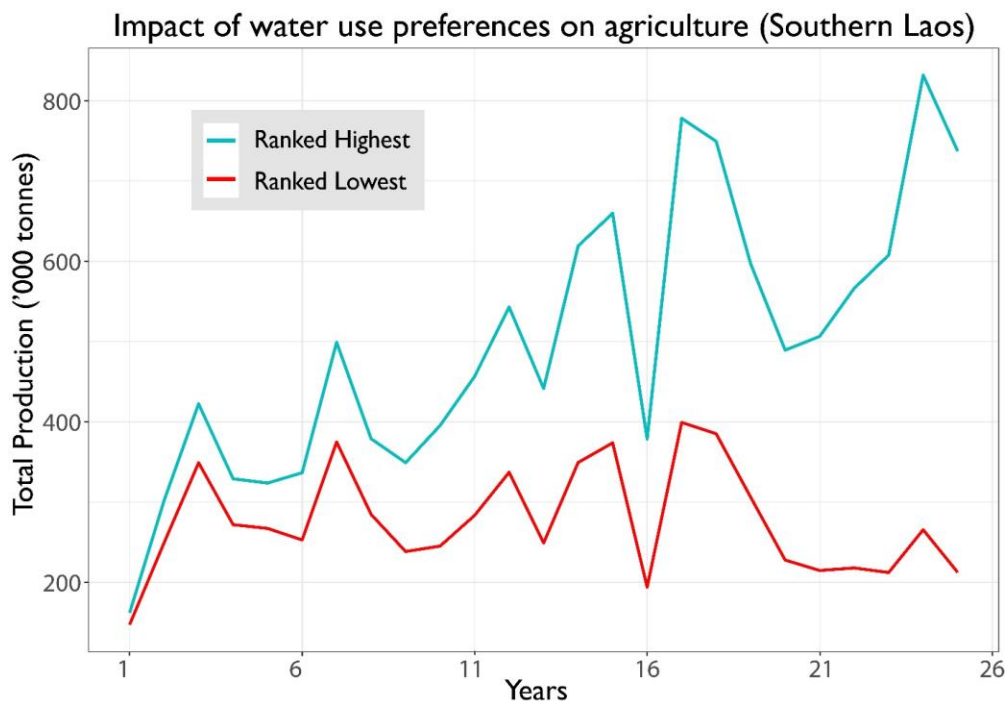
Figure 11: Difference in crop production caused by differing prioritization of agriculture for the Southern Laos agent

Different ecosystem services respond differently to changes in external drivers, depending on the nature of water use. Figure 12 shows a comparison of the effect of different priorities on hydropower generation for the Nam Theun 2 dam in the agent representing Central Laos. As in

the previous example, both the simulated time series are run with similar hydrology to isolate the difference in hydropower generation due only to different agent behavior. For this model, if simulated hydropower generation is less than 90% of historic (for existing dams) or expected (for future dams) mean annual energy, the agent can decide to change its operation rules for the dam to increase hydropower generation. In this model specifically, agents do so by increasing the minimum monthly releases from their reservoirs.

The fluctuations in HP generation from year to year are caused by changes in hydrology, while the differences between the blue and red lines represents the agent preference regarding the relative importance of hydropower. We observe that the annual fluctuations in hydropower generation (due to hydrology) are significantly greater than the slight changes in generation stemming from modified reservoir operations. Time steps with high streamflow conditions lead to very similar outcomes regardless of preference. The difference is more prominent in low-flow conditions where a higher prioritization of hydropower leads to an increased 'minimum' level of hydropower. Despite the fact that the difference between hydropower generation due to a change in prioritization is not as significant as that for the agricultural production, annual differences in hydropower generation can be as high as 8% (210 GWh). In the context of energy shortages in the Mekong, this difference is non-trivial. Another interesting feature to note in Figure 13 is that when the agent decides to increase releases in a time step for larger hydropower generation, generation in the next time step is reduced because of reduced storage. The emergence of this myopic behavior pattern also gives us confidence in the model as it replicates how hydropower generation decisions are made in the real world.
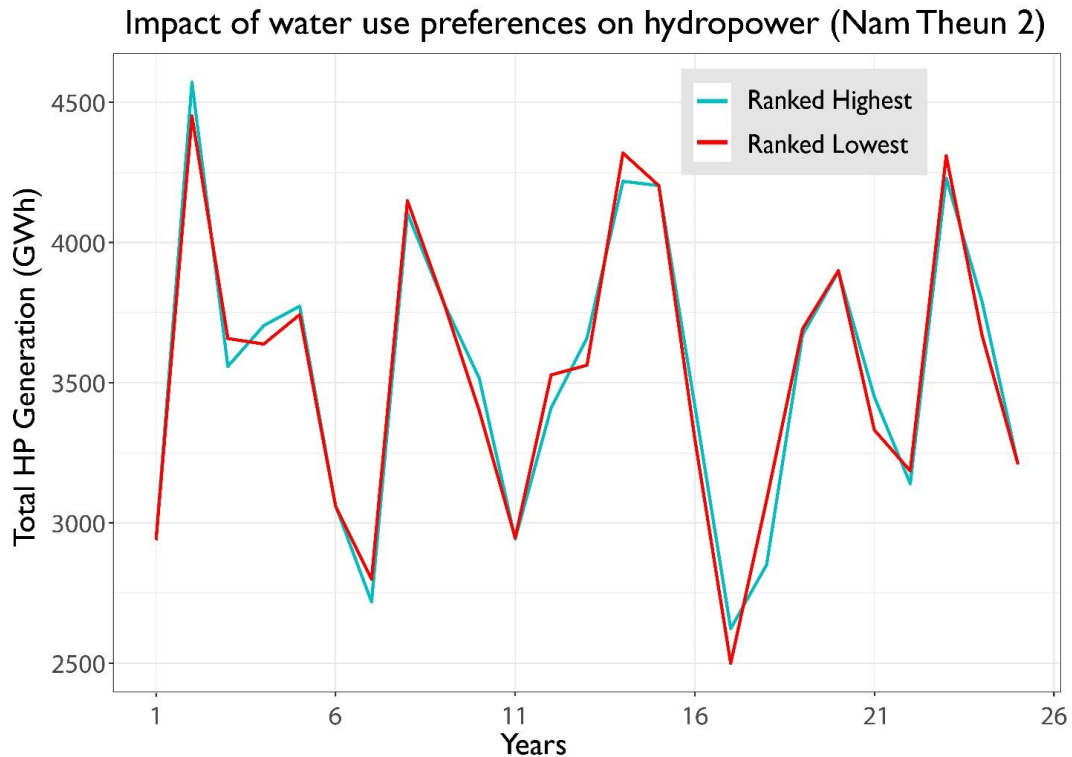
Figure 12: Difference in hydropower generation due to different importance ranking for hydropower for Nam Theun 2 reservoir

Finally, we also investigate the impact of changing priorities on ecologic performance. For each of the 23 hotspots, relevant indicators of ecologic health using the IHA and EFC framework are identified. As explained previously, agents can protect ecological health by choosing to limit water management actions for other water uses (agriculture and hydropower). Simulation results for this model showed that different agent preferences do not have a significant impact on ecological violations. The amount of water available (hydrology) has a much more pronounced impact. A reason for the lack of the negative impact of changes in reservoir operations on ecological performance are that reservoir capacities are low relative to streamflow. It is important to note here that the eco-hydrological indicators we used in the current modeling framework do not account for fish migration patterns and sediment transport, which are among the biggest concerns about hydropower in the Mekong. Future studies can link the current framework with more complex ecological models to address these concerns.

3.4.2 Impact of Agent Cooperation – Niger Demonstration

To illustrate the system-wide impacts of varying level of agent cooperation, we apply this generalized ABM framework to the Niger River Basin. The Niger River drains an area of over 2 million km^2 spanning nine riparian countries in West Africa, making it the ninth largest river basin globally in terms of area. The Niger River is spread across a wide range of ecosystem zones, and the basin is thus notable for its high spatial and temporal hydrologic variability on interannual and decadal scales [*Ghile et al.*, 2014]. Based on GDP, all nine countries of the Niger Basin fall in the bottom quartile of national incomes [*Ogilvie et al.*, 2010]. Agriculture constitutes a large part of the economic output for the region (approximately 33%), with livestock and fisheries also contributing substantially in some areas [*Welcomme*, 1986]. Owing to a lack of a well-developed irrigation system, most of the agriculture in the Niger is rainfed with only 20% of available arable land under cultivation. Investment into water resources infrastructure and institutions offers a potential pathway to economic development for the basin population and several large dams are slated for construction under the existing Niger Basin Authority investment plan. However, the downstream impacts of upstream infrastructure have become a contentious issue.

For the Niger Basin, fifteen agents were identified based on hydrologic characteristics and administrative boundaries. A map of the system showing the agent and subbasin boundaries, and existing and planned water infrastructure is provided in Figure 13. Nineteen ecologic hot spots identified by local ecological experts using the Niger Basin Atlas [*Aboubacar*, 2007], and ten dams (six existing + four planned) are included in the model. For the agricultural module, we simulate irrigated rice and upland crops. A SWAT hydrology model was developed, calibrated and validated with streamflow data from 1985 to 2010. Details on model setup and calibration and validation results for the hydrology model are provided in Appendix B.
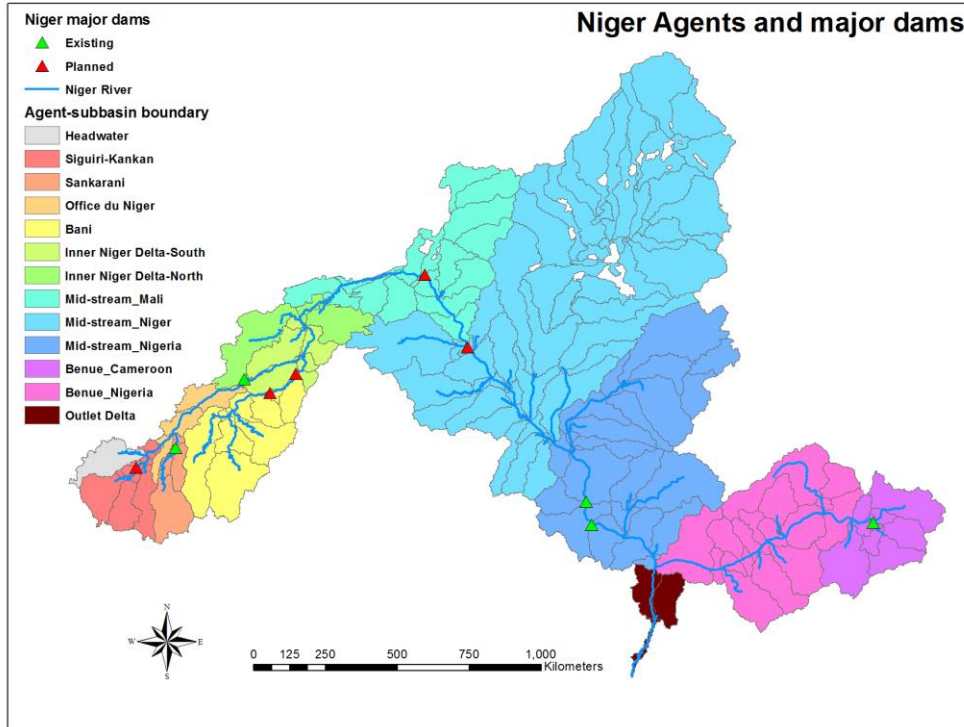
Figure 13: Basin map for Niger River Basin showing agent boundaries and major dams included in the model

We run this model under two different settings and then compare the results to evaluate the basin-wide impacts of cooperation between agents. In the first setting, agents make water management decision solely to satisfy their own objectives without interacting directly with other agents. In the second setting, agents' decisions are driven by both their own objectives, and their willingness to cooperate with other agents. Willingness to cooperate, represented in the model with the level of cooperation parameter (LOC), can be set on a scale of 0 to 1 and signifies the probability of an agent responding favorably to a request from another agent to alter its water management decisions. In this model, agents with reservoirs respond to a downstream request by increasing the minimum flow if storage in the reservoir is above the target storage. For the purposes of demonstration, we set the LOC for agents to 1 to simulate a fully cooperative environment. Both model runs are made with the same set of agent preferences. To illustrate impacts of future

infrastructure development, we run both the simulations under the future state of water infrastructure.

Over the course of the 26-year simulation period, we observe 73 instances of agents requesting help successfully, with many of these requests made during low-flow years. We see that additional releases from an upstream agent willing to cooperate can often, but not always, result in an appreciable increase in crop production compared to when the agents are solely interested in satisfying their own objectives. For example, in year 20 of the simulation, the Outlet Delta agent successfully requests the upstream Jebba reservoir for additional water releases, and experiences an increase in food production of almost 50,000 tons without any decrease in production in the upstream agent.
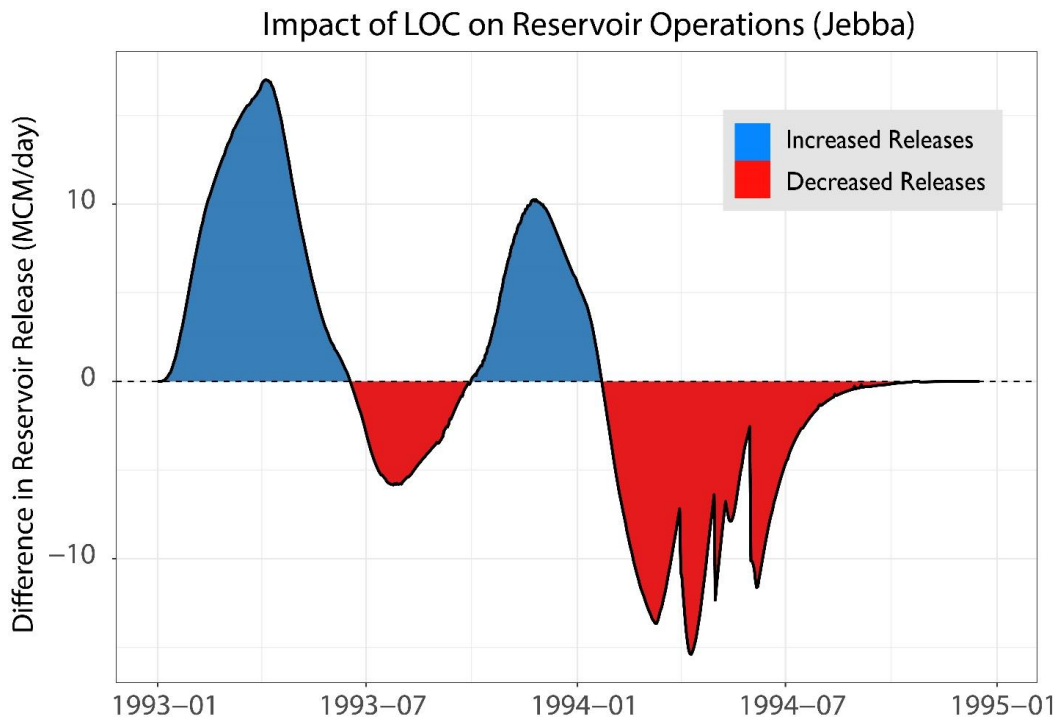
Figure 14: Change in reservoir release caused by the agent's willingness to cooperate with downstream agents. Area in blue (red) represents additional (reduced) water released compared to model runs where agent does not cooperate

Figure 14 and Figure 15 illustrate the changes in reservoir operation and its impact on streamflow downstream when an upstream agent decides to cooperate. For Jebba reservoir, Figure 14 shows the difference in reservoir releases between the 'cooperation' and 'no cooperation' runs, the blue region representing the additional volume that is released based on the decision of the agent to cooperate. Figure 15 shows the available streamflow downstream of the dam under both the simulation scenarios: the red line indicates releases when the agent alters its reservoir operations in response to the request while the blue line shows releases in the model where the agents do not cooperate. It is interesting, but not surprising to note, that additional water released leads to reduced releases in subsequent time steps due to reduced storage.
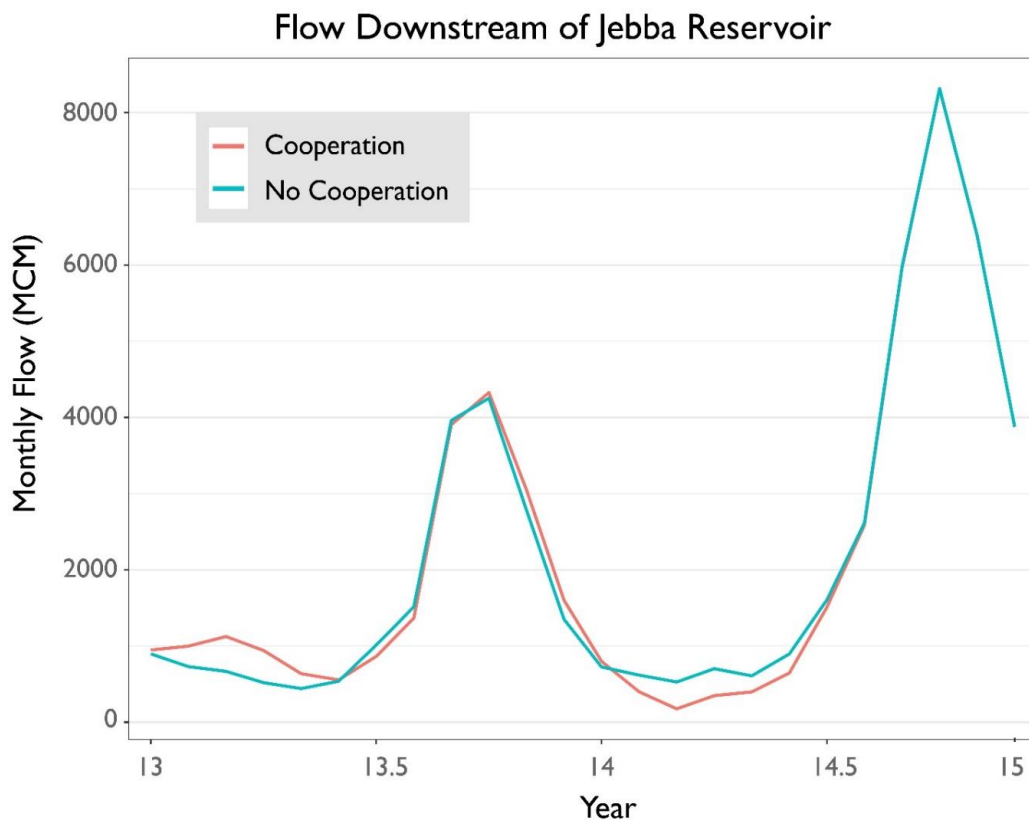
Figure 15: Comparison of monthly streamflow immediately downstream of Jebba reservoir between model runs when agent decides to cooperate and when it does not cooperate.

This change in timing of water availability has the potential to both negatively and positively affect all downstream users, including those that were not part of the negotiation that lead to the altered water management action (i.e. "third party impacts"). The occurrence of third party impacts is dependent on the context; they do not necessarily occur every time, and if they do occur, they can be either positive or negative. In these modeling runs, we observe many instances of varying third party impacts. For example, in response to consecutive years of reduced agricultural production, the Niger Inner Delta (South) Agent requests the upstream Fomi dam for additional releases in year 13 of the simulation. The agent managing Fomi Dam, Siguiri-Kankan, agrees to the request and increases its minimum releases. Not only does crop production in Niger Inner Delta (South) increase as a result, but crop production in Niger Inner Delta (North) is also positively impacted. However, the Office Du Niger Agent suffers from a decrease in food production.

It is pertinent to note here that additional releases do not necessarily increase crop production; it is possible that there are constraints other than water availability that are limiting crop production. In the same year of the simulation as the previous example, the agent representing Mid-stream Niger requests additional releases from Touassa Dam and experiences an increase in crop production. Crop production in the mid-stream does not change appreciably as a result; however, production in another downstream agent, Mid-Stream Nigeria is increased. In the current model, agents make requests when they are unable to meet crop production targets. However, the modeling framework allows for making requests dependent on other factors (e.g. ecological needs).

These third party impacts, also referred to as *externalities* in the natural resource economics literature, are also seen in ecologic performance. The nature and magnitude of third party impacts

on ecologic performance is dependent on the specific ecosystem. Arguably, ecologic health is even more sensitive than agricultural production to changes in the timing and magnitude of streamflow. In these simulations, we see evidence of this impact. In year 9, in response to a request from Mid-Stream Nigeria, Kandaji reservoir releases additional water that (compared to the no cooperation setting) positively affects the ecosystem hotspots in Mid-Stream Niger and Mid-Stream Nigeria, but results in increased violations of ecological targets in the downstream Outlet Delta. In particular, the ecological parameter seen to be violated is the IHA parameter for minimum average 7-day flow. Despite the increase in total annual flow due to the additional releases, the change in the flow timing leads to an ecologically inferior outcome for the Outlet Delta. This finding supports the argument that evaluations of ecological health performed at coarse time scales (e.g. annual) may overlook finer time-scale flow parameters that are critical to ecosystems [*Palmer et al.*, 2005]. In the absence of detailed data relating flow conditions to aquatic health in the Niger Outlet Delta, it is difficult to ascertain the exact impact that the violation of this target would have on the delta's ecosystem.

3.5 Discussion: Dynamic Coupled Natural Human Systems Modeling

The generalized coupled modeling framework presented in this paper adopts many of the principles from the Shared Vision Modeling (SVM) approach [*Palmer et al.*, 2013]. To improve allocation of scarce resources across competing uses, it is crucial to understand the values placed on various water uses by stakeholders in the watershed. For the case study applications, model development was preceded and followed by extensive stakeholder engagements. Before the model development began, an electronic survey of water users in each of the river basins was conducted to analyze perceptions of the relative importance of different water uses. Rules derived from these

surveys improve representation of the interactions between heterogeneous subsystems. Moreover, to make this modeling framework more accessible for users, a web-based interface has been developed where users can perform model simulations with differently specified agent behavior rules [*Zhao and Cai*, 2017].

The online interface allows users to visualize and save results from several modeling runs. Information from the modeling runs made on the online platform can be used to further develop agent behavior rules and have stakeholders evaluate the results to gain insight into emerging development pathways in the basin. In addition to the utility provided by the visualization of the outcomes, the exercise of tailoring the modeling framework to a specific basin requires stakeholders to conceptualize the water system better. A beta version of the website with the model for the Mekong River Basin has been developed and tested with stakeholders in the Mekong.

Third party impacts, which are costs or benefits borne by a party due to the actions of others, have been recognized as an obstacle to promoting cooperative water management practices in a water system with many heterogeneous users [*Petersen-Perlman et al.*, 2017]. While the existence and importance of third party impacts is widely acknowledged, they are not easily quantified, making them difficult to incorporate in stakeholder discussions on water management in transboundary settings. The case study results for the Niger River Basin presented here quantify these third party impacts on agricultural production, hydropower generation and ecological performance. Quantification of the impacts, both positive and negative, of the actions of water users can help develop a shared understanding of the water system dynamics among stakeholders [*Skurray et al.*, 2012]. By offering a way to fully couple human and natural systems with several ecosystem services, with flexibility to incorporate varying levels of importance for heterogeneous

users, the modeling framework presented here can be useful as a tool to stimulate cooperative water management in transboundary settings.

3.5.1 Limitation and Future Work

The case study models developed use observed climate data to develop hydrologic time series for model simulations. Observed streamflow data are used for model simulations under the future infrastructure setting as well. However, significant uncertainty exists regarding future hydroclimatology and its impact on water resources in these basins [*Lauri et al.*, 2012]. A climate stress-test approach where the agent's response to varying hydroclimatological conditions is evaluated can provide insight into sensitivity to climate variables [*Brown et al.*, 2012].

Another useful extension of this modeling framework would be to incorporate seasonal forecasts of water availability into the decision-making process off agents. Water managers often perceive the advantages offered by seasonal forecasts as being low [*Pagano et al.*, 2002], even though the economy-wide benefits of seasonal forecasts can be substantial. This modeling framework can be used to highlight the potential benefits of short-term seasonal forecasts for agents' decisions on water allocation and willingness to cooperate with other agents, and introduce another dimension of stochasticity to the agent decision-making process. The seasonal forecasts used, however, would need to be geographically suitable and temporally appropriate for each agent's operations.

The development of coupled river basin models needs to carefully address several tradeoffs to ensure that the models are scientifically sound and computationally tractable. The focus of this work is to develop a generalized ABM framework that addresses model transparency and model/module reusability [*Parker et al.*, 2003; *An*, 2012]. To address this, the geographic

delineation of our agents are relatively larger than traditional agent-based models (which define individual water users as agents). This is a necessary simplification in order to balance model complexity (or the level of details of simulated decision processes) and computational resource and data availability. Furthermore, it is pertinent to recognize that agent based models are best used to explain existing relationships or phenomena, rather than as prediction tools. Another related limitation associated with large-scale agent-based models is reliance on informal validation. For the case studies presented here, we validate the ABM with internal checks, for instance by comparing modeled and observed hydropower generated (Fig. S4 in Appendix B). We also address this limitation through the use of surveys to inform agent behavior rules.

To further improve the agent decision module, Bayesian decision theory would be a useful avenue of future research to better address uncertainty of human decisions [*Van Oijen et al.*, 2011; *Kocabas and Dragicevic*, 2013]. However, this approach is computationally costly, especially in our setting with a variety of different agents, water use preferences and willingness to cooperate. High performance computing technology might become necessary for this purpose.

The coupled modeling framework described in this paper operates on an annual time step. This means that exchange of information between the ABM and SWAT takes place at the start of every year. The framework can be made more realistic by configuring the models to interact at the finer time scale at which water management decisions are made, i.e. monthly or weekly. While the modeling framework is sufficiently flexible to allow for a range of water management actions, in the modeling framework described here, we model ecological health management in a passive rather than active manner. Active ecologic health management, where the agents make specific decisions (especially with regards to reservoir operations) requires a more in-depth understanding

of the basin ecology than was available for either of the two transboundary rivers used as case studies for this paper.

3.6 Conclusion

Sustainable watershed management requires water managers and policy makers to have a clear understanding of their water system and its interactions with the natural environment. This study develops a spatially scalable, generalized agent-based modeling (ABM) framework consisting of a process-based semi-distributed hydrologic model, SWAT and a decentralized water system model to simulate the impacts of water resources management decisions on the food-water-energy-environment nexus (FWEE) at the watershed scale. The two-way coupling provides a holistic understanding of the FWEE nexus. A novel advancement offered in this framework is the ability of agents to *directly* interact by requesting assistance from other agents based on their level of cooperation (LOC). Quantification of the LOC is especially useful for transboundary river basins with several unique actors with different water management objectives. Among various other future uses, this modeling system has been developed for the CGIAR Research Program on Water, Land and Ecosystems to assess tradeoffs between agricultural production, productivity, other water-based ecosystem services and ecosystem health. To support non-technical stakeholder interactions in developing country settings, where CGIAR operates, a web-based user interface has been developed. This online portal allows for end-user role-play, participatory modeling and inference of prioritized ecosystem services and ecosystem health.

We show the flexibility of this modeling framework by applying it to two large transboundary rivers as case studies and demonstrate its ability to reveal the impact of water use preferences and willingness to cooperate on region-specific and basin-wide outcomes. In the case

studies, we see that agent preferences have a more pronounced effect on crop production compared to hydropower generation. Changing preferences has a relatively smaller impact on ecological health, but that is heavily dependent on the river basin, ecological health indicators and water management actions. Impact of agent cooperation revealed the presence of both positive and negative third party impacts that need to be acknowledged and accounted for when considering cooperative river management in transboundary settings, especially at finer time scales.

CHAPTER 4

EFFECTS OF SPATIAL AND TEMPORAL VARIABILITY ON PERFORMANCE OF GROUNDWATER MARKETS

4.1. Introduction

Water scarcity is recognized as the one of the most serious challenges facing societies globally [*World Economic Forum*, 2016]. Expected increases in population and living standards, especially high in the most water stressed countries, will further exacerbate water shortages and their impact on food and energy production. Discounting freshwater available in the polar ice caps, groundwater constitutes almost 90% of global freshwater, thus making groundwater resource management one of the most important, and critical, natural resource management frontiers [*Koundouri*, 2004]. With the increasing demands on surface waters, groundwater is also increasingly becoming the primary buffer against droughts [*Taylor et al.*, 2013]. However, in recent years, harmful impacts of unmanaged groundwater extraction have emerged. A recent analysis shows that storage in 21 of the 37 largest aquifers in the world has decreased over the past decade, with over a third severely depleted, threatening regional water availability [*Richey et al.*, 2015]

It is in this context of water scarcity and increased groundwater stress that calls for improved groundwater management have been made. One such example is the Sustainable Groundwater Management Act (SGMA) passed by the state of California in response to rapidly depleting groundwater resources [*Xiao et al.*, 2017]. The Law calls for improved groundwater management to ensure sustainable use of the resource and creates groundwater management districts to oversee the implementation, but leaves the particular approach to management up to the districts [*Nelson and Perrone*, 2016].

As is the case with surface waters, centralized governance approaches (also termed 'command and control') have traditionally been adopted for groundwater management globally, such as in the form of groundwater quotas [*Dinar and Wolf*, 1994]. However, in recent years, other more localized and decentralized policies have become increasingly popular as an alternative to the command and control approach. Increased community participation and engagement (Rangan 2016, Garduno et al 2009) has been shown to be particularly effective at mitigating problems arising from the common pool resource (CPR) nature of groundwater. Community management of groundwater can comprise of varying degrees of participation, ranging from simple one-directional provision of information (low) to governance structures where users determine and largely implement management policies (high) [Maheshwari et al 2014]. Along with an improved understanding of the system, community driven management efforts are more likely to result in improved compliance by resource users.

Markets for groundwater present another alternative approach to groundwater management. These markets can be formally instituted, with regulations and clearly defined governing bodies, or can be informal, where they emerge organically as a response to demand for water (often for irrigation purposes)(Easter, Rosegrant, Dinar et al). Informal groundwater markets are especially prevalent in areas with intensive groundwater use (for agriculture), weak governance and lack of capital to install tubewells. e.g. India, Pakistan (Shah et al 2005). In such places, 'spot' markets for groundwater exist where existing well owners sell water physically (Meinzen Dick 1998). A drawback associated with these arrangements is that without sufficient governance, this can lead to excessive groundwater abstraction since selling water is a profitable business by itself. In many other parts of the world with stronger institutional settings, formalized markets for groundwater have been introduced. This approach to groundwater governance uses economic

incentive-based policies, such as the cap-and-trade system, creating financial incentives (in the form of a price) for use of a resource. This paper uses the term groundwater market to refer to a cap-and-trade system for groundwater management. In a groundwater market, tradeable permits are either allocated or auctioned to allow users to access the resource. The total volume of available permits forms a cap on the total groundwater extraction with users allowed to trade the permits allocated to them. Nebraska [*Aladjem and Sunding*, 2015], Texas [*Johnson et al.*, 2009] and Australia [*Wheeler et al.*, 2013] are examples of regions where permit trading programs have been adopted for groundwater management.

While trading permits for groundwater use may lead to increased system-wide economic efficiency, the literature on such incentive-based approaches has simplified the actual context in which such interventions would be enacted, and consequently possibly overestimated their benefits. Groundwater systems are dynamic with aquifer characteristics (e.g. hydraulic conductivity), depth to groundwater and surface water-groundwater interactions varying spatially. This hydrogeologic variation in groundwater can lead to uneven distributional impacts in the absence of well-designed trading regulations [*Brozovic et al.*, 2010]. These uneven distributional impacts, amplified in low-transmissivity aquifers, can lead to drying of wetlands, streamflow reductions, or land subsidence. Possible economic benefits notwithstanding, the presence of uneven distributional impacts can make implementation of incentive-based policies challenging. Analysis of performance of groundwater markets, with the explicit intent of addressing distributional impacts has been rare [*Skurray et al.*, 2012]. Groundwater management policies cannot be meaningfully evaluated if the models used do not realistically simulate hydrogeologic conditions. To represent the spatial and temporal heterogeneity in groundwater conditions across

a region, models for groundwater markets need to be supplemented with physically based hydrogeologic models [*Mulligan et al.*, 2014].

In addition to the need to address spatial variation, possible temporal variation caused by future changes in climate need to be addressed in groundwater market designs [*Loch et al.*, 2013]. Climate variability and change can impact groundwater directly, mainly through changes in temperature and precipitation, and indirectly, through change in irrigation-water demand due to reduced surface water availability. A thorough investigation of the sensitivity of a market to changes in climatic conditions can provide useful insight to policy makers regarding appropriate market design to optimally adjust for changing conditions. Sustainable groundwater management that addresses these changes needs to be informed by integrated models that are able to incorporate the interactions between surface water, groundwater and human activity [*Taylor et al.*, 2013].

This work builds upon the growing literature on distributional impacts of incentives-based groundwater management policies. We compare the economic and environmental performance of an incentives-based policy (i.e. groundwater market) with a command and control approach (water quotas) under climate change and hydrogeologic heterogeneity. We quantify the distributional impacts associated with groundwater trading with a physically based groundwater model. This study systematically evaluates climate change impacts on groundwater dynamics and the resultant impact on groundwater trading through a stress testing approach (Brown et al 2012). We develop a stylized example of groundwater use in the Republican River Basin, overlying the Ogallala aquifer in the High Plains of the United States, as a case study. We develop a multi-agent system model where individual benefits of each self-interested agent are maximized subject to bounds on irrigation requirements and water use permits. This economic model is coupled with a calibrated physically based groundwater model for the study region. Section 2 provides a review of the

current literature on models for groundwater management, Section 3 details the methodology for the models, Section 4 presents and discusses the modeling results, limitations and future research opportunities are presented in section 5 followed by a conclusion.

4.2. Literature Review

Groundwater management has been identified as one of the major natural resource management challenges of the 21st century, especially in the context of climate change [*Gorelick and Zheng*, 2015]. Effective groundwater policies need to be instituted within a quantitative framework. Initial quantitative analyses evaluating the efficacy of groundwater policy instruments represented groundwater using single cell or 'bath tub' models [*Feinerman and Knapp*, 1983]. This assumption implied that the aquifer is unconfined, bottom-less, and has an infinite hydraulic conductivity; it also ignores spatial heterogeneity. Prominent in these studies was *Gisser and Sánchez* [1980] who showed that for an aquifer with relatively large storage capacity, there is very little difference in welfare losses between optimal groundwater allocation and free market competition. However, subsequent studies assessing the validity of their findings [*Knapp and Olson*, 1995] found that a significant difference did exist between groundwater extraction under optimal control and unregulated competition [*Brill and Burness*, 1994; *Brown et al.*, 2006]. More recently, work by *Brozović et al.* [2010] has shown that ignoring the spatial heterogeneity in an aquifer significantly affects welfare gains from optimal management and *Mulligan et al.* [2014] showed similar impacts for use of price and quota-based management interventions. Recognition of the importance of realistically capturing groundwater dynamics spurred interest in economic studies that model aquifer as multi-cell basins, with varying spatial resolution [*Katic and Grafton*, 2012].

A growing body of literature highlights the importance of accounting for spatial heterogeneity while evaluating groundwater policy. Using irrigation well level data, Palazzo and Brozovic [2014] demonstrate the effects of heterogeneity (both in farmer behavior and aquifer characteristics) on economic outcomes of groundwater management policies. Building on this work, Guilfoos et al [2017] present a framework coupling an economic model (representing a groundwater market) with to assess performance of policies in the context of a dynamic system with significant heterogeneity. Their findings further emphasizes the importance of accounting for hydrologic and economic differences between groundwater users by showing the large welfare losses accrued if these differences are ignored. More recently, there have been efforts to further improve the representation of the hydrogeology through the use of physically-based groundwater models that are able, among other things, capture the dynamic streamflow-aquifer feedback and more holistically quantify groundwater pumping drawdown effects. . Some of these studies have used optimization models coupled with physically based groundwater models [*Yu et al.*, 2003; *Reeves and Zellner*, 2010]. *Mulligan et al.*, [2014] compare the economic and environmental performance of an idealized groundwater market with taxes and caps on groundwater use. They find that optimal allocation through the idealized market leads to reduced environmental impacts and increased economic benefits. In another study, *Bauman et al.* [2015] address the heterogeneity in users by using multi-objective optimization to model 'imperfect' surface water trading between agricultural, municipal and industrial users having different objectives in the Western US. In an attempt to model a more realistic water market, the authors incorporate transaction costs and find that these costs noticeably reduce economic efficiency and highlight their distributional impacts. This work however, does not incorporate any physical representation of the hydrology or account for groundwater use.

More recently, groundwater management models that minimize externalities resulting from groundwater use have been developed. Smart water markets provide an avenue for optimal management of groundwater to control the externalities resulting from groundwater overuse. These markets are essentially electronic clearinghouses simultaneously matching many buyers and sellers using optimization algorithms that combine the advantages of decentralized permit ownership with the coordination advantage of central processing [*Murphy et al.*, 2000]. In theory, not only can smart water markets account for spatial heterogeneity, they can also mitigate distributional impacts and environmental externalities that result from over use of a common property resource such as groundwater. Using groundwater irrigation in Marlborough, New Zealand as a case study, *Raffensperger et al.* [2009] show that smart water markets can increase the reliability of environmental flows and reduce transaction costs and users' risk. The Twin Platte Natural Resource District in Nebraska, recently became the first region to establish an exchange of groundwater use permits via a smart water market [*Young*, 2016].

Not only does market design need to account for spatial heterogeneity, but it also needs to be robust to temporal variation, most notably future changes in climate. The impact of climate change on groundwater has received much attention recently [*Green et al.*, 2011; *Treidel et al.*, 2012]. Climate variability and change can impact groundwater directly, mainly through changes in temperature and precipitation, and indirectly, through change in irrigation-water demand due to reduced surface water availability. Due to the high uncertainty in GCM projections, particularly those for future precipitation, the impact of climate change on groundwater systems is uncertain [*Döll and Fiedler*, 2008]. Global analyses on the effect of climate change on irrigation demand project increased groundwater irrigation requirements in almost 70% of irrigated area globally

[*Döll*, 2002]. In addition to the effect of mean changes in climate, changes in daily rainfall distributions are also posited to affect recharge in some aquifers [*Crosbie et al.*, 2013].

Water markets have been proposed as one of the solutions to offset the differential impacts of climate change. Existing literature and past evidence, primarily from Australia, suggests that markets for surface water are effective in mitigating effects of a drier climate [*Beare & Heaney*, 2002; *Loch et al.*, 2013]. A review of water markets in the Murray Darling Basin (MDB) in Australia documents the increases in efficiencies brought about and concludes that water markets helped the water use structure in the country to adjust to changing climate conditions and was effective at reducing total economic impacts and production losses [*Wheeler et al.*, 2013]. A review of existing literature suggests that while studies have attempted to evaluate the impact of climate change on surface water markets [*Jiang and Grafton*, 2012; *Marchlik*, 2014]], an assessment of the impact of future changes in climate on groundwater market dynamics has not been performed.

4.3. Methodology

This study extends the analysis performed by *Mulligan et al*, [2014] comparing the performance of optimal water allocation and free market access under different groundwater policy instruments. This analysis aims to (1) evaluate the differential effects climate change on performance of groundwater markets and non-tradeable water quotas, (2) quantify the uneven distributional impacts that result from an imperfectly designed groundwater market, and (3) compare the economic and environmental performance of non-tradeable water quotas to a realistic groundwater market. To do so, we modify the economic optimization agent-based model developed by *Mulligan et al*, [2014] to incorporate groundwater permit trading between users, and couple it with a calibrated physically based groundwater model. The models are linked through

the agent's groundwater pumping decision (optimized decision variable in the economic model) which is then input to the groundwater model to calculate updated groundwater levels and streamflows, which affects subsequent pumping decisions. The coupled model is run under scenarios with varying agent characteristics, groundwater allocations and climate conditions.
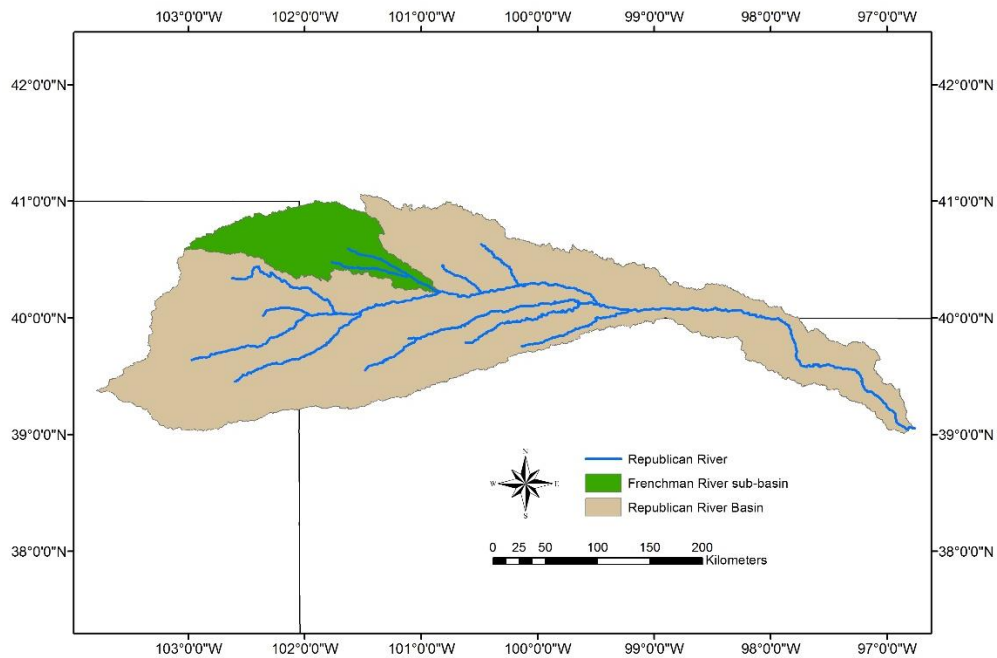
Figure 16: Study region for the analysis overlying the High Plains aquifer

4.3.1. Study region: geography (location, area), agriculture, climate

As a case study for this coupled modeling framework, we develop a stylized example of agricultural water use in the Frenchman River sub-basin. Spanning 2,900 square miles across Nebraska and Colorado, this subbasin is located in the northwest corner of the Republican River Basin, as shown in Figure 16. The Republican River Compact Authority (RRCA), established in 1959, oversees allocation of state water rights in the Basin. The Upper Republican Natural Resources District (NRD) within Nebraska, overseeing implementation of water management policies, spans most of the Frenchman River Basin. Most of the crop water requirements are met

with groundwater, with conjunctive water use rarely practiced in the study area (Palazzo and Brozovic 2014). Overlying the Ogallala aquifer (also known as the High Plains aquifer), the Republican River and the groundwater flow eastward. Climate in the Frenchman River subbasin can be classified as semi-arid, with average annual precipitation of 32 inches. Irrigation accounts for approximately 95% the total groundwater use in the region [*Rodell and Famiglietti*, 2002]. Intensive groundwater pumping in this region, primarily for agricultural purposes, is well documented and has been the subject of many investigations [*Sophocleous*, 2005]. The increase in large-scale pumping has led to reductions in streamflow and a rapidly depleting groundwater table in some parts of the basin, emphasizes the need for improved groundwater management [*Scanlon et al.*, 2012]. The study area is one of the few areas in the United States to have well quantified and enforced groundwater rights, stemming from a need to limit transboundary streamflow impacts on neighboring states. The impact of groundwater pumping on the surface water-groundwater interaction is the primary focus of management efforts in Nebraska and Kansas.

Transaction costs can be an important determinant of the effectiveness of water markets [*Howe et al.*, 1990; *Garrick and Aylward*, 2012], and should be addressed when evaluating the performance of a market. High transaction costs create significant lags in permit transactions [*Neuman*, 2004], and have been identified as a barrier to successful implementation of market-based water allocation [*Colby*, 1990]. For our study region, Palazzo and Brozovic (2014) make a case for why transaction costs in this region would expected to be low. Among their reasons they cite (i) the existence of some water trading without a formal market, suggesting potential gains from trading are greater than transaction costs; (ii) already completed certification of irrigated area which clearly defines and quantifies groundwater rights (iii) comprehensive well metering and

enforcement and monitoring of groundwater pumping making efficient trading more likely. For these reasons, we do not include transaction costs as part of this analysis.

4.3.2 Groundwater model

The calibrated MODFLOW groundwater model used in this study was developed by the RRCA to assist with water allocations stipulated in the Republican River Compact [*Republican River Compact Administration*, 2003]. We briefly mention the salient features of the calibrated model here; detailed explanation of the model input and setup can be found in the model documentation. The simulation model runs under a monthly stress period with a bi-weekly time step and contains approximately 30,000 active rectangular grid cells, each 1 square mile in size. Monthly averages for precipitation and temperature over time 1950-2000 are used to calculate the baseline climatic inputs (recharge and evapotranspiration) for the simulations. Observations from 34 rain gages and 3 climate stations across the modeling domain are interpolated to assign precipitation and temperature values to each grid cell. Recharge from precipitation at each grid cell is determined using a recharge versus precipitation curve developed by the RRCA for different soil types across the basin, while area weighted evapotranspiration rates are calculated based on the Hargreaves method for each grid cell. For phreatotype vegetation, the Hargreaves method with appropriate equivalent crop coefficients is employed. For crop irrigation requirements, the Hargreaves equation is calibrated to the Penman-Montieth equation. For this analysis, while the simulation model for the entire Republican River Basin is run, pumping decisions are updated for grid cells only in the Frenchman River. Pumping rates for cells outside of the Frenchman River subbasin are fixed at the flow rates for the latest year (2000) available in the RRCA model. Groundwater levels at the end of the simulation run from 1918-2000 from the original RRCA

model are used as the starting hydraulic heads for this analysis. The River package in MODFLOW is used to simulate the interaction between groundwater and surface water. Changes in groundwater head (resulting from the various groundwater fluxes) have an impact on the rate and direction of flow between groundwater and surface water (streamflow).

4.3.3 Agent-based model: agent characteristics

Agent characteristics in the Frenchman River subbasin as used by *Mulligan et al.*, [2014] are used in this study and briefly summarized here. Using model reduction methods, pumping wells across the Frenchman River Basin are clustered into fifty agents of varying sizes based on the similarity of stress imposed on the groundwater system [*Mulligan and Ahlfeld*, 2016]. Each agent represents a farmer; the same agent delineation is used throughout the different model formulations and scenarios. Each agent makes two decisions: which crop to grow, and how much to grow subject to constraints on land and water availability. These decisions determine the amount of water the agent must pump. In this modeling framework, the agents can choose between soy and corn, the two crops representing the majority of agricultural production in the region. Productivity of agents is determined by two key parameters: crop yield and crop irrigation requirements. Five different sets of values for these parameters are developed to sufficiently randomize agent characteristics such that model results are not impacted by the uncertainty associated with agent productivity.

Groundwater irrigation requirements are calculated after accounting for effective precipitation. For each precipitation change considered, we calculate the effective precipitation (rainfall that can be used for irrigation). The balance water requirement for the crops is met with groundwater irrigation. The deficit irrigation strategy adopted in this model assumes that the

farmer adjusts the amount of irrigated land based on the pumping decision. If the farmer is constrained below the required irrigation depth for his/her land, the model allows the farmer to increase irrigation depth above the regulatory limit on a subset of the irrigated area, while at the same time reducing total irrigated area and increasing dryland area. For instance, consider a farmer who possesses 50 acres of land and requires 10 inches of water for corn. Due to regulatory or economic constraints, the farmer decides to use only 5 inches of water for corn for a given season. Then, the model allows the farmer to apply 5 inches of water to half of the 50 acres, such that the 25 acres will be irrigated with 5 inches of water for corn while the other 25 acres remain unirrigated. This farmer behavior is also adopted by Palazzo and Brozovic (2014) for a similar study of groundwater trading in our study area.

4.3.4   Agent-based economic model formulation

The agent-based economic model is described in the two sections below. In the first section, design of the 'baseline' model in which agents maximize individual profits subject to fixed constraints on water usage (allocated groundwater quotas) is provided. In the second section, we describe the changes made to model design to introduce trading between agents.

4.3.4.1 Decentralized optimization with fixed quotas

In the agent-based economic model, for each agent there is an objective function in which individual profits are maximized. The objective function shown in equation (1) below contains all revenues and costs faced by the agent. Table 1 provides definitions for the different variables. The total costs faced by each agent is the sum of energy costs for groundwater pumping and operating costs. The total revenue for each agent is a function of the amount of crop produced (determined

71

through a linear crop production function) and the crop price. For model runs in which agents are allowed to trade water allocations (groundwater market), the revenues/costs of trading allocations are added to the objective function. The constraint in equation (2) bounds the pumping to limits on available land area and crop irrigation requirements. The constraint in equation (4) limits pumping to the allocated groundwater quota.

Maximize

$$\sum_{c=1}^{N}\left\{\left[\frac{p_c y_{a,c} d}{w_{a,c}} - \frac{h_{a,s}\gamma_w p_e d}{e} - \frac{f_c d}{w_{a,c}}\right] Q_{a,c,s}\right\} \qquad (1)$$

subject to

$$0 \leq \sum_{c=1}^{N} Q_{a,c,s} \leq Q_a^u \qquad (2)$$

$$Q_a^u = max_c \frac{A_a w_{a,c}}{d} \qquad (3)$$

$$\frac{d \sum_{c=1}^{N} Q_{a,c,s}}{A_a} \leq CAP \qquad (4)$$

Each model run has a 50-year time period, with each agent's decisions optimized each year. The optimization is carried out using the Active-set optimization algorithm in the R programming language. For each agent, the decision variable that is optimized is the amount of groundwater to pump at the start of the cropping season subject to constraints on water allocated and land available. Based on groundwater use in the previous year, updated depth to groundwater for each agent is calculated at the beginning of each cropping season. The depth to groundwater determines the pumping costs for each year. Return flows are assumed to be 20% of pumping volumes, with a pumping efficiency of 70%. Overhead costs (excluding real estate rental values and taxes), based on the 2016 crop budget reports for corn and soybean range between 4%-9% of total costs. Hence, these fixed costs are not included in the objective function.

Table 1: Variables used in the agent-based economic model

Variable	Definition
$Q_{a,c,s}$	Flow rate decision variable (L^3/T)
Q_a^u	Upper bound for flow rate
a	Agent (well site)
s	Pumping season
c	Crop
N	Total number of crops
A_a	Maximum land area (L^2)
CAP	Water use cap (L)
p_c	Selling price of crop c ($)
$y_{a,c}$	Crop yield (bushel/L^2)
d	Pumping duration (T)
e	Pumping efficiency
h	Total lift (L)
γ	Specific weight (F/L^3)
$w_{a,c}$	Crop irrigation requirements (L)
p_e	Electricity price ($/P-T)
f_c	Farm operating costs ($/$L^2$)

4.3.4.2 Groundwater market formulation

To model a groundwater market that allows agents to trade allocated permits, we use the penalty-based decentralized optimization algorithm proposed by *Yang et al*, [2011], represented by equation (5).

$$\max F_i (x_i, p_i | w_i) = \max[f_i(x_i) - p_i(x_i - w_i)] \qquad (5)$$

Where x_i represents the water used, p_i represents the water price, w_i represents the water use permit for the agent, and $f_i(x_i)$ represents the water use benefit. As in the formulation described previously, the model assumes that all agents maximize water use benefits. In the formulation described above, a positive (negative) difference between x_i and w_i, i.e. $x_i > w_i$ ($x_i < w_i$) represents the amount of water an agent is willing to buy (sell) at the given price.

The algorithm for determining the price of water for a particular water use cap is as follows:

For each level of groundwater quota, the total water usage by each farmer in the absence of trading is determined. (This is the average annual groundwater used by the farmer when the particular cap is in effect).

The sum of all water usages under a particular cap, A_c, is used to constrain the algorithm and ensure that the solution from the price loop is feasible.

The solution algorithm starts with $p_i = 0$ at which all the agents use all the water that they can possibly use because selling permits is not economically advantageous. However, this results in water usage greater than the allowable A_c. This situation, although unrealistic, allows the numerical search loop to find an initial solution through which the price of water can then be increased to reach an equilibrium between A_c and groundwater extracted.

The price of water is incrementally increased until equilibrium is reached.

The system reaches equilibrium and the algorithm stops when the sum of the modeled water use approaches the sum of the water use permits (A_c, i.e. $\sum x_i = \sum w_i$).

This groundwater market setup assumes that all agents have equal access to buying groundwater permits and hence all agents face a uniform equilibrium water price. While all agents face a uniform equilibrium water price, each agent will have a unique marginal value of water owing to the spatial heterogeneity in aquifer conditions. The use of the physically based groundwater model helps indirectly capture the effect of this heterogeneity on each agent's marginal value of water.

4.3.5 Scenario analysis

The coupled economic and groundwater model are driven with different combinations of water allocations, temperature and precipitation changes to illustrate their respective impacts on

the two groundwater management policy approaches. Six different groundwater allocations, in terms of inches per unit area (depth), indicating varying levels of water scarcity are used to compare the performance of water quotas and groundwater markets. Water allocations are assigned uniformly for all agents.

As part of this study, we perform a climate stress test, which systematically perturbs the climate inputs to test the sensitivity of the system to precipitation and temperature [*Brown et al.*, 2011]. In our modeling framework, changes in precipitation affect groundwater directly by altering the aquifer recharge and net irrigation requirements; it affects groundwater indirectly through changes in streamflow and thus baseflow. Changes in temperature affects the evaporation from shallow groundwater and crop evapotranspiration, ultimately affecting irrigation requirements.

The ranges for the climate perturbations, relative to historically observed climate, are informed by the range of changes projected for the study region in the Fifth Coupled Model Intercomparison Project (CMIP5) GCMs. Projections of future climate for this region suggest an increase in mean temperature, and display significant uncertainty in precipitation changes. Precipitation is varied from -30% to 30% of historic average with 15% increments and temperature from 0 to 4º C with 1 degree increments. Climate shifts are applied to the baseline precipitation and temperature assigned for grid cells in the modeling domain uniformly across space and time. The updated climate inputs are used to calculate the precipitation recharge and evapotranspiration values. Groundwater irrigation needed is also updated for the different changes in precipitation.

In total, 750 model runs for the fixed groundwater allocation and groundwater market settings (6 allocations x 5 precipitation x 5 temperature x 5 sets of agent characteristics), each 50 years long are conducted for this study.

4.4. Results and Discussion

This section begins with results comparing the economic and environmental performance of water quotas and groundwater markets under climate change. Next, uneven distributional impacts from groundwater trading are quantified. Finally, the impact of changes in climate on groundwater dynamics are explored and discussed.
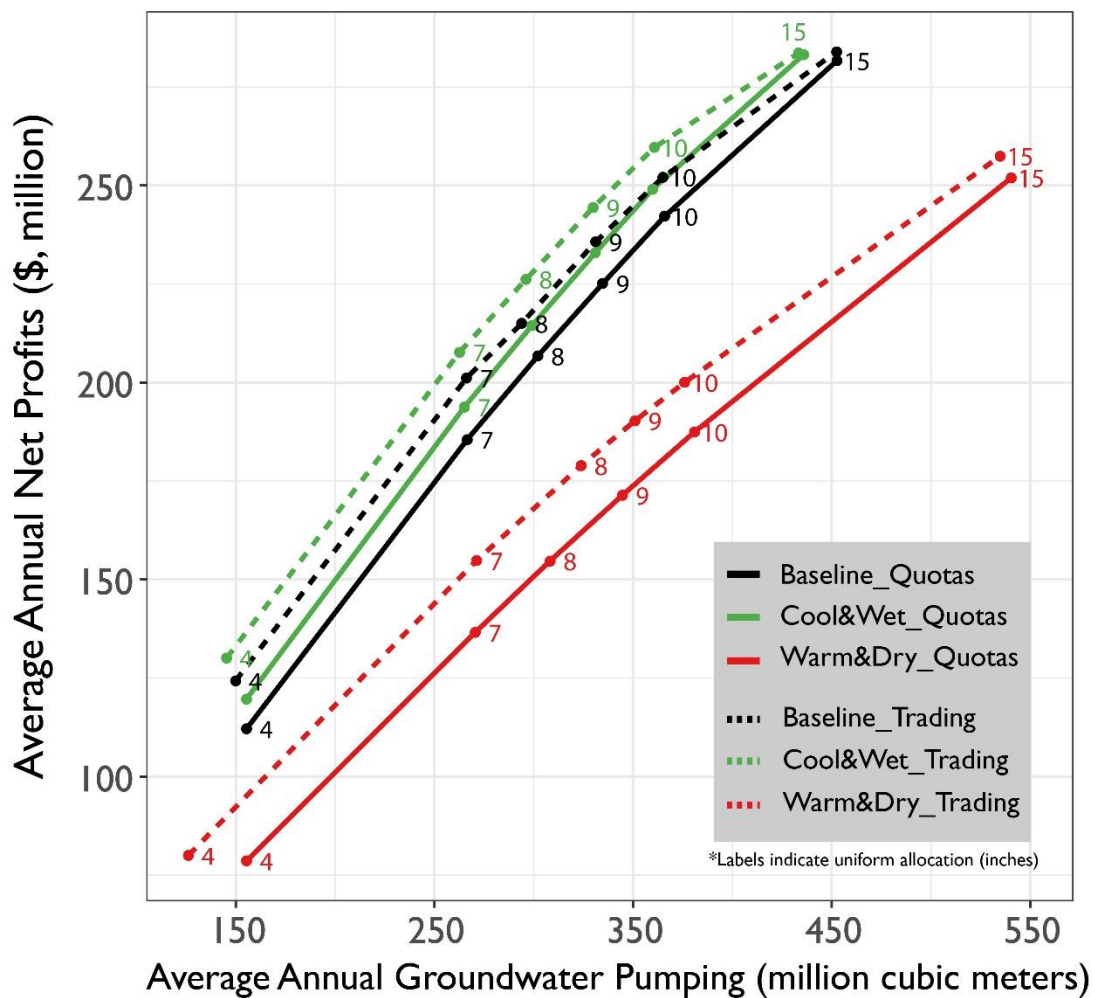
Figure 17: Total annual average agent profits and groundwater pumping for different allocations and varying climates for a groundwater market and water quotas

Figure 17 shows how average annual system wide profits change with the average annual groundwater pumping. The solid black line shows the profits when agents are provided a uniform

allocation and not allowed to exceed that (i.e. quotas on groundwater use) while the dashed line represents the profits when the agents are allowed to trade their allocations. The difference between these lines is the change in benefits when farmers are allowed to trade their groundwater allocations. The figure shows that increased groundwater pumping leads to increased economic benefit, with gains from trading depending on the groundwater allocation and the resulting price of water. Gains from trading are lowest at the extreme water allocations due to limited trading. Under very restrictive water allocations (bottom left), fewer trades take place due to the high water price resulting from high scarcity. Similarly, when allocations are sufficiently high to allow all agents to use as much water as needed, there is little incentive to trade (top right). Benefits of trading allocations are highest when the allocations create the 'optimal' level of scarcity and can increase revenues by up to $20 million (~10% of total revenues). A higher variation in crops and water usage than is observed in this region would be expected to lead to larger gains from trading [*Zeff et al.*, 2016].

The figure also shows how the benefits of groundwater trading would change for possible changes in future climate. Cooler and wetter future climate conditions lead to slightly reduced groundwater pumping and increased crop profits. The warmer and drier future has a more pronounced negative impact on crop profits. Due to the increased groundwater irrigation needs in a warmer and drier future, crop profits for a given level of groundwater use are significantly lower. The figure shows the extent to which trading can help mitigate the effect of climate change on total profits. The greatest benefits of trading are under the warmer and drier climate.
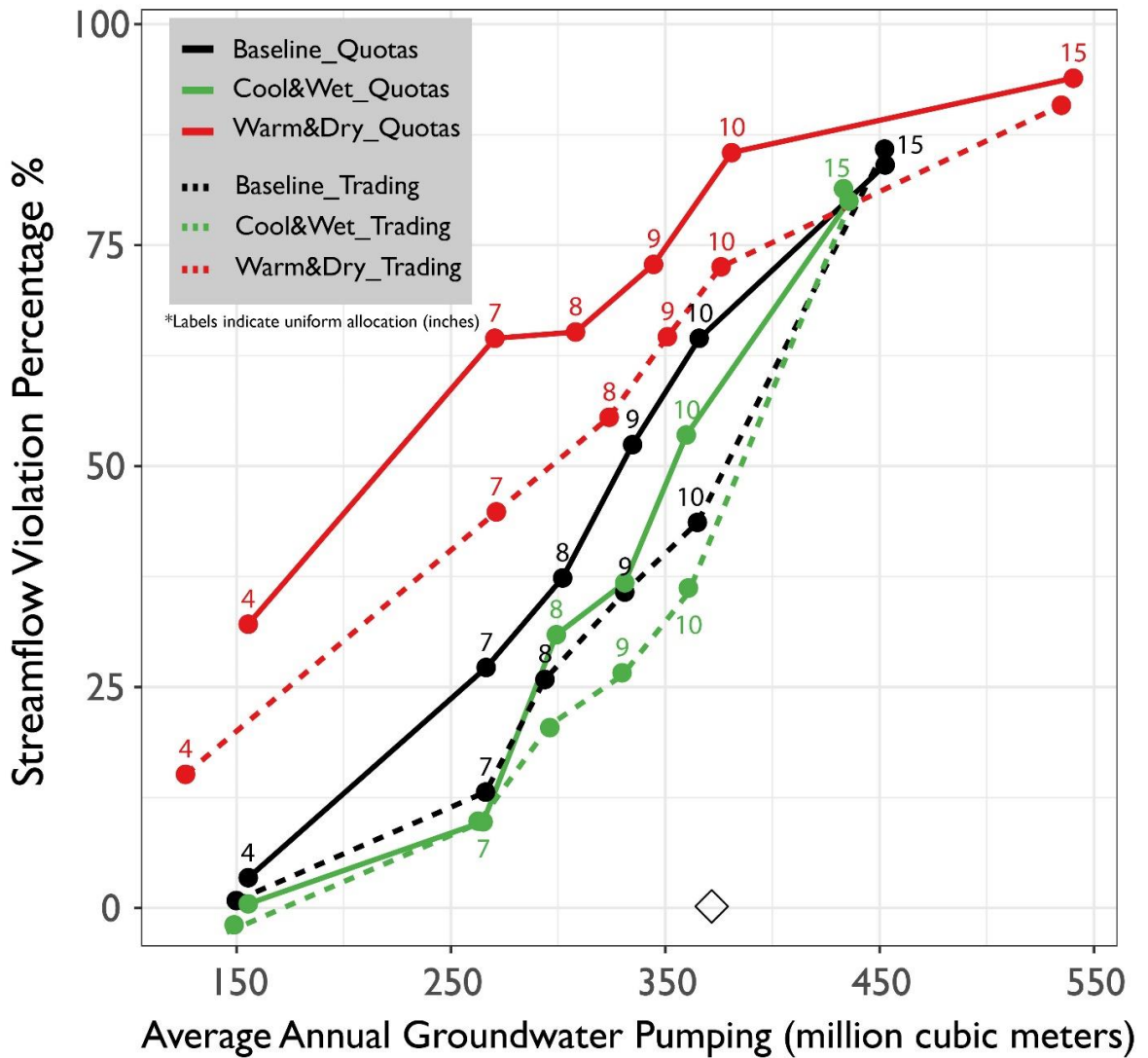
Figure 18: Average annual streamflow violations as a function of groundwater allocations for varying climates and management policies. The solid lines show results for the model runs where agents are assigned fixed quotas, while the dotted lines show results from models runs where agents can trade their allocated quotas. The black colored line show violations for model runs under historic climate, while the red and green lines show violations under warmer/drier (30% decrease in precipitation and 4° C warming) and cooler/wetter (30% increase in precipitation and no warming) climate respectively.

Next, we evaluate the tradeoff between economic gains and environmental performance for the different groundwater management policies. We gage environmental performance by *streamflow violation percentage*, which is the percentage of occurrence when modeled streamflow is less than the streamflow targets at 17 stream cell locations across the basin. Streamflow

violations occur when modeled flow is less than 75% of the 1990-2000 average flow determined from the RRCA MODFLOW model output. These targets are unrelated to actual targets outlined in the Republican River Compact. The data points in the top-right corner of Figure 18 show the economic and environmental outcomes under relatively unrestricted access to groundwater (15 inches). Not surprisingly, this unconstrained groundwater pumping where environmental externalities are not penalized results in the highest economic benefits and the least environmentally sustainable outcome. In the absence of groundwater management, farmers act in their own interests to maximize their profits. The 'costs' of environmental degradation are spread across all users. Since farmers do not directly experience these costs, there is no incentive to use groundwater 'sustainably' if there are no regulations on groundwater use.

Figure 18 provides a comparison of the performance of a realistic and 'perfect' water market. The diamond at the bottom right corner of the figure shows the economic and environmental outcomes when a 'perfect' water market is in place. This point represents the maximum profits that can theoretically be achieved on a system-wide level without any ecological damages. In the absence of a central planner with perfect foresight, we see that groundwater trading (dashed lines) is closer to this optimal outcome than a policy where groundwater quotas are imposed in the system (solid lines)

Allowing trading between agents leads to a lower streamflow violation for a given level of societal benefits because as the price of groundwater increases, less efficient farmers reduce their water usage and sell their permits to the more efficient farmers. Since a greater proportion of water is used by the more productive water users, crop production per unit of water used increases. The model runs are performed with various sets of randomized agent characteristics (crop yield and crop irrigation requirements), so the difference in performance shown in the figure is exclusively

due to the increased efficiency of groundwater markets. Increasing streamflow violations indicate a falling groundwater table resulting in higher cost of pumping groundwater. However, because the pumping costs are low relative to the benefits of pumping, declining groundwater levels do not change the pumping behavior of the farmers and slow down groundwater depletion.

The figure also shows the impact of groundwater trading and changes in climate on average streamflow violations. While the coupled model is run with several combinations of climate changes, the climate futures shown here represent the bounds of changes. The figure shows that violations for a given water allocation increase significantly under a warmer and drier future, while allowing agents to trade partly reduces those violations due to the increase in efficiency of water use. These environmental benefits from trading exist under all of the climate scenarios shown but are greatest in a warmer and drier future. Under the warmer and drier climate, the groundwater pumping associated with each allocation is also greater, particularly when the allocation is greatest. This is because in a warmer future, crop water requirements increase and reduced precipitation leads to further increased groundwater irrigation. Since groundwater pumping costs are low relative to crop profits and maintenance costs, the increased costs of pumping do not deter agents from trading. An interesting finding observed in these results, not shown here, is that the price of groundwater for a given allocation changes by very little over the 50-year simulation period despite the changes in groundwater depth. This is similar to the findings of *Mulligan et al.* [2014] who showed that when pumping costs were low relative to other costs and benefits, increases in pumping costs due to lower groundwater table did not lead to a reduced groundwater usage.
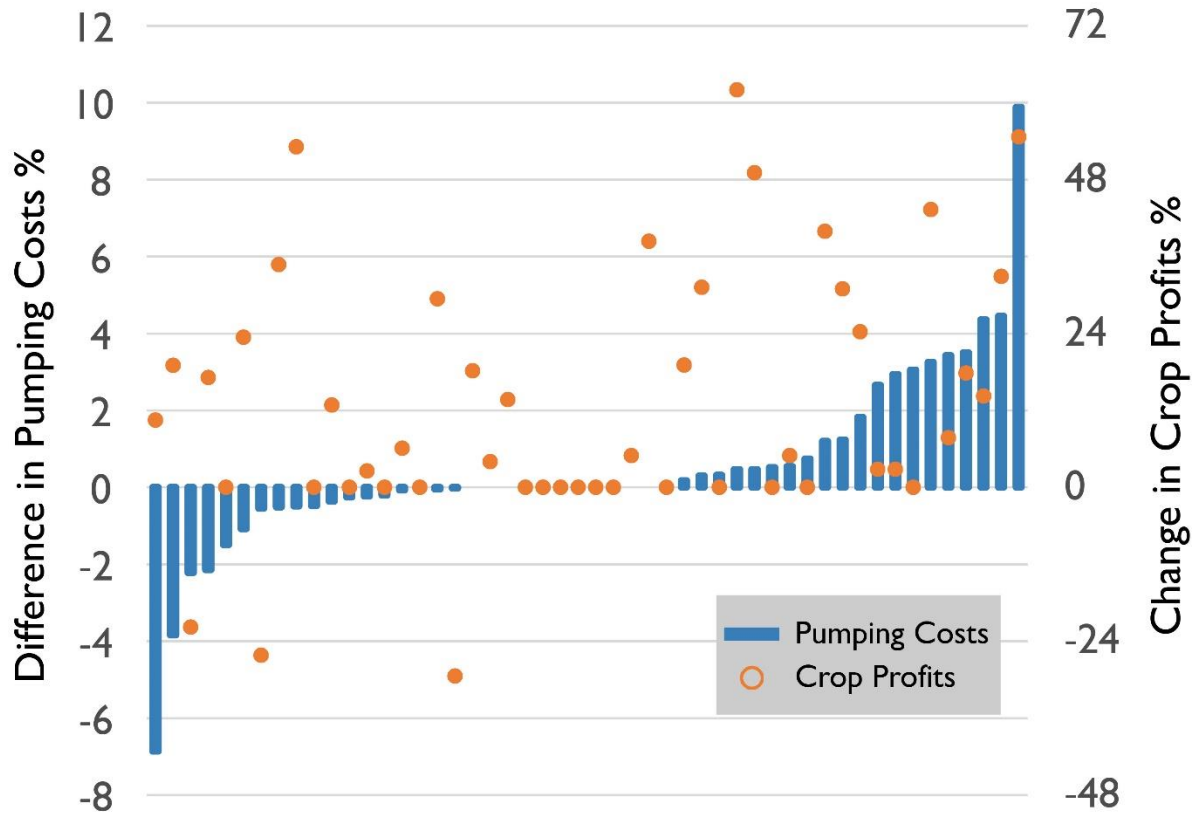
Figure 19: Distributional impacts of groundwater trading for a given water allocation. The primary (left) axis shows the difference in pumping costs (shown in blue) experienced by agents due to modified pumping by neighboring agents, while the secondary axis shows the associated change in crop profits (shown in orange) due to trading.

Improperly designed water markets where water trading does not account for the spatially heterogeneous hydrogeologic conditions can lead to uneven distributional impacts that may make an economically advantageous groundwater market politically infeasible. Figure 19 illustrates the uneven distributional impacts, in terms of difference in per unit pumping costs, resulting from trading between agents for a given level of water use. The difference in pumping costs for each agent caused by groundwater trading is calculated using equation (6).

$$\% \ difference \ in \ per \ unit \ pumping \ costs = (\frac{PC_{trade} - PC_{no \ trade}}{PC_{no \ trade}}) - (\frac{PV_{trade} - PV_{no \ trade}}{PV_{no \ trade}}) \ (6)$$

where *PC* represents the annual average pumping costs and *PV* represents the annual average pumping volume. The secondary axis shows how the associated crop profits (shown in orange) change for each agent, underlining the presence of winners and losers in the market. Higher crop profits indicate increased groundwater pumping (net buyers). Some agents, despite increased groundwater pumping, enjoy a decrease in pumping costs due to reduced groundwater pumping from adjoining neighbors (winners). Negative impacts are experienced by agents whose pumping costs increase despite no increase in their own pumping (losers). While the shortcomings of groundwater markets have been qualitatively addressed, this work is the first attempt at quantifying the distributional impacts associated with a cap and trade system using a process based spatially dynamic hydrogeologic model coupled with an agent based farmer decision model.
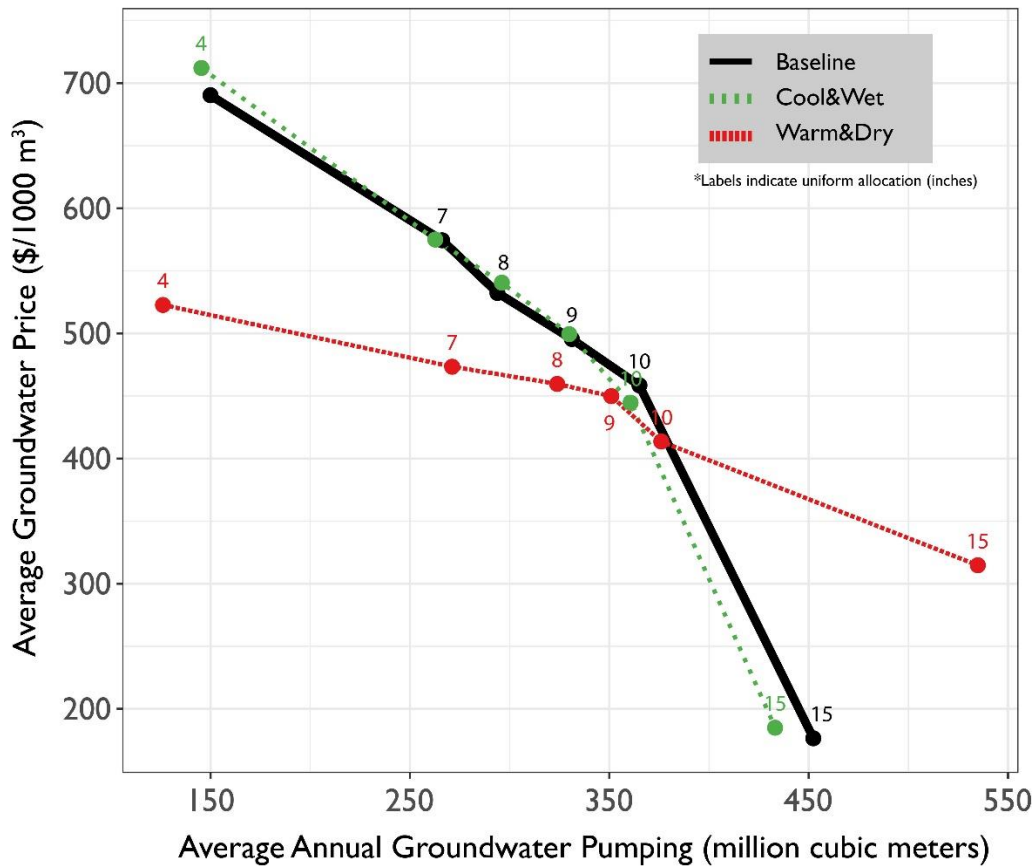
Figure 20: Average annual groundwater price and groundwater pumping for different allocations and varying climates

Figure 20 shows the equilibrium groundwater price versus annual groundwater pumping for different allocations of groundwater, under various future climates averaged over the 50-year simulation. Under all climate scenarios, as allocation increases, groundwater scarcity decreases and leads to reduced groundwater price. The figure shows a noticeable increase in the price elasticity of groundwater demand under a warmer and drier climate. At the lowest water allocation, the warmer and drier climate results in slightly reduced groundwater pumping and significantly reduced price of groundwater. This result is initially surprising because a more restrictive allocation under a warmer and drier climate would be expected to increase scarcity, and drive up the price of the resource. However, further investigation reveals that under this restrictive allocation, a high number of agents leave their farms fallow leading to a lower demand for groundwater and thus, a lower groundwater price. As groundwater allocation increases, fewer agents are driven out of the market and the demand and associated price for groundwater becomes comparable across the three climate scenarios. Under allocation that approaches unrestricted access, the associated groundwater price and groundwater pumped in the warmer and drier climate future is significantly higher because of increased groundwater irrigation requirements and thus, greater competition for the resource (scarcity).

An alternative to a cap-and-trade system for groundwater management is directly pricing its use on a per volume basis (tax). The respective merits for managing a natural resource by controlling its price (taxes) or quantity (permit trading) have been discussed extensively in the environmental economics literature. Figure 20 allows for a comparison of the outcomes associated with these two different approaches under climate change.

For a cooler and wetter (green line) climate, there is no significant change from historic climate in the range of groundwater price and pumping. Under the warmer and drier climate (red

line), the range in groundwater price is significantly reduced while the range of corresponding pumping is increased. This potential variation in groundwater pumping and price due to changing climate can be manipulated with different groundwater policies. The extent of the variations influences which policy is most suitable. For instance, assuming that the safe yield for the aquifer is 400 million cubic meters (MCM), a tax on groundwater to maintain sustainable usage would be $350/1000 m^3 under current climate. However, in the warmer/drier future climate scenario, the agent's willingness to pay for groundwater changes. Under the tax of $350/1000 m^3, the agents are projected to cumulatively pump around 470 MCM, 70 MCM more than the safe yield. If the decision maker places a high importance on reducing variation in pumping (ensuring sustainable groundwater pumping levels), then implementing taxes may not be the most suitable policy; a cap and trade system would be more suitable. However, in that case the resulting reduction in potential variation in groundwater pumping would come at the cost of increased possible variation in groundwater prices. A compromise between the two policies may be to set up a trading market with price controls. The system would work by allocating a total number of marketable groundwater permits (equal to the safe yield) and a price ceiling for exceeding the allocations. If the future climate is warmer and drier, the price ceiling provides an escape valve for farmers and prevents the agents from being priced out of using groundwater.

In this study, we do not account for non-agricultural land uses in our objective function; i.e. what happens with the portion of the field that is not planted. It is possible that this fallow land will have non-zero value. To accurately estimate the potential economic benefits of this land, much more information on the regional economy and farmer behavior would be required and is outside the scope of this study.
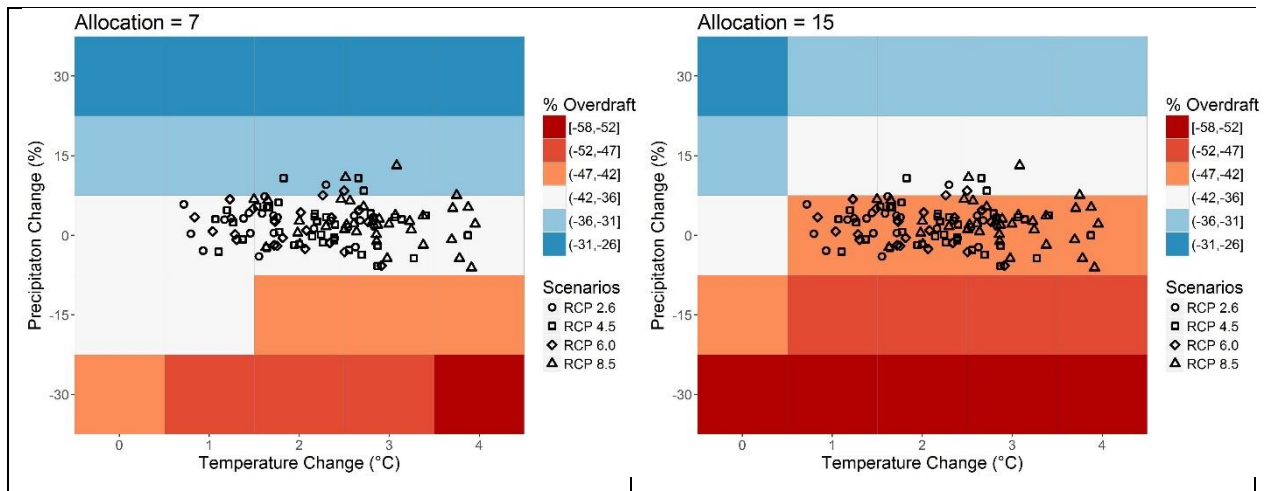
Figure 21**:** Sensitivity of groundwater overdraft (Overdraft = Evapotranspiration + groundwater pumping - recharge) to changes in precipitation and temperature for two different groundwater allocations (7 inches and 15 inches). CMIP5 GCM projections for different emission scenarios are overlain

Next, we illustrate how a range of changes in climate affects the level of groundwater overdraft. Currently, the rate of groundwater pumping exceeds the recharge in many parts of the Ogallala Aquifer resulting in declining groundwater tables. Changes in temperature and precipitation could stress the aquifer even more. Climate response surfaces in Figure 21 show how groundwater overdraft changes with climate, and how these impacts manifest themselves for different water allocations. Groundwater overdraft is calculated as the difference between recharge into the aquifer and the sum of evapotranspiration and groundwater pumping, accounting for the return flow from groundwater pumping. We calculate the groundwater overdraft from the water balance for the last year of the 50-year model run.

Two interesting results are observed in Figure 21. First, the results suggest that groundwater overdraft is sensitive to changes in *both* precipitation and temperature, with a higher sensitivity to changes in precipitation. For a given temperature change, groundwater overdraft varies more with changes in precipitation than it does for changes in temperature for a given

precipitation change. This can be observed visually by comparing the changes in shading across rows and columns in both the response surfaces.

Second, comparison of the climate response surface between the two allocations suggests that the change in groundwater overdraft from current climate conditions is greater for the higher allocations, where agents are more dependent on groundwater irrigation. A likely reason for this increase in groundwater overdraft is the increased pumping by agents who under current climate conditions pump below the allowable allocation. GCM projections from CMIP5 for different emission scenarios are overlain. While there is significant variability in the future projections of precipitation, all projections indicate warming. For the available projections, the results suggest that with the lower allocation, groundwater overdraft would not significantly change from what it is under historic climate. However, for the higher allocation, modeling results suggest that groundwater overdraft increases from that under current climate conditions (shift from white to orange region).

4.5. Limitations and Future Work

Groundwater is a common resource property, meaning that one agent's use can affect other groundwater users. When the location of pumping is changed as a result of trading, the distribution and magnitude of the impact of that pumping changes. Results presented here-in highlight the uneven distributional impacts when one-to-one trading of permits is allowed. This one-to-one trading does not account for the non-uniform impacts of groundwater pumping that is caused by the spatially heterogeneous aquifer conditions. To account for these differences, trading coefficients between agents that are based on the ratio of accrued marginal impacts need to be defined. These trading ratios will in effect, create a spatially varying price for groundwater. In

addition, environmental violations are tracked but not penalized in the current modeling framework. The benefits of markets compared to the system with water quotas would be greater were there a price on environmental violations.

While this analysis did not address the choice of groundwater allocation mechanism, it is nevertheless an important policy decision. The allocation of permits determines the financial impact on stakeholders and resultantly their willingness to participate. Unsustainable allocations where the water is over-allocated also leads to environmental degradation. In this analysis, although groundwater permits are allocated uniformly across all users, socioeconomic and political factors may make non-uniform allocation more suitable. An interesting extension to this work would be to explore different methods of allocating permits to assess their economic impact on users and basin-wide environmental outcomes.

Results of this analysis should be viewed in context of some key limitations, including constant model parameters over time (productivity, farmer operating costs, crop prices) and assuming a linear relationship between stream depletion and groundwater pumping. In addition, while crop water requirements are assumed to change linearly with temperature for this analysis, recent studies have shown non-linear relationships between crop water requirements and temperature [*Fischer et al.*, 2007]. While we acknowledge these shortcomings, we believe they do not significantly undermine the key findings. Nevertheless, future endeavors addressing these limitations will further strengthen the outcomes from this analysis.

4.6. Conclusion

Increasing population and climate variability are stressing groundwater resources in many parts of the world, prompting calls for better management of groundwater. Incentives-based

policies, such as a groundwater market, have been identified as promising solutions to manage groundwater, however quantitative evaluations of the performance of these markets under uncertain climate and administrative costs are rarely performed. Using a calibrated physically based groundwater model with an agent based farmer decision model, this work compares the respective performances of a groundwater market and water quotas accounting for spatial and temporal variability in the Frenchman River Subbasin overlying the High Plains aquifer. The study quantifies the uneven distributional impacts of groundwater trading and shows how changes in climate affect groundwater market dynamics.

Results of this analysis suggests that changes in climate significantly influence groundwater market dynamics, affecting the amount of groundwater pumping with the impact varying under different allocations. The study also finds that allowing users to trade groundwater allocations leads to modest improvements in economic performance. For a given level of water use, a groundwater trading system results in fewer environmental violations (measured in terms of impact on streamflow). The results show that economic gains from trading are unequally distributed across the users, with some users worse off due to third party impacts.

This work provides key policy insights for regions considering groundwater markets as an instrument to sustainably manage groundwater. To account for the spatially variable groundwater conditions and mitigate uneven distributional impacts, trading ratios should be incorporated in groundwater transfers between users. With regards to temporal variability, a thorough assessment of impact of changes in future climate on market dynamics should be performed to determine the appropriate policy features (e.g. price controls). While groundwater markets offer a promising alternative to traditional command and control management of groundwater, region-specific

assessments are needed to determine whether the benefits promised by these markets are worth the

potentially considerable administrative costs incurred in setting them up.

CHAPTER 5

EVALUATING IMPACT OF DIFFERENTIAL CLIMATE CHANGE IN CALIFORNIA THROUGH A SPATIALLY AND TEMPORALLY DISAGGREGATED WEATHER GENERATOR

5.1 Introduction

With a population of over 40 million, the eighth biggest economy globally, internationally significant agricultural production, and a climatology particularly susceptible to climate anomalies, California provides a compelling example for investigation of impacts of future changes in climate. Climate change is already having a profound impact on California's water resources, as evidenced by changes in temperature, precipitation, snowpack, and river flows [*Cayan*, 2013] that are expected to continue and amplify in the future. This potential change in weather patterns will exacerbate both drought and flood risks and add additional challenges for water supply reliability across the state [*Sicke et al.*, 2013].

An extensive body of literature investigating California's climate exists [*Dettinger*, 2011; *Swain et al.*, 2016; *Allen and Luptowitz*, 2017]. Precipitation in California is characterized by considerable inter and intra-annual variability, larger than anywhere else in the US. This large variability stems from the fact that only a few storm events comprise the bulk of the state's annual precipitation [*Steinschneider and Lall*, 2015]. Drought occurrence in the state is thus closely linked to the number of these large storms that results from landfalling atmospheric rivers [*Ralph and Dettinger*, 2011]. Also important from a drought perspective is the persistence of precipitation on longer time scales. Low-frequency precipitation variability has been identified as an important characteristic of California's climate where drought episodes have been found to occur approximately every 15 years over the 20th century [*Dettinger and Cayan*, 2014]. This 15-year cycle is not associated with the El-Nino Southern Oscillation (ENSO, 3 to 7 year cycle) or the

Pacific Decadal Oscillation (PDO, 30 to 60 year cycle), and the underlying mechanism of this cycle is still an open research question. An increasing, but statistically insignificant, trend in frequency and magnitude of precipitation over the past century in California has been observed.

Temperatures have shown a warming trend, with the state as a whole experiencing an increase of 1.1 to 2° F in mean temperature over the past century [*CA DWR*, 2015a]. The relatively few studies that have investigated whether this warming trend varies seasonally have found evidence of a greater temperature increase in summer months than in winter months [*Killam et al.*, 2014]. An investigation of whether these trends differ geographically; i.e. whether low-lying coastal areas are warming differently than the high-altitude Sierra Nevada region has not been previously performed. The resultant impact of these possible spatial and temporal variations on hydrology in California is thus not well understood. This work aims to fill this research gap.

The most recent model projections suggest an increase in temperatures and an intensification of future droughts in California [*Diffenbaugh and Ashfaq*, 2010]. Given California's very sharply defined wet season, it is especially vulnerable to extended anomalies in atmospheric circulation patterns [*Van Loon et al.*, 2014]. While enhanced precipitation in northern California is projected for the future, considerable uncertainty exists regarding these projections [*Neelin et al.*, 2013]. Situated between the drying subtropics and moistening midlatitudes, California lies in a region of climate change uncertainty [*Simpson et al.*, 2014].

The effects of future changes in climate on hydrology and water management in California have been studied extensively. Projected increases in temperature are expected to affect the timing of snowmelt in the Sierra Nevada, leading to increased runoff during the winter and consequently lower runoff in the spring season [*Dettinger and Anderson*, 2015]. A key factor behind this change in timing of snowmelt is the elevation of a basin compared to the freezing line location during the

winter (snow accumulation) and spring (snowmelt period) [*Miller et al.*, 2003]. This loss of snowpack essentially translates to a reduction in storage from a water resources management standpoint, and has implications for reservoir operations trying to balance needs for water supply and flood protection [*Brekke et al.*, 2004; *Vicuna et al.*, 2010]. Prior studies have found changes in precipitation to have a relatively smaller impact on streamflow compared to temperature shifts [*Vicuna et al.*, 2007].

The aforementioned findings were obtained using a variety of approaches. Initial efforts to study the effect of climate change on hydrology in California developed statistical relationships to determine streamflow sensitivity to climate change in major basins [*Revelle and Waggoner*, 1983]. With the advances in climate modeling, studies began making use of General Circulation Model (GCM) derived climate at coarse resolutions [*Lettenmaier and Sheer*, 1991]. Improvements in climate models, coupled with an increasing use of downscaling approaches using regional climate models, led to use of finer resolution climate data [*Knowles and Cayan*, 2002; *Miller et al.*, 2003; *Vanrheenen et al.*, 2004]. More recent studies have shifted from using single GCMs to model ensembles to determine projections of future climate change for specific time periods (e.g. 2040, 2070, 2100) [*Zhu et al.*, 2005; *Hydrocomp*, 2012]. Consistent with the earlier Coupled Model Intercomparison Project (CMIP) projections (CMIP3 and before), a majority of these scenario-based studies consider climate that is generally warmer and drier.

Evaluation of the hydrologic response to climate change using specific GCMs and climate futures provides a limited representation of future climate. A few studies investigate a wider range of possible future climates. *Willis et al.*, [2011] use an ensemble of 11 GCMs with multiple emission scenarios to evaluate risk of flooding in the Sacramento River Basin, while *Groves and Bloom* [2013] analyze water management policies for California's Central Valley System (CVS)

using 6 GCMs with CMIP3 emission scenarios, A2 and B1. Even though these studies consider a relatively wide range of future changes in climate, these changes are insufficiently sampled. To overcome this issue, *Ray et al.*, [2018] use Decision Scaling (DS) to evaluate CVS performance over a wide range of sufficiently sampled possible future climates. They systematically explore uniform changes in temperature (0° to 4° C) and precipitation (-30% to 30%) to summarize the CVS's sensitivity to climate change. In vulnerability-based approaches such as DS, the performance of a system is evaluated using systematic sampling of plausible future climates, developed typically using stochastic weather generators, to identify climatic conditions that can cause the system to fail [*Brown et al.*, 2012]. This is in contrast to scenario-based approaches where system performance is tested for a given set of climate model projections that may not necessarily highlight a system's vulnerabilities, and where results are contingent on the projections and downscaling approach that happen to be used. In the DS approach, once the system's vulnerabilities to climate states have been identified, then the level of concern associated with those climate states can be assessed using climate projections (e.g. GCMs, historical observations or paleoclimatological simulations). This allows for a separation of the articulation of system response to climate from the use of GCM projections of future climate conditions. In this study, we demonstrate a methodology to investigate hydrologic effects of seasonal variation in climate change using the DS approach.

Seasonal variation of the hydrologic cycle between the summer and the winter for the middle to high latitude regions, allows for different responses to additional incident radiative energy from increasing GHG concentrations [*Nigam et al.*, 2017]. For regions with short and sharply defined precipitation seasons, such as California, changes in seasonality can have an especially pronounced effect on hydrology [*Vano*, 2015; *Rice and Emanuel*, 2017]. Analyses of

trends in seasonal temperature and precipitation in the Pacific Northwest in the US reveal that while anthropogenic forcing is the leading predictor for long-term warming, ENSO and PDO are the primary modulators of seasonal temperature trends on the decadal time scale [*Abatzoglou and Barbero*, 2014; *Abatzoglou et al.*, 2014]. Elsewhere, seasonal changes in climate in the Columbia River Basin have been attributed to changes in large-scale circulation patterns and regional surface energy budget where summer warming and decreased summer precipitation was found to result from enhanced upper-level ridging across the region [*Rupp et al.*, 2017]. Interannual variability in temperature was found to decrease during the cool seasons and increase in the summer while it was found to increase for precipitation across all seasons. While existing studies investigate spatial and temporal changes in hydrologic response to climate change in the Pacific Northwest [*Shrestha et al.*, 2012; *Werner et al.*, 2013], this has previously not been performed for watersheds in California.

In this paper, we build on the work by Ray et al. [2018] to investigate seasonality in the DS approach. We develop a spatially and temporally disaggregated stochastic daily weather generator that is used to generate climate time-series embedded with regionally and seasonally varying climate change in California. While Ray et al., [2018] explore step changes in climate, transient changes in climate are explored in this work. The generated climate time series are then used to drive hydrologic models to examine the resultant effect on water availability. We compare this vulnerability-based methodology with a scenario-based approach that uses downscaled GCM projections, and assess the effect of downscaling approach on hydrology. We use the water supply served by the San Francisco Public Utilities Commission (SFPUC) to 2.7 million people in the San Francisco Bay Area as a case study for this analysis. The varied topography and geography of the different sources from which San Francisco receives water provides an ideal setting for this study.

5.2 Methodology

This study develops a stochastic daily weather generator that is capable of simulating changes in climate that vary spatially and temporally as part of a climate vulnerability assessment. Prior to the weather generator development, data analysis of the observed climate across the San Francisco regional water system is conducted to explore spatial and temporal correlations, investigate the presence of spatial and temporal trends in precipitation and temperature, and determine the connection between large-scale atmospheric processes and regional climate. Downscaled GCM climate projections for the study area are obtained for comparison with this vulnerability-based approach. This baseline data analysis is used to inform the design of the different components of the stochastic weather generator and application of climate shifts. Hydrologic models for five watersheds comprising about 95% of total SFPUC regional water supply in the Central Sierra Nevada (Upcountry) and San Francisco East Bay watersheds are developed and calibrated. The climate time series obtained from the weather generator and downscaling approaches (BCCA and LOCA) are used to drive the calibrated hydrologic models to evaluate impact of climate change on water availability.

5.2.1 Study area and data availability

San Francisco and adjoining areas are provided water through the Hetch Hetchy Regional Water System (RWS), a municipal utility operated by SFPUC. The RWS supplies water from three different regions: the Tuolumne River watershed (referred to as the Upcountry), East Bay and Peninsula watersheds, shown in Figure 22. Each of the different regions supplying water for SFPUC has a unique topography and climatology. Approximately 85% of the total water supply comes from the Upcountry watersheds, about 10% from the East Bay and the remainder from the

Peninsula watershed [*SFPUC*, 2016]. The split between these three sources varies annually depending on the current hydrology and operational circumstances.
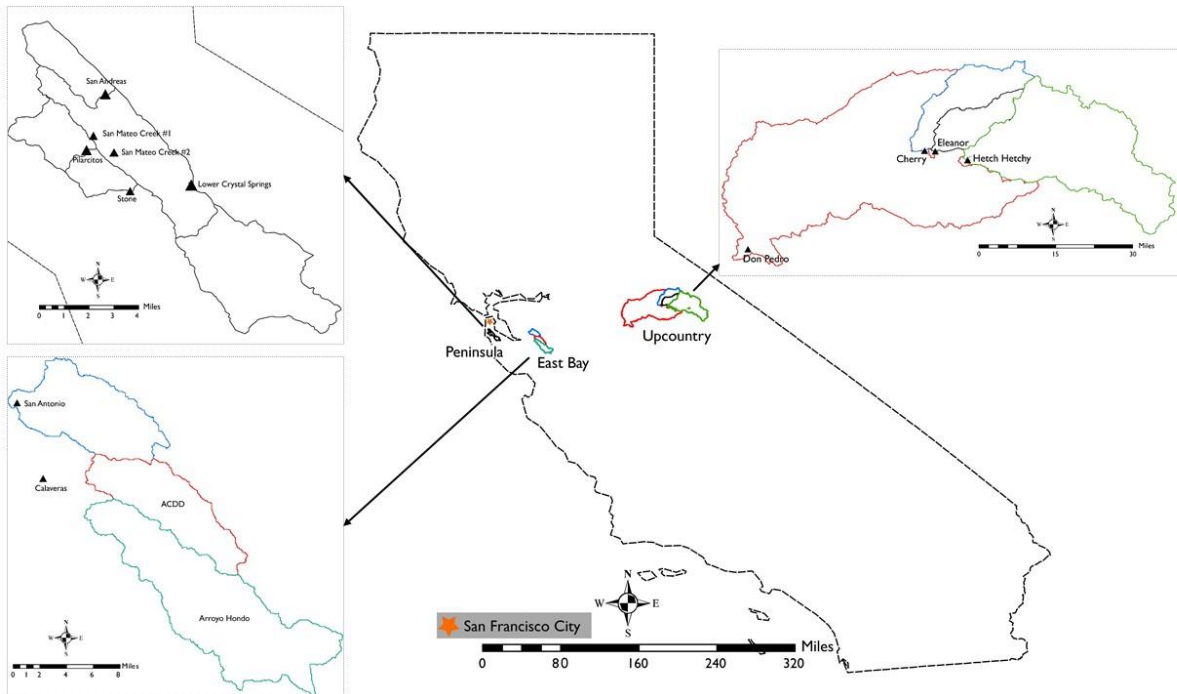
Figure 22: Map showing watersheds for the three regions that SFPUC receives waters from

To realistically simulate weather data, the weather generator is parameterized with the observed climate in a region. Observed precipitation data from 25 gages, and temperature data from 14 gages spread across the system are obtained from a variety of sources. Figure 23 shows the length of records of daily data available for the temperature and precipitation gages. Long time series (> 50 years) of daily precipitation are available for some gages in each region; long time series of observed temperature are available for fewer gages. The available weather data represents a reasonably comprehensive summary of climate for the study region. Figure 24 shows the elevation of each of the precipitation gages for which data is available and illustrates the altitudinal differences between the three watersheds.
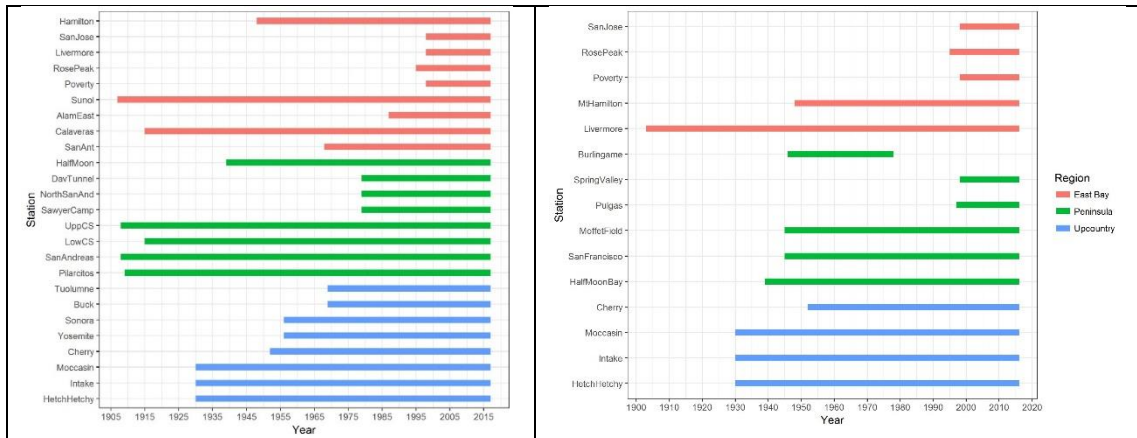
Figure 23: Length of daily precipitation (left) and daily temperature (right) records for gages across the SFPUC system
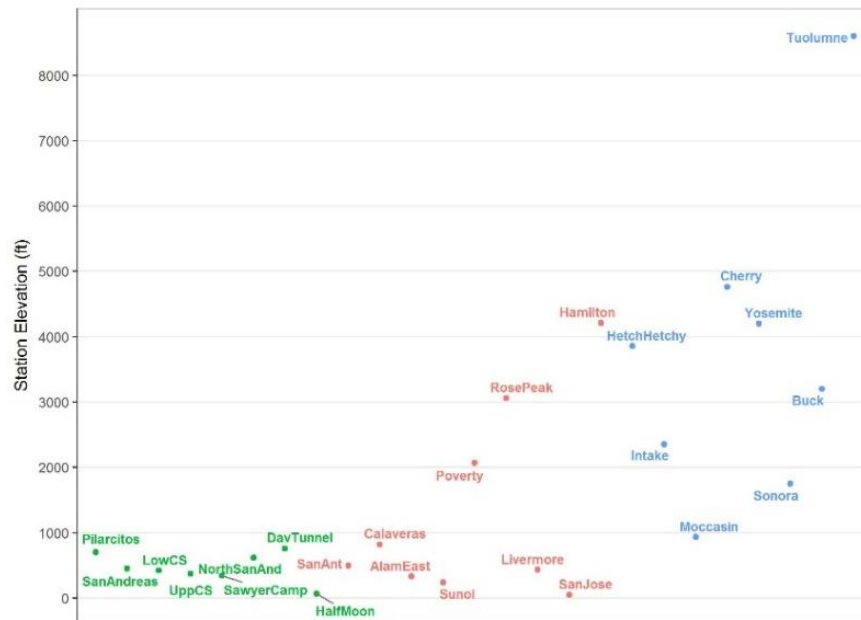
Figure 24: Station elevations for the 25 precipitation gages with available data across the SFPUC system. Stations are color coded by region (Blue = Upcountry, Red = Alameda, Green = Peninsula)

The SFPUC obtains water from watersheds distributed across three distinct regions, each with a potentially unique climatology. The correlational structure between the climate variables across the different gages was explored to inform the spatial design of the weather generator. The Alameda and Peninsula watersheds exhibit a similar climatology that is significantly different from the Upcountry watersheds. Figure 25 shows the correlation in daily precipitation between the different gages. Gages within the same region exhibit relatively high correlation (R= ~0.7-0.9).

97

Precipitation in the Peninsula and Alameda watersheds is also well correlated (R~ 0.6 – 0.8). Upcountry precipitation is not as correlated with Peninsula or Alameda precipitation although the correlations are still positive (R~ 0.2 - 0.3).
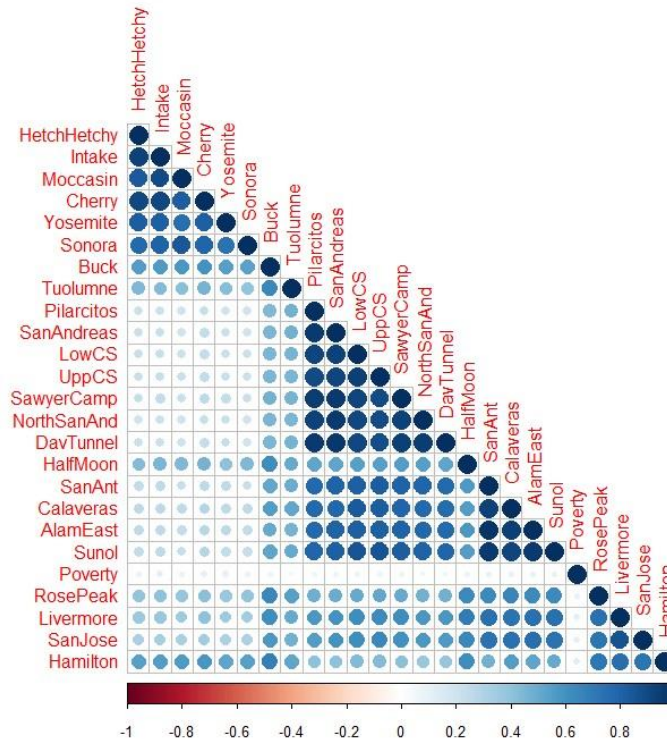
Figure 25: Correlation in observed daily precipitation for gages across the SFPUC system. Color indicates the sign of the correlation; circle size and color intensity indicates the magnitude of the correlation.

5.2.2 Trends in Temperature and Precipitation

Before generating synthetic time series of future climate, it is necessary to accurately establish baseline historical climate conditions across the different watersheds and investigate teleconnections affecting climate in the study region. Given these well-documented trends in the 20th century in California's climate [*Killam et al.*, 2014], we conduct time series analyses on the trends for precipitation and temperature across the SFPUC watersheds to determine the nature of

the trends (i.e. deterministic or stochastic), and understand the spatial and temporal variation in these trends.

Mean maximum (T_{max}) and minimum (T_{min}) temperatures for the dry (April-September) and wet seasons (October to March) for the Peninsula watersheds are plotted in Figure 26 and Figure 27 respectively. Also shown on these plots is a trend line, where the region in grey represents the 95% confidence interval for the trend line. Both T_{min} and T_{max} for the Peninsula watersheds exhibit an increasing trend, with the strongest trend observed for the dry season T_{max} where the 95% confidence interval band is the narrowest. A possible reason behind this significant increase could be the heat island effect where built up areas (concrete, road surfaces etc.) absorb considerable amounts of incident solar energy and radiate heat. Trend analysis at a monthly level shows greatest increases in June-September. Similar results are also observed for the Alameda watersheds.
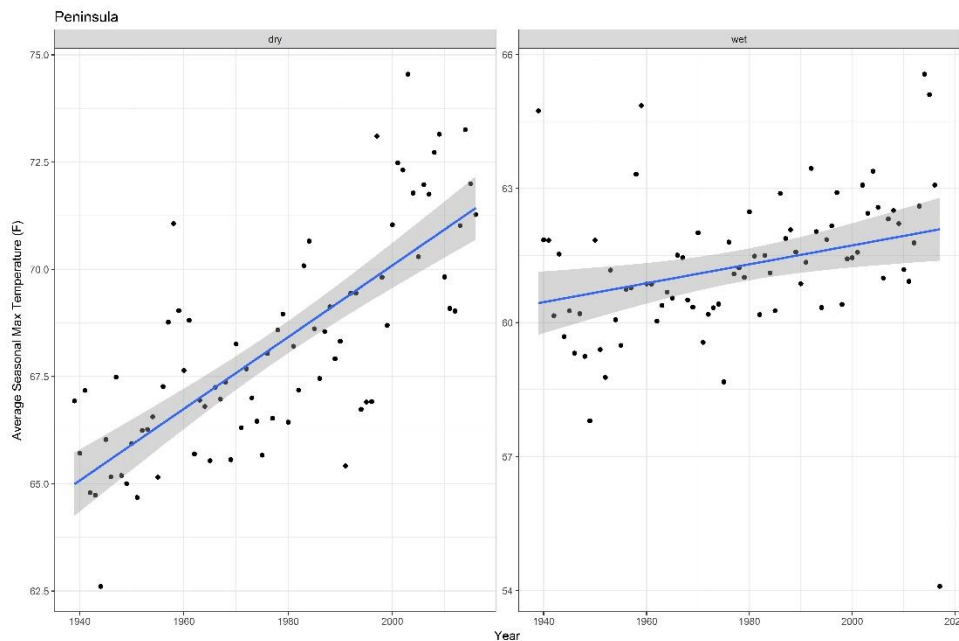
Figure 26: Seasonal average maximum temperature across the Peninsula watershed for the dry (April to September) and wet seasons (October to March)

99
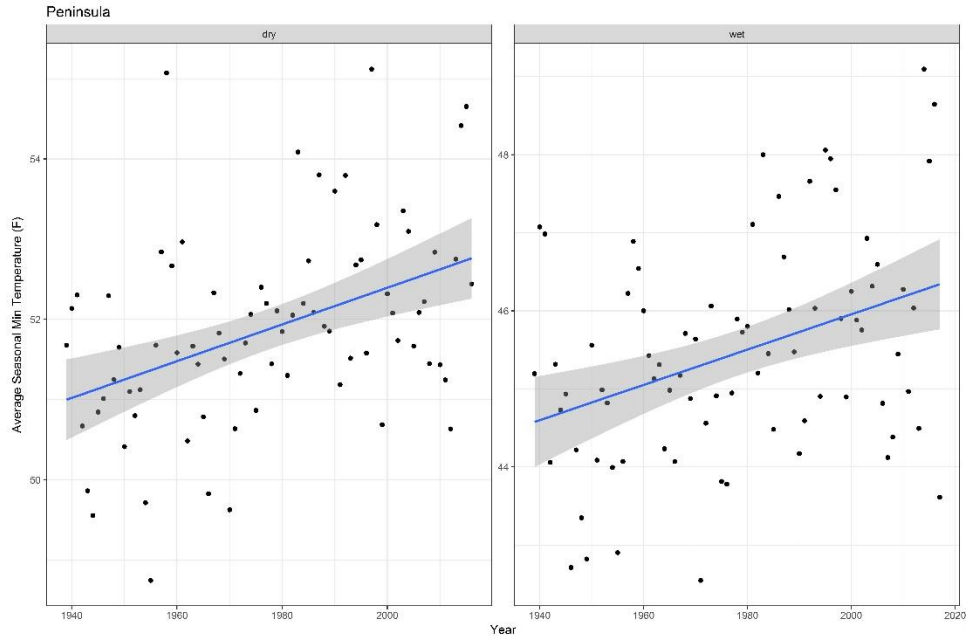
Figure 27: Seasonal average minimum temperature across the Peninsula watershed for the dry (April to September) and wet seasons (October to March)

Figure 28 and Figure 29 show the basin-wide average T_{max} and T_{min} for the Upcountry watersheds for the dry and wet seasons respectively. While a linear trend is fit to these plots, it is interesting to note a U-shaped distribution of temperature for the period where data is available. T_{max} for both the dry and the wet season have a decreasing trend, while T_{min} is observed to have an increasing trend. However, the time series clearly exhibit flow frequency variability, with a cooler mid-century and warmer early and late parts of the record. The change in temperature in the Upcountry watersheds is especially important because that can affect the phase of precipitation and thus not only the volume but also the timing of flows into the Upcountry reservoirs (e.g. change in precipitation from snow to rain). Earlier analyses have shown that over the last several decades, rising temperatures in the Sierra Nevada and northern California trigger decreasing snowpack and earlier snowmelt [*Barnett et al.*, 2008]. For the SFPUC, these changes may change water availability based on water rights.
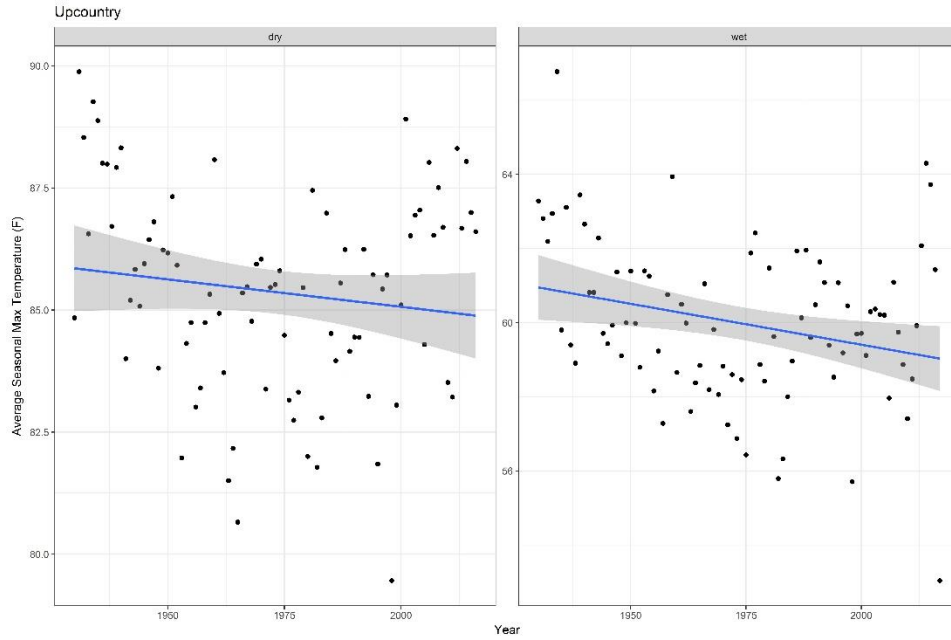
Figure 28: Seasonal average maximum temperature across the Upcountry watershed for the dry (April to September) and wet seasons (October to March)
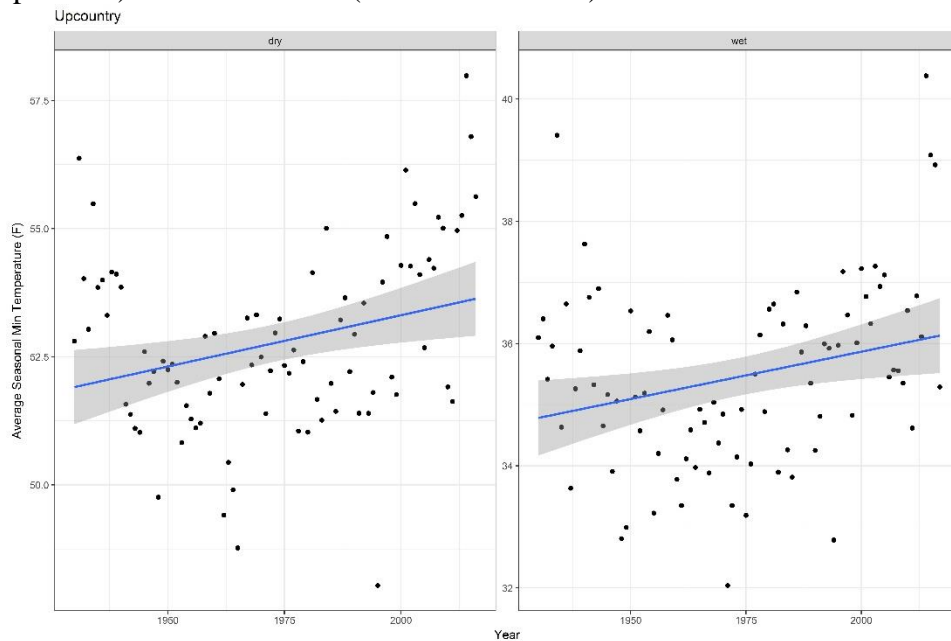
Figure 29: Seasonal average minimum temperature across the Upcountry watershed for the dry (April to September) and wet seasons (October to March)

Figure 30 shows the Mann Kendall (MK) statistic for trends in temperature for both T_{max} and T_{min} in each of the watersheds in the dry and wet seasons. The two horizontal lines (-1.96 and +1.96) denote the 95% significance level; an MK statistic between the two lines is not statistically significant. As seen in the scatterplots previously, the strongest trends are those for T_{max} and T_{min}

in the Peninsula and East Bay watersheds. The increasing trend in T_{min}, in both the dry and wet season, for the Upcountry watersheds is also statistically significant. Tests were performed to determine the nature of the observed trend; all of the trends were found to be deterministic. Similar trend analyses were also conducted for precipitation across the different watersheds. None of the gages showed statistically significant trends in precipitation, a finding consistent with that in the existing literature [*Killam et al.*, 2014].
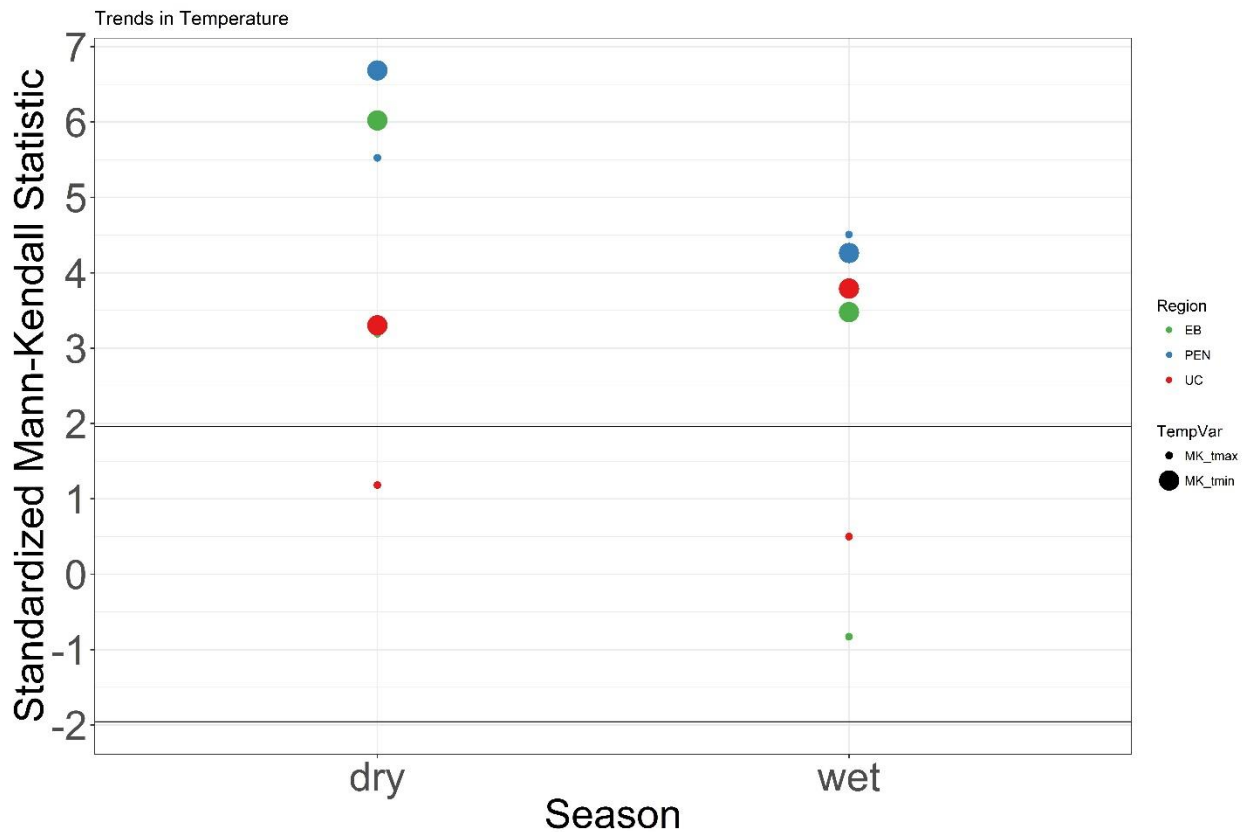
Figure 30: Standardized Mann-Kendall statistic for each of trends observed in seasonal maximum and minimum temperature across the SFPUC watersheds

5.2.3 Low frequency variability

The impact of large-scale climate patterns on precipitation in California is well documented [*Dettinger et al.*, 1998]. The ENSO has been shown to influence precipitation in the State, especially in Southern California. Evidence for the effect of ENSO on precipitation in the Delta

region is inconclusive. Understanding these effects is important because they are typically the source of structured low frequency variability found in an observed weather time series. Since low frequency variability is a key factor in the occurrence of drought, preserving these effects is required to create a weather generator that reproduces the local climate conditions.

We investigate the historic precipitation record for presence of low frequency variability. Figure 31 shows the wavelet power spectrum for precipitation records for the Hetch Hetchy (Upcountry) and Pilarcitos (Peninsula) gage stations. Statistically significant (90%) low frequency signals occur at the 11, 12 and 13 Fourier periods corresponding to 12.1, 13.6 and 14.9 years. This quasi-periodic 15-year cycle in the precipitation signal has been identified previously in the literature but surprisingly has received little further attention. This signal is also visible in the paleo-records for the past 200 years, but not before that [*Meko et al.*, 2014]. The climatic patterns responsible for this signal are not currently well understood. While not significant at the 90% confidence level, a 'bump' in the low frequency signal at 5 years (associated likely with ENSO) is also observed.
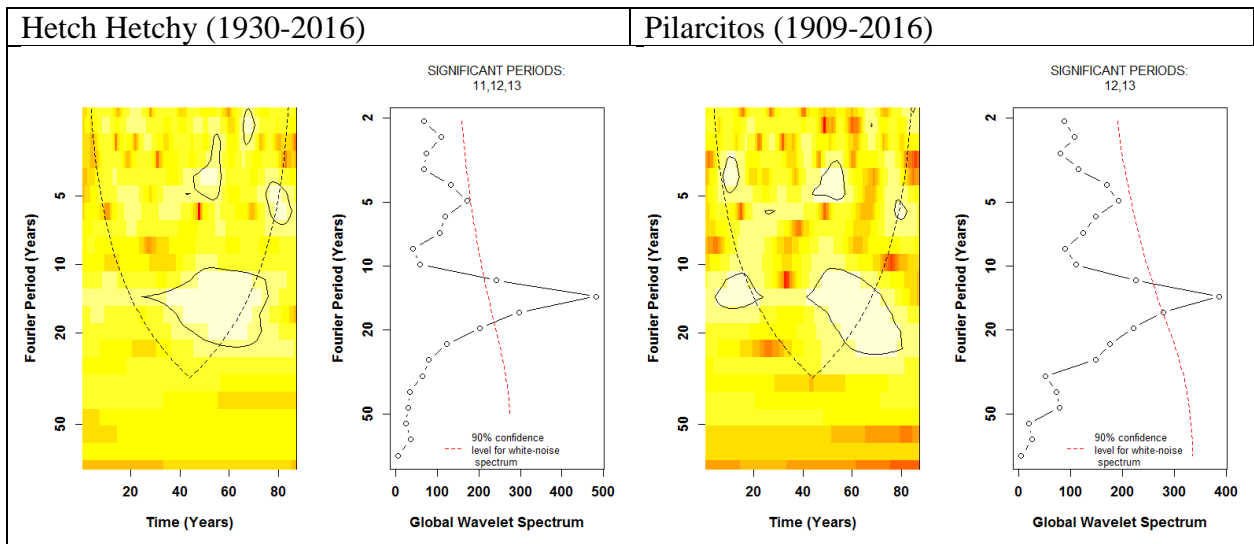
Figure 31: Wavelet power spectrum for average annual precipitation at the Hetch Hetchy and Pilarcitos gage stations

5.2.4 GCM downscaling

GCM climate change projections are too coarse and biased to be used directly for a hydrologic impact assessment, and need to be downscaled to a finer resolution before they can be used to drive hydrologic models [*Fowler et al.*, 2007]. There are two components to downscaling: spatial downscaling and bias correction. Bias correction refers to an approach where known systematic errors ('biases') in GCM projections over a region are removed. There are two primary methods for spatial downscaling: dynamical and statistical. Dynamical downscaling approaches make use of regional climate models (tailored to the region of interest) and use GCM output as boundary conditions. While it can provide a much more realistic representation of the physical processes in a region, dynamical downscaling can be computationally prohibitive, especially for larger domains and for processing several GCM ensembles with over centuries-long climate time series.

Statistical downscaling makes use of historically observed empirical relationships between finer scale climate variables and coarser GCM output. Implicit in this approach is the assumption that the relationship between coarser scale climate and finer scale climate variables remains stationary. Constructed analogs (CA) has emerged as a popular statistical downscaling method, especially for North America [*Brekke et al.*, 2013]. CA methods search for a set of observed days (typically 30) that most closely match a given GCM output day when the observations are coarsened to the GCM grid. Bias corrected constructed analog (BCCA) and Localized Constructed Analog (LOCA) [*Pierce et al.*, 2015] are two commonly used sets of downscaled GCM data products that make use of the CA method [*Bracken*, 2016].

There are three key differences between the LOCA and BCCA approaches. BCCA selects a set of 30 analog days where climate most closely matches a given GCM grid cell daily climate

across the entire downscaling domain. LOCA selects the set of 30 analog days based on how well the observed days match the GCM climate over ~1000 km region around the point being spatially downscaled. The second key difference is that while the BCCA approach calculates optimal weights for the selected 30 days to generate downscaled climate, LOCA selects only one of the 30 days that is most similar to the point being downscaled at a ~100 km scale. This has important implications as the LOCA approach thus avoids the problem of spurious precipitation drizzle generation and damping of precipitation extremes that result from using a weighted average of 30 days (as is done for BCCA). The third key difference between the LOCA and BCCA data products is in the bias correction method. BCCA uses quantile mapping for bias correction that can lead to a loss of the GCM predicted climate change signal depending on the climate variability of the given region. LOCA avoids this problem by making use of a three-step process that preserved the climate signal.

Given the internal climate variability observed in California's climate, and the spatial climate variability across our study area, the choice of GCM downscaling approach used to evaluate hydrologic impacts of climate change may influence findings. In this study, we compare BCCA and LOCA downscaled climate data and its projected effect on SFPUC watersheds. We also compare the downscaled GCM projections with climate simulation produced using a stochastic weather generator. We obtain downscaled GCM ensembles for both the BCCA and LOCA approaches [*Maurer et al.*, 2007]; retaining only the 10 models that have been identified by the Climate Change Technical Advisory Group (CCTAG) [*CA DWR*, 2015b] to simulate California climatology well. The models selected for this analysis are all from RCP 8.5 emission scenario. For BCCA, we were only able to obtain 7 of the 10 models for the RCP 8.5 emission scenario.

5.3 Weather generator setup

Stochastic weather generators (SWG) can be used to perform exhaustive assessments of a system's vulnerability to climate conditions across multiple temporal scales, including changes in mean climate and variability [*Katz*, 1977; *Wilks*, 1998]. SWG are mathematical models that produce time series of weather data that preserve the temporal and spatial characteristics for a given location or region. To ensure that the "synthetic series" generated accurately represent a given region's climatology, the parameters of the weather generator are conditioned on the existing meteorological records. Typically, SWG are used to produce a new realization of a time series of weather variables that exhibit the same statistics as the original historical record, thus producing an ensemble of time series that samples the historical or "natural" variability [*Steinschneider and Brown*, 2013]. The simulated realization is then perturbed to alter climate characteristics to represent possible changes in future climate. To more realistically simulate changes in future climate and hydrology, weather generators need to be able to account for seasonal and spatial differences and be able to replicate and perturb climate variability important for a given system.

The daily weather generator developed for this study, adapted from *Steinschneider and Brown* [2013], is composed of two primary modules. It couples an autoregressive wavelet decomposition for simulating the observed low frequency structure in the annual climate with a KNN resampling scheme to simulate spatially distributed, correlated, multivariate weather variables over a region. The bootstrapping technique, resampling from the study-region simultaneously, perfectly maintains the spatial correlations between the three watersheds and cross-correlations between the weather variables.

Given the long wavelength low-frequency variability observed in the precipitation in the region, a long time series of climate variables on which to condition the weather generator is

desired. In addition, the resampling technique used in this weather generator requires that input time series of temperature and precipitation over the same time-period. Weather generators often make use of gridded climate products where corresponding time series of temperature of precipitation are available for large study regions.

For this analysis, we investigated the suitability of using gridded climate data by comparing it with the local observations. We perform a comparison of gridded climate datasets with observed precipitation to assess whether the gridded data satisfactorily replicate observed data. Two gridded climate datasets, CONUS and Daymet, were evaluated for two precipitation gages in the Alameda watersheds. Daymet and CONUS datasets provide daily weather data at a 1 km^2 and 6.25 km^2 spatial resolution, respectively. Figure 32 shows a comparison between the observed daily precipitation and gridded precipitation from the CONUS dataset. The gridded climate data were observed to not replicate observed precipitation satisfactorily in either location. Figure 33 shows the comparison between observed and gridded temperature for gage stations in each of the study region. The gridded temperature is adjusted to account for the difference in altitude between the gage station and the average grid elevation. The gridded temperature is seen to perform better relative to gridded precipitation for all three watersheds. Except for T_{min} at the Rose Peak where the gridded temperature has a negative bias, no biases can be visually observed. In sum, it was determined that the gridded precipitation products were not suitable for use but the gridded temperature data, which is advantageous due to the much longer record than the local data, could be used for the weather generator.
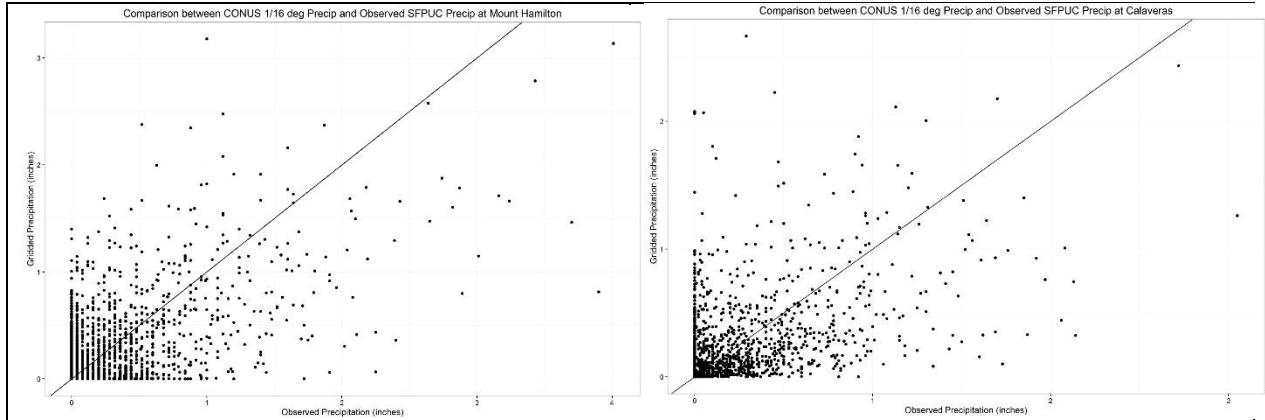
Figure 32: Comparison between observed precipitation and CONUS gridded climate data for two precipitation stations in the East Bay watershed
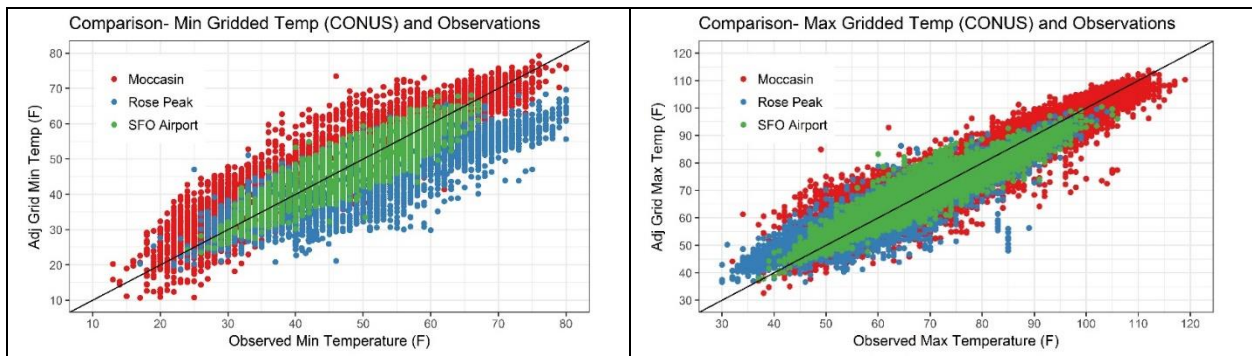
Figure 33: Comparison between observed temperature and CONUS gridded climate data for gages stations across the three watersheds

We select 13 precipitation gages that have the longest records and are representative of precipitation across the three watersheds as input for the weather generator. These include 4 gages from the Peninsula watershed (Upper Crystal Springs, Lower Crystal Springs, San Andreas, Pilarcitos), 3 from the Alameda (Sunol, Calaveras, Hamilton), and 6 from the Upcountry region (Hetch Hetchy, Intake, Moccasin, Sonora, Yosemite, Cherry). For each of the gages, daily precipitation data from 1956-2016 is available. Combined with the gridded temperature data available from 1915-2011, the weather generator was therefore conditioned on 55 years of climate data from 1956-2011.

The first part of the weather generator is comprised of a wavelet autoregressive model (WARM) that is able to reproduce a time series of climate exhibiting a similar spectral structure

to the observed data and avoids the problem of simulated data being overdispersed at the interannual timescale. The WARM approach, using a wavelet transform, decomposes a given time series into different orthogonal signals that represent low-frequency signals and residual noise components. For each of these components, a linear autoregressive (AR) model is fit. The simulated time series is then generated by summing each components' simulation. Details regarding the implementation of the WARM approach and the wavelet transform can be found in *Steinschneider and Brown* [2013].
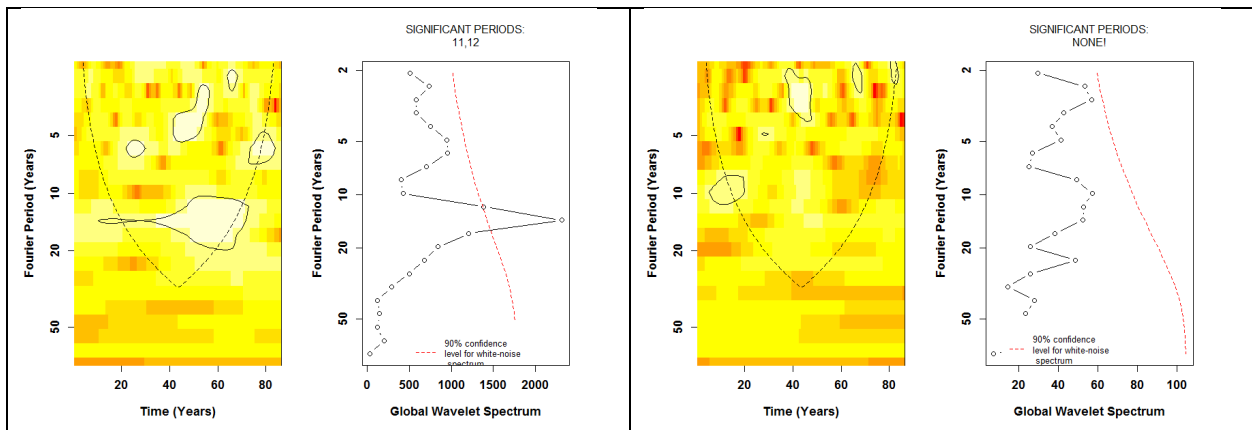
Figure 34: Wavelet power spectrum for the 1st principal component (left) and the 2nd principal component (right) of annual precipitation across the 9 selected gage stations

Typically, the WARM approach is applied to annual area-averaged precipitation over the region of interest. Because there are significant differences in climatology across our region of interest, we instead use principal component analysis (PCA) to obtain an annual time series to preserve the variability between the stations that would be lost if they were simply averaged together. The PCA on annual precipitation for the 13 stations reveals that the first two Principal Component (PC) account for 90% and 5.3% of the variability in the data respectively. We investigate the characteristics of the PCs to determine their suitability for use in the weather generator. Figure 34 shows the wavelet power spectrum for both the PCs, which reveals the previously observed low frequency is embedded in the first PC. The second PC is not seen to

109

exhibit any low frequency signal. Figure 35 shows maps showing correlations between the PCs and sea level pressure (SLP) and sea surface temperature (SST). Similar to annual precipitation in the region, the first PC is correlated with both SLP and SST in areas typically associated with ENSO or the PDO. The second PC is not correlated with either. Since the second PC is not seen to be associated with any climate patterns, we only apply the WARM to the first PC. The 50-year WARM simulated time series are inverted using the gage station loadings from the PCA to obtain simulated annual precipitation at each of the 13 gage stations with the low frequency signal embedded.
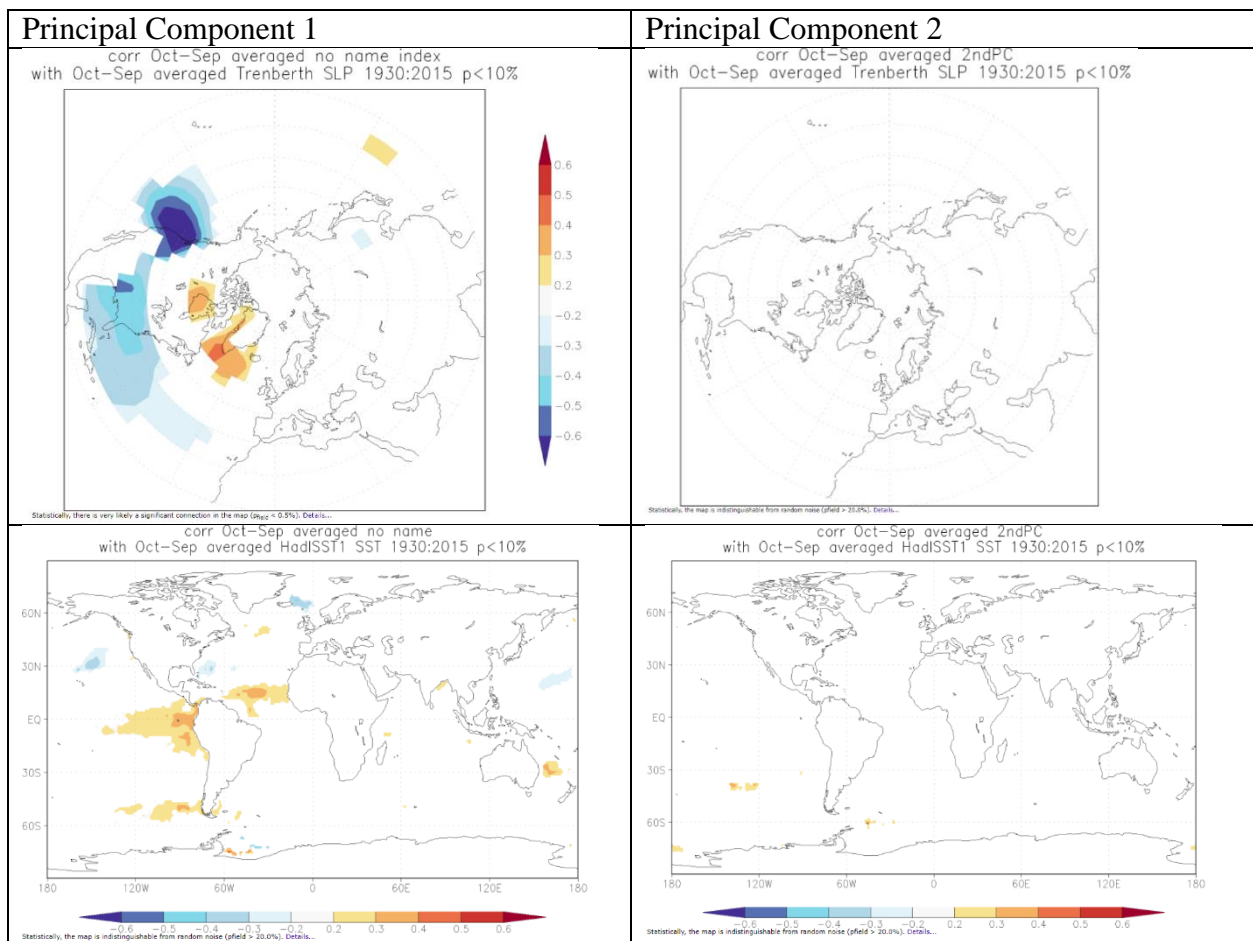
Figure 35: Correlation plots for the first two principal components against averaged sea level pressures (SLP, top) and averaged sea surface temperatures (SST, bottom)

Next, we distribute the annual precipitation time series to the monthly time scale using the method of fragments [*Silva and Portela*, 2012]. For each gage, we first determine which year, k, in the observed record had the most similar annual precipitation to the simulated annual precipitation X_k. We calculate the proportion of annual precipitation in each month for year 'k' and use those proportions to distribute the simulated precipitation, X_k, to monthly values. This produces a time series of monthly precipitation at each gage station. A KNN resampling algorithm is then used to generate daily values for all the weather variables based on the simulated monthly precipitation. For each month M, a vector of simulated precipitation P_s of length 9 (the number of gage stations) is available. We calculate the Euclidean distance, d_j, between P_s and each of the Q vectors of observed monthly precipitation for the same calendar month. We order the distances d_j from smallest to largest and assign weights to the k smallest distances using the discrete kernel function presented below, where j indexes the first k ordered distances d_j.

$$K[d^j] = \frac{\frac{1}{j}}{\sum_{j=1}^{k} \frac{1}{j}} \qquad (6)$$

This approach assigns the greatest weight for the nearest neighbor and smallest for the kth nearest neighbor, with the weights summing to 1. K is set equal to the square root of the number of years of observed data (N=81) as suggested by *Lall and Sharma* [1996]. One of the k-nearest neighbors is then sampled based on these developed weights and the historic month associated with that neighbor is recorded. Daily weather variables for the chosen month in the observed record are then obtained. This is repeated for all months in the simulation to generate a daily time series of time precipitation at each gage station, and gridded T_{max} and T_{min} across the entire system.

Given that droughts present an important challenge to the water utility's ability to meet water demand, a set of 100 daily climate traces for the entire system are generated and sorted

based on the drought severity represented by the precipitation time-series in each trace [*Whateley et al.*, 2016]. We measure drought severity using the sequent peak algorithm to determine the maximum cumulative departure from mean precipitation in each time series. It is calculated as follows:

$$K_t = \max\{0, K_{t-1} + D_t - P_t\} \tag{7}$$

$$K^* = \max\{K_t\} \, over \, all \, t = 1,2, \ldots . t \tag{8}$$

where K_t = cumulative precipitation deficit at time step t, D_t = mean annual precipitation, P_t = precipitation at time step *t*. The maximum cumulative precipitation deficit (K^*) can thus be considered a measure of drought severity, with higher values indicating prolonged periods of reduced rainfall. For each climate trace, K^* is normalized across all the gages and the mean K^* calculated. The traces are ranked based on the severity of drought; seven traces representing the 1st, 10th, 25th, 50th, 75th, 90th and 99th percentile drought severity are selected as representative sequences to be used for the subsequent hydrologic impact assessment. Each of these traces provides a 50-year simulation of climate and together, provide a good representation of natural variability.

5.3.1 Application of climate change

The simulated climate sequences are perturbed incrementally to simulate a wide range of future climate changes. To determine a realistic range for the climate perturbations, we investigate the 2020-2070 CMIP5 climate projections for temperature and precipitation changes across the watersheds in the dry and wet season respectively. The temperature projections for all watersheds, across the different representative concentration pathways (RCP), suggest a warmer future with up to 5° C increase in mean temperature. Greater warming in the summer months than the winter

months is projected. A slightly greater increase in temperature is projected for the Upcountry watershed, compared to the East Bay/Peninsula watersheds. For precipitation, no clear direction of change can be determined from the projections.

Based on the CMIP5 projections, precipitation is varied from -20% to 20% of historic average with 10% increments and temperature from 0 to 5° C with 1 degree increments to produce 30 different combinations of climate change. These changes in climate are applied in a transient manner over the 50-year period. To enable an assessment of the hydrologic impact of differential change in climate across the SFPUC watersheds, climate change is applied in two ways: (i) uniformly across space and time, and (ii) differentially across space and time. The resultant hydrology from these two approaches is then compared.

The observed historical trends in maximum and minimum temperature are consistent with the GCM projections of increased warning in the summers. However, the trend analysis indicates a greater warming in the local watersheds (East Bay and Peninsula) than the Upcountry watersheds, contrary to GCM projections. We decide to use the observed trends in temperature to simulate the spatial and temporal variation in climate change. Due to a lack of observed trend in historic precipitation, and no clear direction of change in GCM projections, we only explore spatial and temporal differential changes in temperature. Historical trends in T_{max} and T_{min} and for each region (Peninsula, East Bay and Upcountry) in each season (winter and summer) are calculated using the non-parametric Theil-Sen estimator. These trends are applied to the simulated climate sequences, while maintaining the overall climate change consistent with the uniform climate change setting as shown in Equations 9 and 10.

$$X_{it}^* = X_{it} + C.Y + U_{r[i]s[t]}.Y \qquad (9)$$

$$\sum_{i=1}^{n} \sum_{t=1}^{m} U_{r[i]s[t]} \cdot Y = 0 \qquad (10)$$

where X_{it} is the vector representing simulated climate (T$_{max}$ or T$_{min}$) for each day t at each grid cell i in a given year; r represents the region a grid cell i is located in; s denotes the season; Y represents years since the start of the simulation; the uniform climate change applied is represented by C and $U_{j[i]s[t]}$ denotes the spatially and temporally unique trend applied. For example, for a 2° C increase in temperature, in the uniform climate change sequences, the uniform warming trend (C) is applied to the entire region to produce climate that is 2° C warmer by the end of 2070. In the non-uniform climate change, the observed trends ($U_{r[i]s[t]}$) are superimposed on the uniform warming trend (C). These observed trends are scaled to have zero mean to ensure the average warming across the regions is still 2° C . Figure 36 illustrates the spatial patterns of the average dry season maximum temperature in the Upcountry and East Bay regions with spatially and temporally varying climate change, with a 1° C overall temperature increase by the end of 2070. Compared to the uniform warming case, the spatially and temporally varying climate change results in (slightly) greater warming in the East Bay watershed.
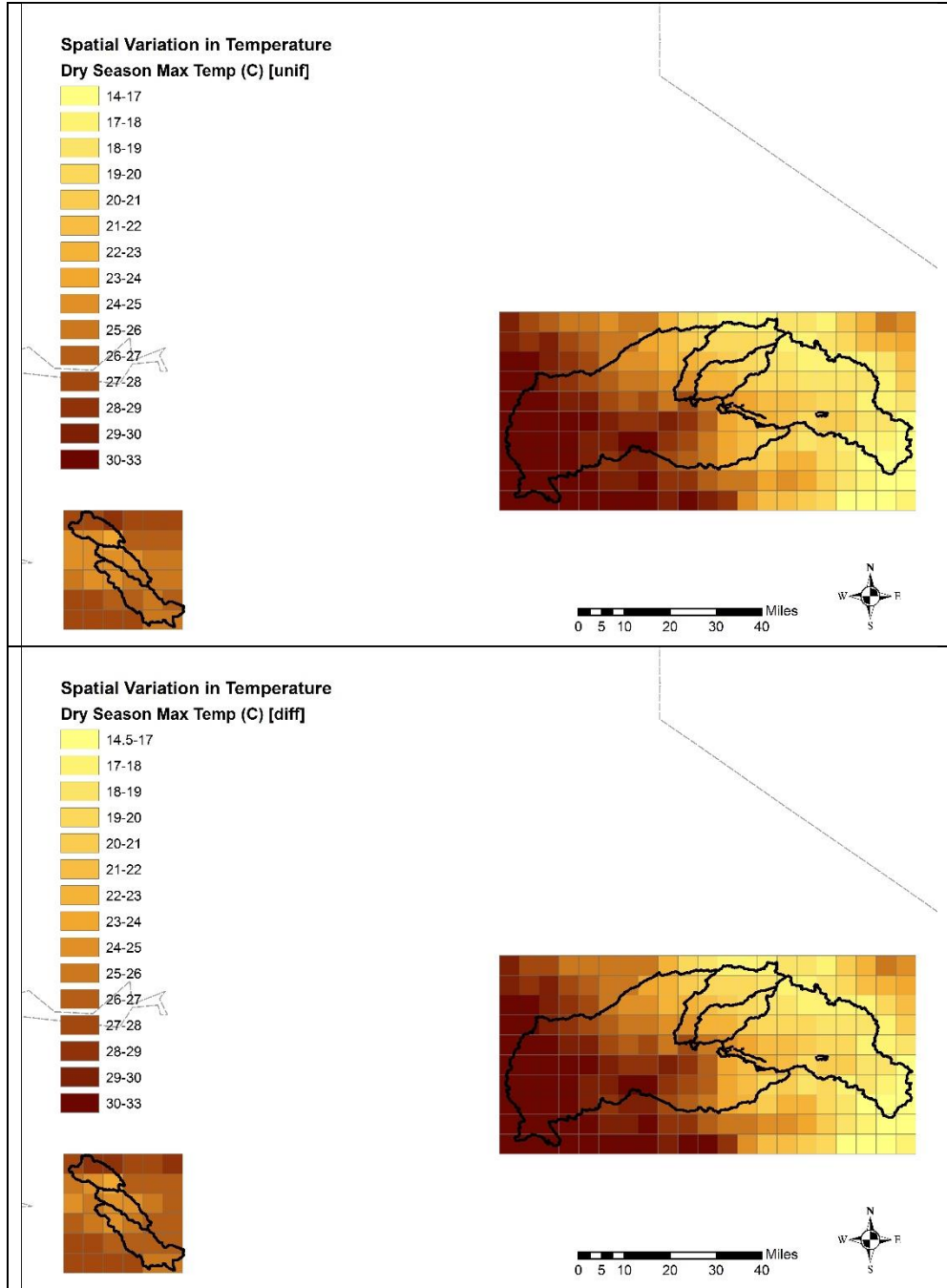
Figure 36: Spatial patterns of dry season average maximum temperature with uniform (top) and spatially and temporally varying climate changes (bottom)

5.4 Hydrologic model development

To represent hydrologic processes in the contributing watersheds for RWS, a suite of five hydrologic models is used for this study. Summary of each watershed's hydroclimatology is shown in Table 2. Each of the hydrologic model used here simulates 'unaltered' daily streamflow entering into SFPUC reservoirs using daily time-series of temperature and precipitation as model inputs. Hydrology in only the Upcountry and East Bay watersheds is considered in this study; the Peninsula watersheds are not included since they comprise a relatively small (<5%) of total system storage and are heavily regulated.

Table 2: Summary statistics for the five watersheds for which hydrologic impacts of climate change are evaluated

Watershed	Basin area (km^2)	Mean annual precipitation (mm)	Mean annual T_{max} (C)	Mean annual T_{min} (C)	Mean annual runoff (MCM)
Hetch Hetchy	1174	914.4	19.3	5.2	972
Cherry-Eleanor	509	1200	19.0	4.8	563
Arroyo Hondo	206	606	16.3	9.1	40.2
Alameda Creek	105	532	17.7	9.9	17.4
San Antonio	101	454	22.9	9.0	7.7

5.4.1 Upcountry

Three major reservoirs are located in the Upcountry watersheds—Cherry, Eleanor and Hetch Hetchy. Cherry and Eleanor reservoirs are connected through a pipeline, and hence treated operationally as one reservoir. Precipitation-Runoff Modeling System (PRMS) models developed by SFPUC to simulate inflows into the reservoirs (Cherry-Eleanor and Hetch Hetchy) are used to simulate the Upcountry hydrology for this study.

5.4.2 East Bay

The East Bay watersheds comprise of the Arroyo Hondo, Upper Alameda Creek (above Alameda Creek Diversion Dam), and San Antonio subwatersheds. These subwatersheds provide inflow to SFPUC owned facilities, including, respectively, two major storage reservoirs, Calaveras and San Antonio, and a diversion facility, the Alameda Creek Diversion Dam, which diverts water to the Calaveras Reservoir.

Despite the relatively small area of the Alameda watersheds, average annual precipitation varies considerably within the region due to altitudinal differences. The highest point in the watershed, Mount Hamilton, has an elevation of 4,400 feet above sea level. Most of the precipitation in the region falls during the winter months, with very little precipitation during the April-September period. Because of the small area and concentrated precipitation period, many streams in the watersheds are ephemeral. Furthermore, the combination of the steep terrain and winter storms with high precipitation intensity makes the streams extremely 'flashy', necessitating careful management of the reservoirs into which the watersheds drain.

5.4.2.1 Model setup

For each of the three subwatersheds in this region, Sacramento Soil Moisture Accounting (SAC-SMA) models were developed to generate inflows into the SFPUC reservoirs under a variety of climate change scenarios. The SAC-SMA model, a lumped conceptual hydrologic model, was coupled with a river routing model to estimate the hydrologic response of the watershed. The coupling with the river routing model makes it fully distributed and suitable for the significant topographic and climatic heterogeneity of the region. We use the acronym SAC-SMA-DS to refer to the distributed version of this coupled model. In addition to the river routing model, SAC-SMA-

DS consists of modules representing soil moisture accounting, evapotranspiration and runoff routing (i.e., unit hydrograph) processes. Potential evapotranspiration (PET) in the SAC-SMA-DS method is calculated using the Hamon method, which uses daily mean temperature and daylight hours to determine daily PET. For river channel routing, the linearized Saint-Venant Equation is used.

The location of each subwatershed in the Alameda hydrologic region is shown in Figure 37, while Table 3 shows the model configurations for the Alameda subwatersheds, including the area and the number of HRUs of each subwatershed.

Table 3: SAC-SMA-DS configurations for the Alameda sub-watershed

Subwatershed	# of HRUs	Calibration/Validation Periods
Arroyo Hondo	23	Calibration: 1997-2006
Alameda Creek	10	Validation: 2006-2014
San Antonio	13	

The significant variability in precipitation due to altitudinal differences requires finer resolution climate input than would be available from a single precipitation gage. The PRISM dataset [*Daly et al.*, 2015] provides long-term averages for monthly precipitation at each grid cell across the watershed, at a ~4 km grid scale. Spatial correlations (unique for each month) from the PRISM dataset were used to estimate daily precipitation at each grid cell in the basin, with daily precipitation data from gages at Mt Hamilton, Calaveras Res and San Antonio. For each grid cell, the nearest precipitation gage was used. The PRISM climate grid was also used for the spatial discretization needed for modeling hydrologic processes. i.e., the HRUs in the Alameda region were defined by PRISM climate grids.
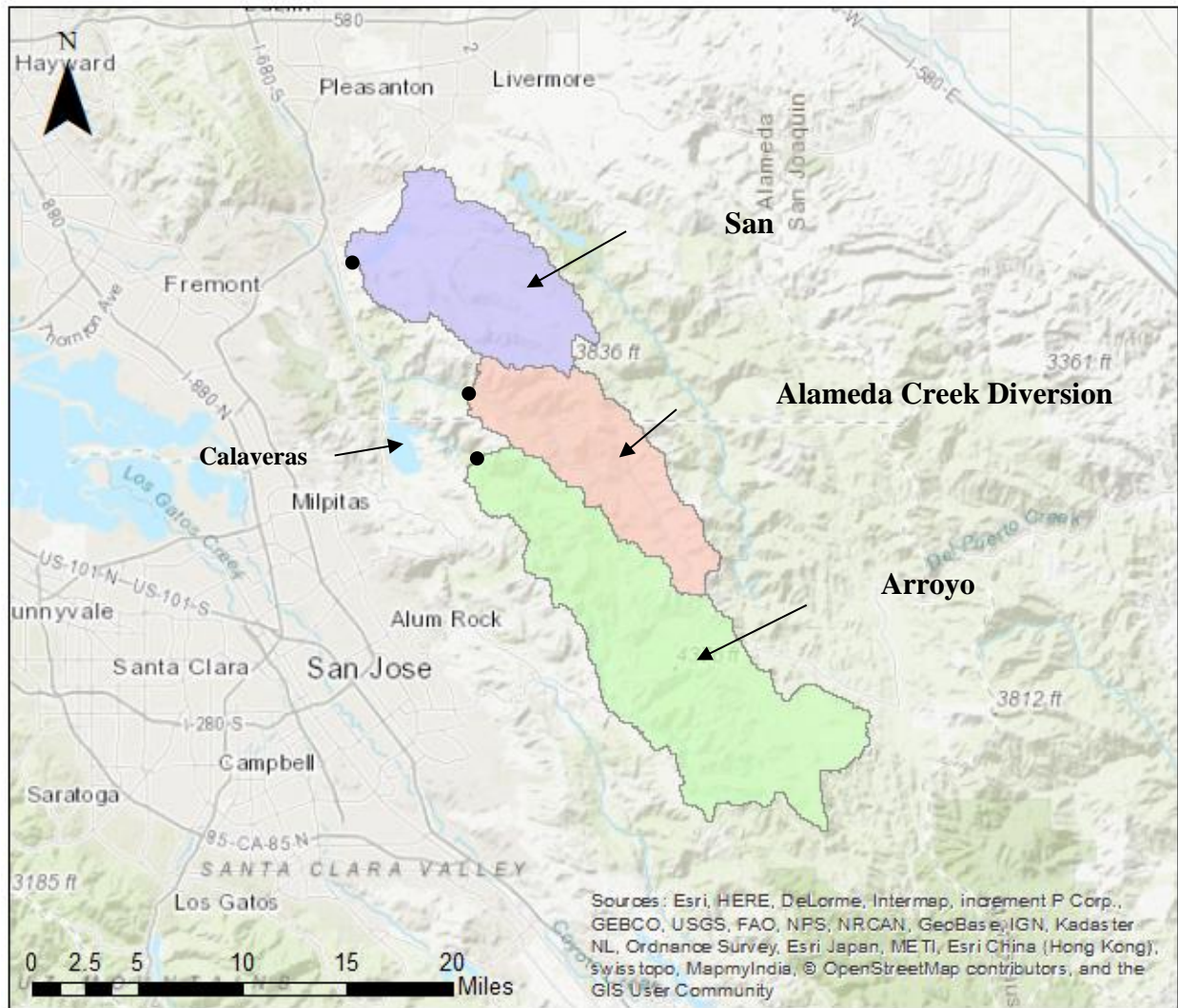
Figure 37: Alameda hydrologic region subwatersheds. Subwatershed outlets are shown as black dots.

5.4.2.2 Calibration

The three hydrologic models were calibrated to observed streamflow at the three main water facilities. The Arroyo Hondo hydrologic model was calibrated to observed streamflow at the USGS Arroyo Hondo gage just upstream of the Calaveras Reservoir. Flows less than 30 cubic feet second occur over 80% of the time in the Arroyo Hondo but represent only 11% of total flow by volume.

Observed streamflow is available from 1995-2015. The available data was split into half for calibration and validation, with the first two years of observations used for model warm-up. Observed streamflow from 1997-2005 was used for model calibration, and the model was validated using streamflow from 2006-2014. Hydrologic parameters for each HRU were calibrated using genetic algorithm (GA) as the optimization method.

The objective function used in the GA is based on the Kling-Gupta Efficiency (KGE) metric (Gupta, et al., 2009), which equally weights model mean bias, variance bias and correlation with observations. The KGE is appropriate for settings where there is significant variation in streamflow, as in the Alameda region.

The objective function is comprised of the KGE metric applied to three equally weighted components of the flow regime observed in the hydrograph and found to be particularly important for SFPUC operations: 1) modeled daily flow, 2) logarithmically transformed daily flow, and 3) monthly summary flow (April-September). The logarithmically transformed daily flow component emphasizes low flow conditions generally. The summer monthly flow component recognizes the importance of environmental streamflow releases during the warm low flow period and further emphasizes total summer volume as opposed to just low flow conditions. An average of the three components is used in the objective function.

During the iterative calibration process, a trade-off between estimation of peak flow and low-flows was observed. Improved model performance during the summer months was seen to slightly reduce model performance with regards to winter flows. However, this trade-off did not materially affect calibration, due to the equal weighting of the components.

As mentioned previously, the climatology and topography of the region means that streamflow is characterized by large periods of low flow, comprised of baseflow, with large peaks

resulting from winter storms. Flow separation is performed in the hydrologic models to more realistically replicate the different sources of streamflow. In the calibrated hydrologic model, baseflow accounts for approximately 20% of total annual flow.

Figure 38 shows sample observed and simulated monthly hydrographs with NSE and pBias for the entire time series for the Alameda hydrologic region. NSE shows very good monthly performance, with 0.72, 0.90, and 0.89 for San Antonio, Alameda Creek Diversion Dam, and Arroyo Hondo, respectively. In addition to these basic comparisons, model calibration and validation results for a wide range of different metrics of interest, including for different temporal scopes. A representative sample of these validation results for monthly flows, total annual flow, and average annual 60-day maximum flow is shown in Appendix C.
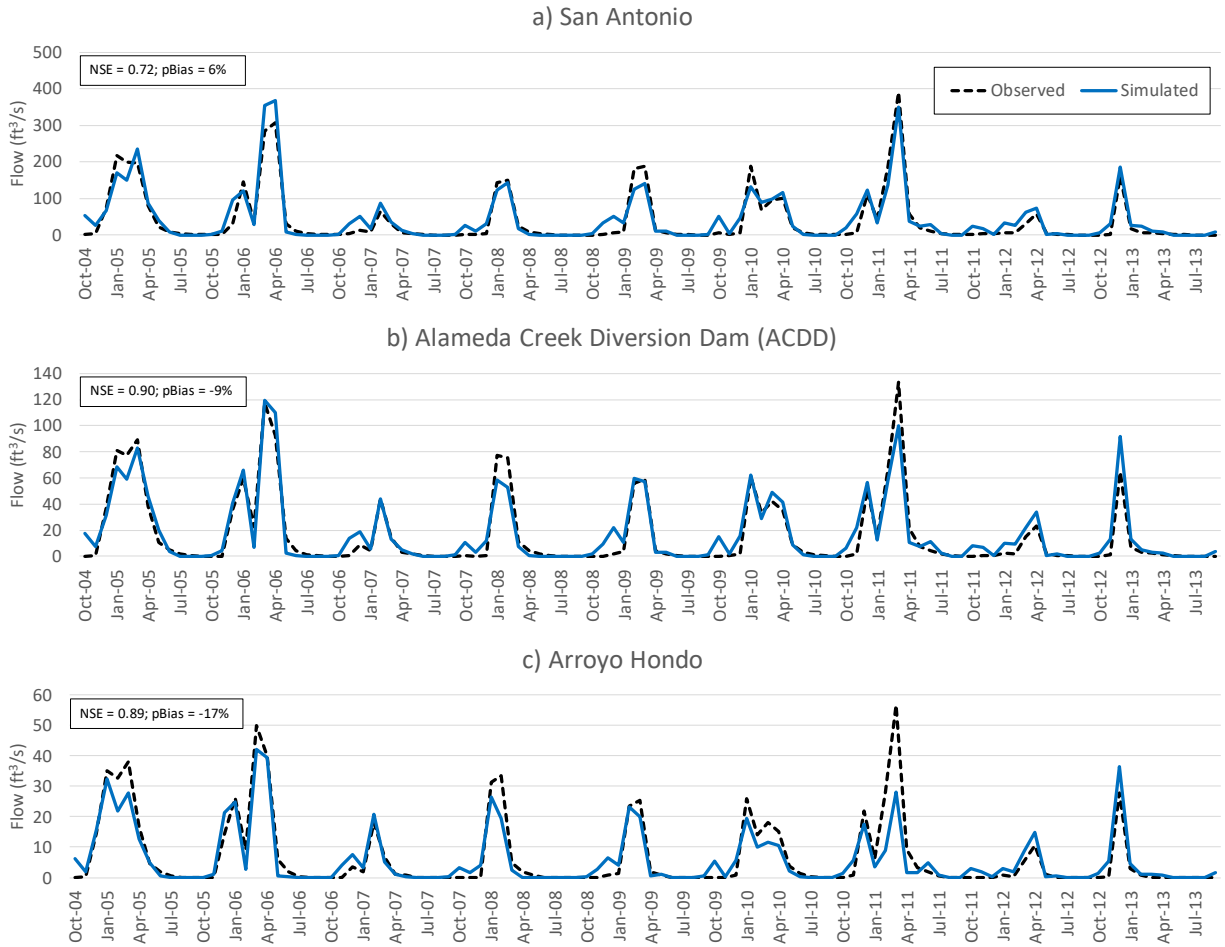
Figure 38: Observed and simulated hydrographs for the Alameda hydrologic region, with Nash-Sutcliffe Efficiency (NSE) and percent bias (pBias). NSE and pBias are for the entire series, not the subset shown here.

5.5. Results and Discussion

5.5.1 Weather generator performance

The weather generator is run to produce climate realizations of daily precipitation and temperature, each 50 years long (length of historic record used). We evaluate the performance of the weather generator by comparing the characteristics of each weather variable at different time scales.
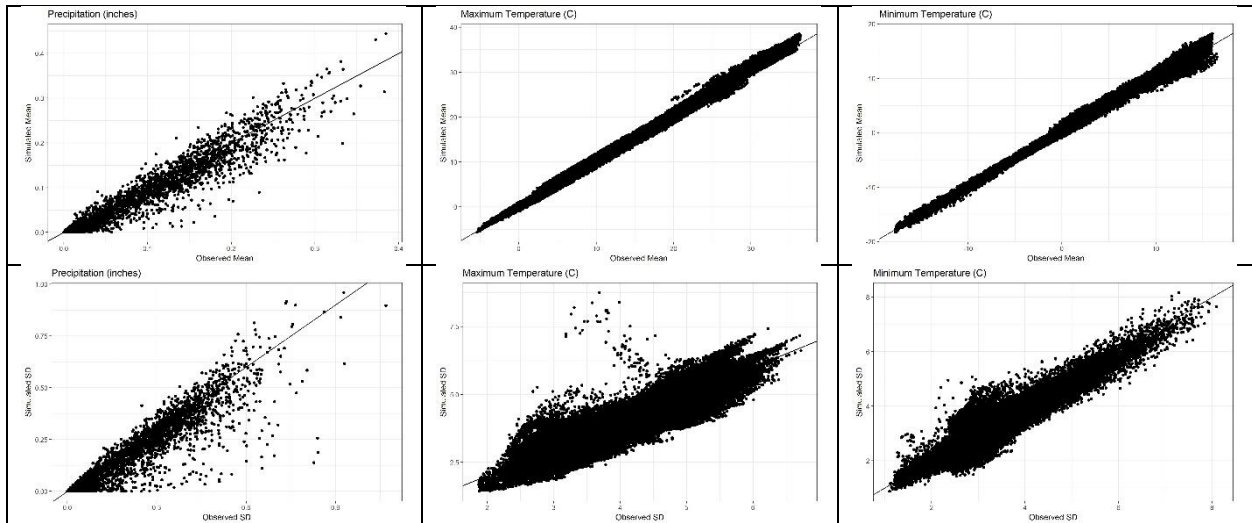
Figure 39: Mean and standard deviation of daily precipitation, maximum temperature and minimum temperature for all stations/grid cells and months, Median values across 50 different simulations are shown against the observed values
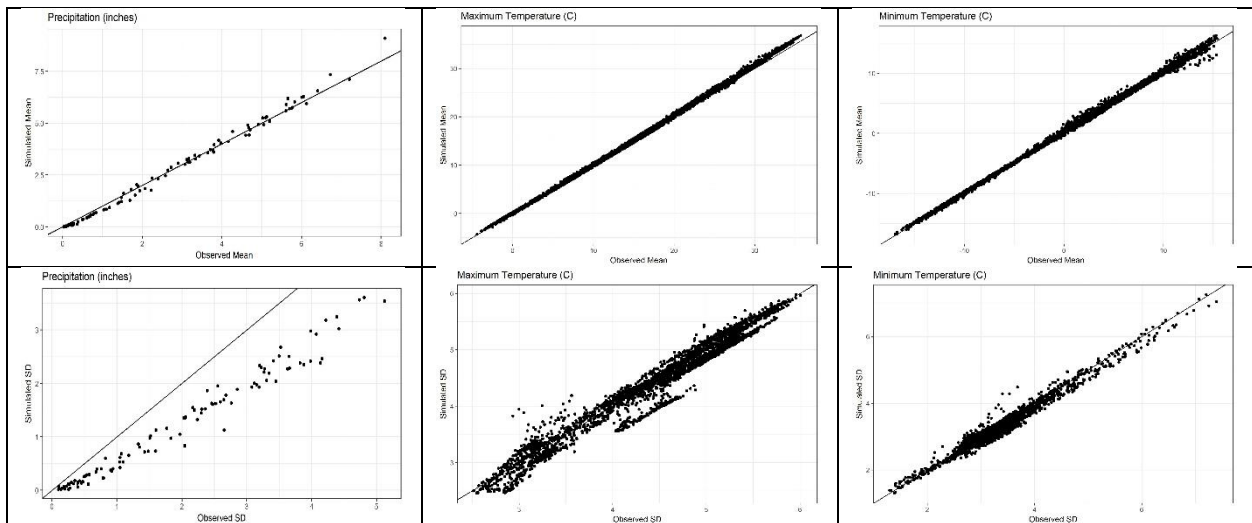
Figure 40: Mean and standard deviation of monthly precipitation, maximum temperature and minimum temperature for all stations/grid cells and months, Median values across 50 different simulations are shown against the observed values

Figure 39 shows the mean and standard deviation for daily precipitation, maximum temperature and minimum temperature for all combinations of months and gage stations/grid cells. The median values of these statistics over the 50 different simulations are used for comparison with the historic statistics. The results show good performance of the simulated time series. The standard deviation of daily temperature in some cases tends to have a higher standard deviation.

Figure 40 shows a similar comparison at a monthly time scale. The results show again a good

performance except for the under-estimation of standard deviation of monthly precipitation.
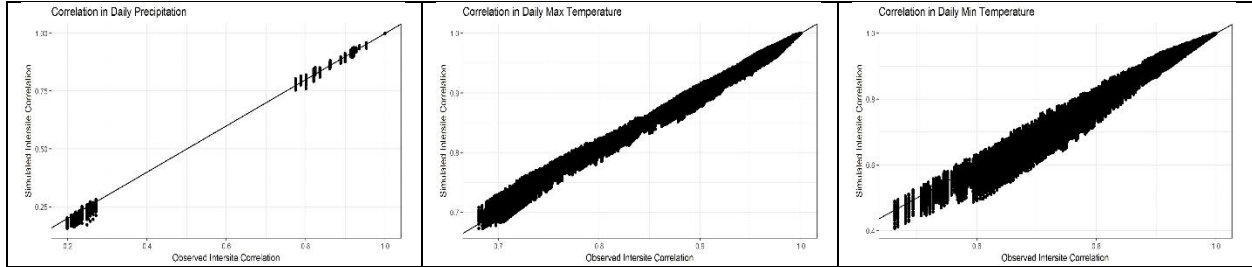
Figure 41: Intersite correlations for daily precipitation, maximum temperature, and minimum
temperature. Median values across 50 different simulations are shown against the observed
values for all stations/grid cells.

Figure 41 shows the intersite correlations of a given variable across different stations

(precipitation) and grid cells (temperature) for daily data, using the median values from the 50

simulations. Because we resample the climate variables together for the entire system, the results

show that the correlation between the sites is well maintained. Similar results for cross correlations

between different variables for a given site are also observed (not shown here). Figure 42 shows a

comparison between the historic and simulated average annual precipitation across the different

gage stations.

Figure 43 presents a measure of drought severity based on annual precipitation simulated

by the weather generator for a precipitation in each of the three regions, and compares it to the

observed record. The distribution of the drought severity of 100 simulated annual precipitation

time series at each gage is shown using box plots. The figure shows that for the precipitation gages

in the local watersheds (Calaveras (East Bay) and Pilarcitos (Peninsula)), the simulated annual

precipitation time series accurately reproduces the observed drought severity (solid pink dot). For

the Hetch Hetchy gage, the simulated annual precipitation on average tends to underestimate the

drought severity, suggesting an overestimation of precipitation.
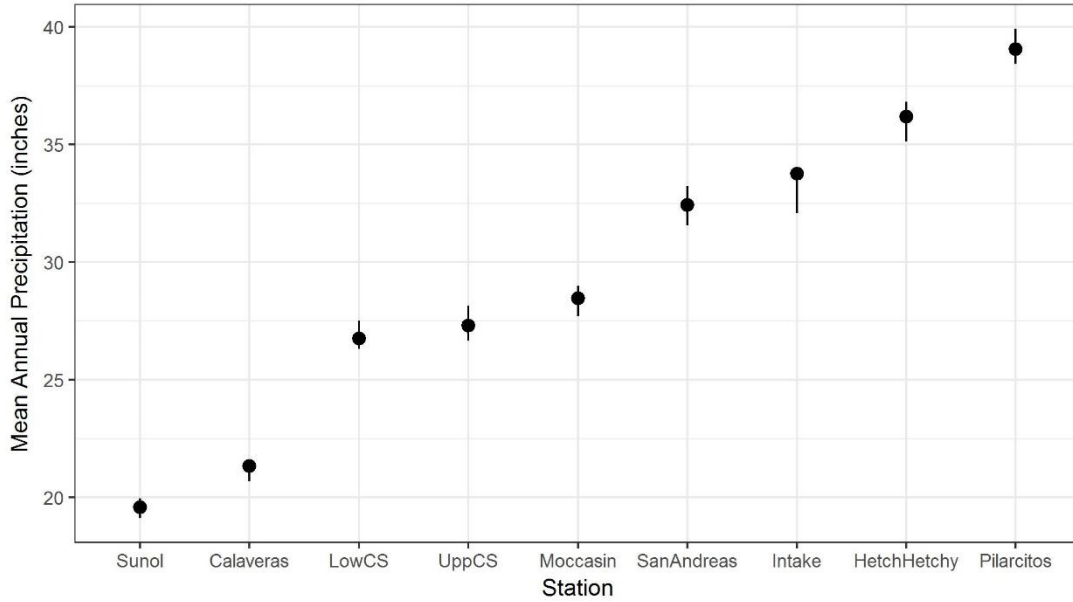
Figure 42: Distribution of simulated annual average precipitation across the different stations. The solid dot represents the observed annual precipitation while the lines represent the range of the simulated data.
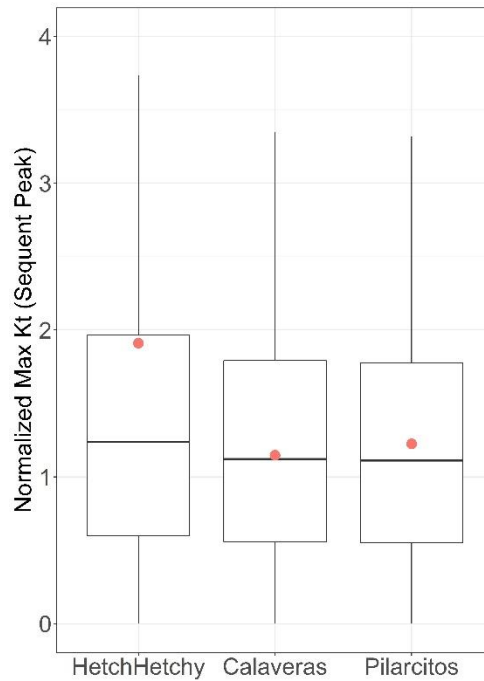
Figure 43: Drought severity simulated by the weather generator annual precipitation for the Hetch Hetchy (Upcountry), Calaveras (East Bay) and Pilarcitos (Peninsula) watersheds. The solid pink dots indicate the drought severity based on the observed record.
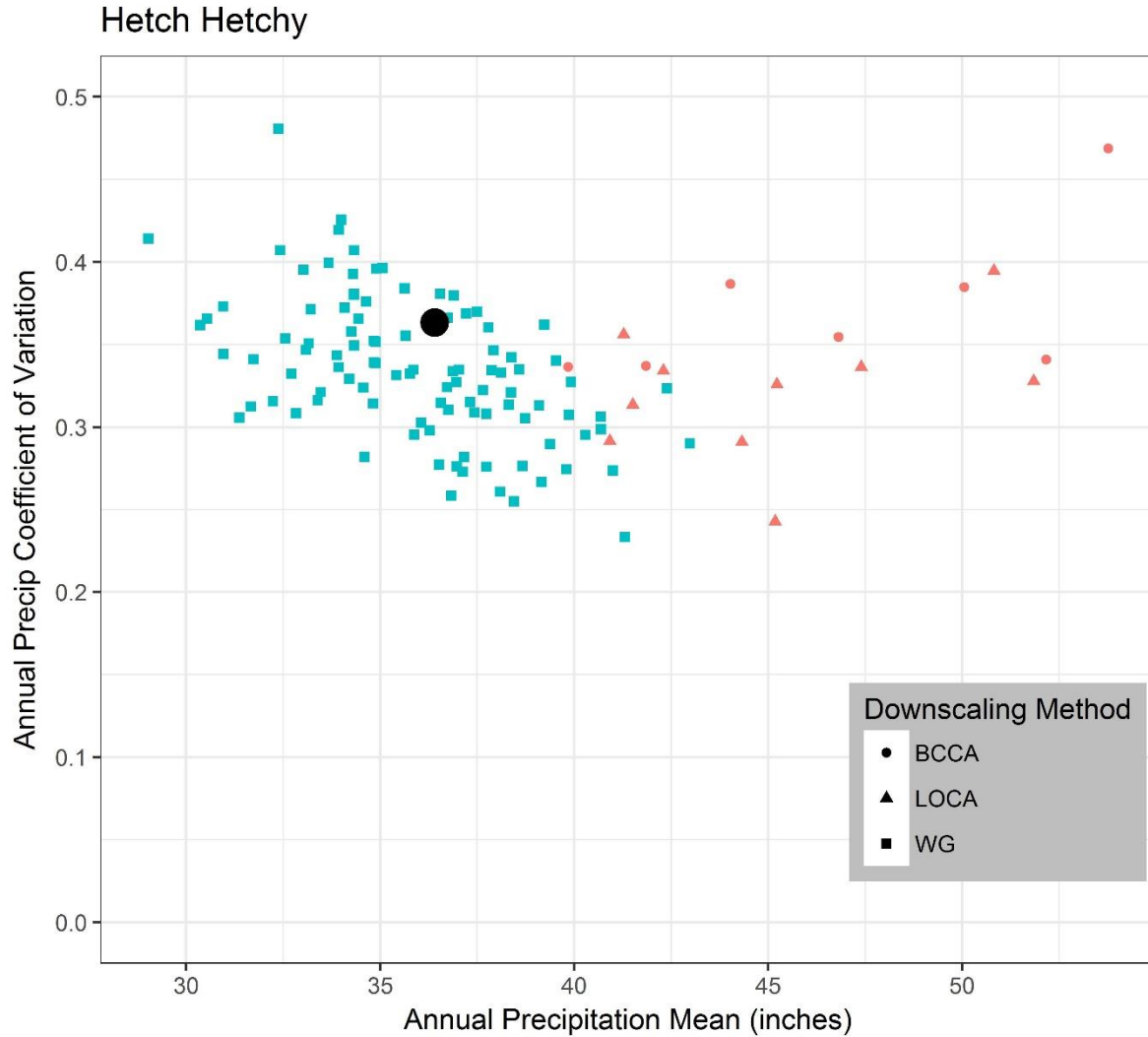
Figure 44: The mean and coefficient of variation of annual precipitation at the Hetch Hetchy precipitation gage. Statistics for observed (black), simulated (blue), and GCM projected (red) precipitation are shown. Shapes denote the different downscaling method used.

Figure 44 shows a comparison of changes in the magnitude, frequency and variability for simulated precipitation at the Hetch Hetchy gage using different downscaling approaches. 100 weather generator runs, each 50 years long, run under baseline conditions (no climate change) are shown. The ensemble of GCM projections of 2020-2070 included in the study for this region indicate an increase in both the mean and standard deviation of annual precipitation over the historic average (black circle). A slight decrease in coefficient of variation is also observed. The lag-1 autocorrelation (not shown) values exhibited by the projections are similar to the low value

of observed autocorrelation (0.03) for precipitation at this gage station. No systematic difference can be observed in the precipitation projections from the BCCA and LOCA downscaling. The weather generator runs exhibit climate characteristics comparable to the observed record and present a range of plausible climates that can be run to evaluate the effect of internal climate variability on regional hydrology. The weather generator is used in this study to explore a much wider range of future climate than those offered by the GCMs.

5.5.2 Impact on hydrology
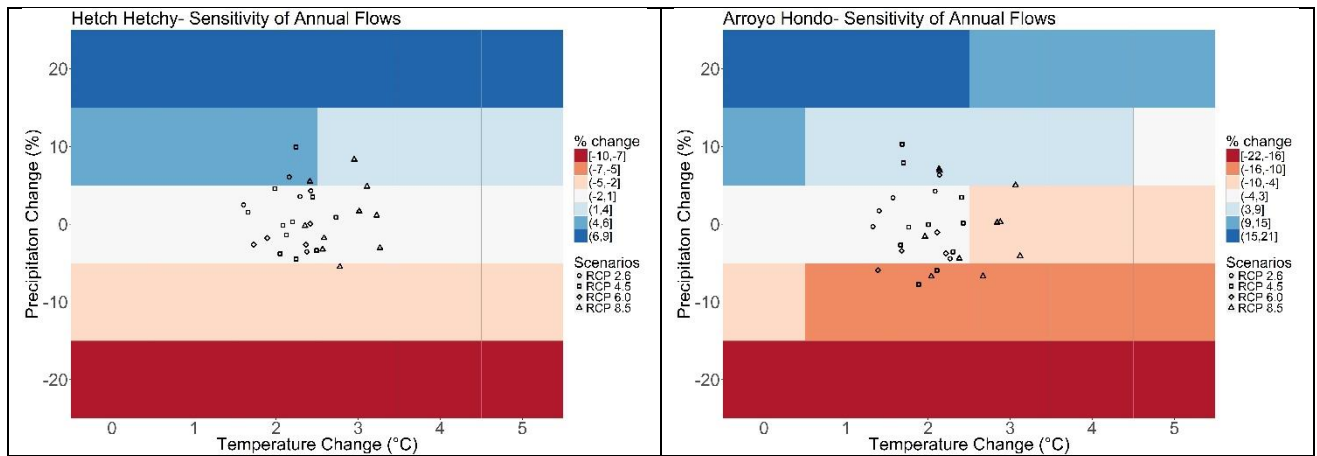
Figure 45: Sensitivity of mean annual runoff to changes in temperature and precipitation for the Hetchy Hetchy (left) and Arroyo Hondo (right) watersheds. CMIP5 GCM projections for different emission scenarios are overlain.

The stochastic weather generator was used to simulate a variety of plausible future climates, which are used to drive the hydrologic models. Figure 45 shows the sensitivity of mean annual inflows to the Hetch Hetchy (Upcountry) and Arroyo Hondo (East Bay) watersheds to changes in temperature and precipitation, in form of a climate response surface. The hydrologic impact for the median climate trace is shown, as described in the methodology section. The response surface shows the percentage change in mean annual inflows under various combinations of change in precipitation and warming compared to mean runoff under the no climate change

127

setting. The intensity of change is reflected in the shade of color (darker for greater percentage change), while the direction of the change is shown by the color (red hues for decrease in mean annual inflow). The change in the color and intensity of the response surface horizontally and vertically indicates the relative sensitivity of the inflows to temperature and precipitation. For example, in Figure 45 for a given temperature change, as we move vertically (different precipitation changes), we observe changing shades and color, while for a given precipitation change, as we move horizontally (different temperature changes).

Figure 45 shows that mean annual inflows to the Hetch Hetchy reservoir are only moderately sensitive to temperature, but are highly sensitive to changes in precipitation. This is in contrast to findings in earlier studies based on GCM projections that suggested precipitation change to have less influence on hydrology [*Lettenmaier and Sheer*, 1991]. For a 20% decrease in precipitation and 5° C increase in temperature by 2070, the mean annual inflows decrease by around 10%. This magnitude of change is consistent with those noted in more recent studies of flows in the Tuolumne River [*Vicuna et al.*, 2007; *Hydrocomp*, 2012]. While temperature change is expected to affect magnitude of flows in the Sierra Nevada watersheds, the more important impact in terms of hydrology is in the shifting of the hydrograph due to earlier melting. As temperature increases, MAAF-15 and MAAF-60 is seen to increase. This is likely a result of greater warming leading to greater rate of snowmelt in the winter/spring seasons, coupled with a larger proportion of winter precipitation falling as rain instead of snow.

Inflows into Calaveras reservoir from the Arroyo Hondo watershed show a greater sensitivity to temperature changes as well as precipitation changes. Unlike the Hetch Hetchy, the Arroyo Hondo watershed is not snowfed. Temperature influences hydrology in the local watersheds (including Arroyo Hondo) primarily through changes in evapotranspiration. Higher

128

temperatures are seen to lead to decreased flows; this effect is especially more pronounced in the dry summer months. Evapotranspiration comprises a relatively larger part of the total water budget for Arroyo Hondo than it does for the Hetch Hetchy watershed; this leads to a comparatively higher percentage change in Arroyo Hondo annual runoff for a given temperature change.

Overlain on both climate response surfaces are bias corrected spatially downscaled CMIP5 projections of climate change for different emission scenarios from the GCMs identified by the CCTAG. The GCMs project for both the regions, an increase in warming. There is less agreement regarding changes in precipitation; for the Hetch Hetchy watershed, a few projections suggest a minimal decrease in precipitation while others show an increase. For Arroyo Hondo, there is a wider range of projected precipitation changes.

The climate response surfaces shown above are for spatially and temporally uniform changes in temperature. Next, we examine the extent to which spatially and temporal differential changes in temperature affect resulting hydrology. To isolate and determine the effect of different seasonal warming trends, we compare various measures of hydrology under differential climate change with those observed for uniform climate change within each of the watersheds. Among the hydrologic measures compared are mean annual flows, mean summer and winter flows, and MAAF-15 and MAAF-60. For all of the watersheds across all variables, we do not observe a significant difference between the two approaches.

To determine whether representation of spatial differences in warming affect hydrology, we compare the ratio of total flows between the Upcountry and the East Bay watersheds. We calculate average aggregate basin-wide flows for each of the regions (Upcountry and East Bay) under uniform and spatially varying climate change respectively. These two ratios are then compared to assess whether the proportion of flows across the two regions varies across the

different simulations. In the spatially varying climate change, a greater warming trend is applied to the East Bay watersheds compared to the Upcountry watersheds. Again, little to no change in the proportion of flows between the uniform and spatially varying climate change is observed.

The negligible hydrologic impact of differential climate change observed here is primarily because of the relatively little small differences in the trends applied. While warming in the East Bay is observed to be greater than in Upcountry, the difference in the warming translates to less than 1 C° change over 50 years across the regions.
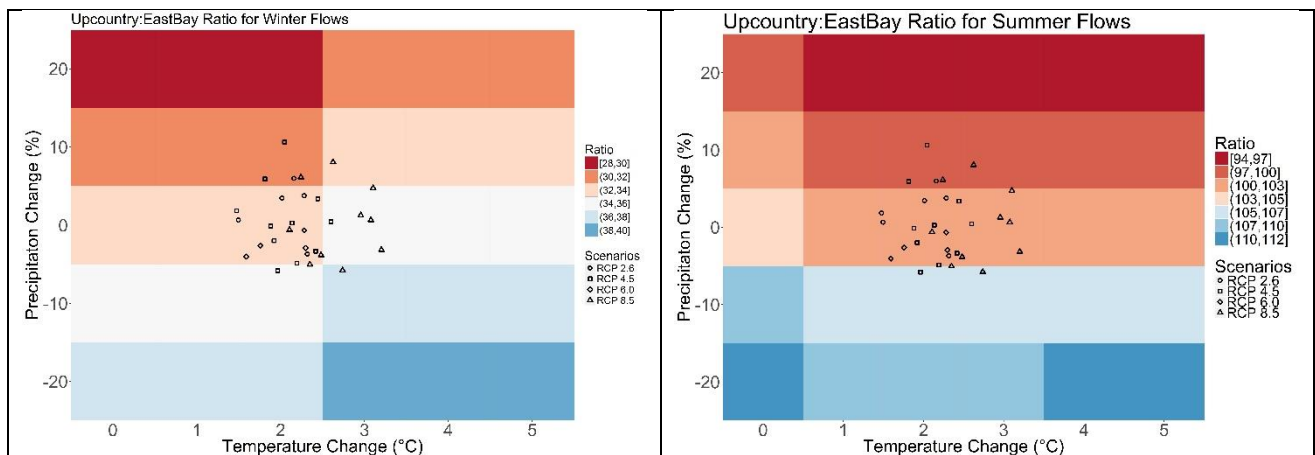
Figure 46: Ratio of basin-wide flows between Upcountry and the East Bay watersheds for the winter (left) and summer (right) seasons respectively, under climate changes.

Figure 46 shows the sensitivity of Upcountry:East Bay (UC:EB) basin-wide flow ratios to different combinations of uniform precipitation and temperature changes in the winter and summer seasons respectively. We observe that the ratios are sensitive to changes in both temperature and precipitation. Under baseline conditions (no climate change), the UC:EB ratio of basin-wide winter flows is 34. For an increase in temperature, the winter flow ratio increases due to a combination of increased Upcountry flows and decreased East Bay flows. A uniform basin-wide increase in precipitation is associated with a decrease in ratio.

A similar response to precipitation change is observed for the UC:EB summer flow ratio as well. For temperature changes, the opposite effect is seen: increasing temperatures lead to

decreasing ratio. In general, greater variation in the UC:EB ratio for summer flows compared to the winter flows is observed. This likely stems from the greater variability in summer flows in the East Bay watersheds.

This change in flow ratios is important for SFPUC from an operational standpoint because it indicates the extent to which the utility's water supply is dependent on flows in the Sierra Nevada.
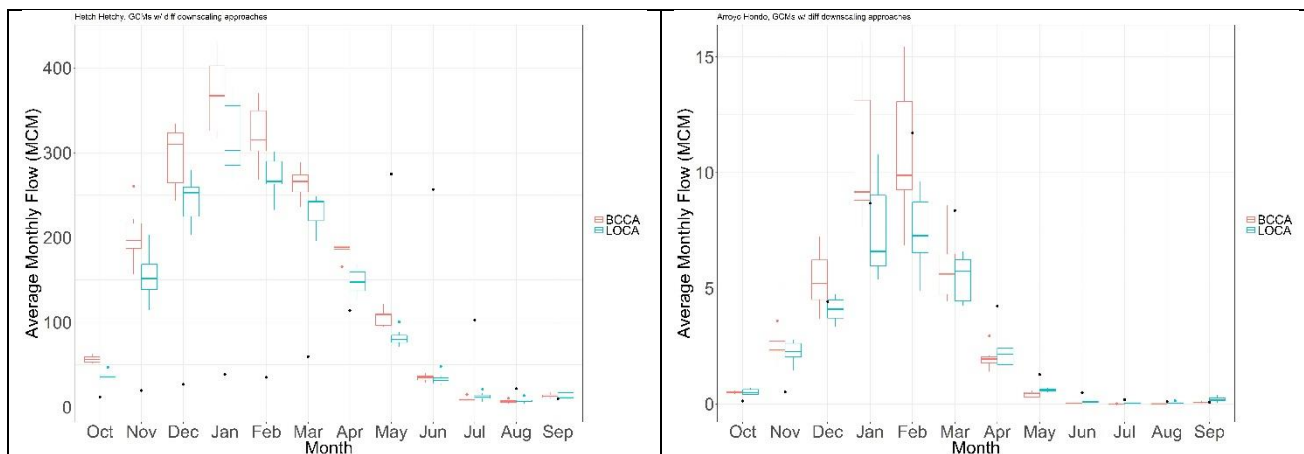
Figure 47: Average monthly flows for the BCCA (blue) and LOCA (red) GCM climate projections for the Hetch Hetchy (left) and Arroyo Hondo (right) watersheds. Solid black dots represent the observed monthly flows.

Next, we examine the impact of the different GCM downscaling approaches on hydrology. Figure 47 shows average monthly flows in the Hetch Hetchy (left panel) and Arroyo Hondo (right panel) watersheds for the BCCA (red) and LOCA GCM projections. The solid black dots show the observed monthly flows in the watersheds. For both the watersheds considered, projected monthly flows based on the BCCA projection tend to be higher than those for the LOCA projection, especially in the winter season when most of the flow occurs. For the Hetch Hetchy basin, a significant shift in the hydrograph is observed; peak flows shift four months earlier from May to January. This finding, consistent with the existing literature [*Lettenmaier and Sheer*, 1991], translates to a reduction of storage since an increase in risks of winter floods would require flood

131

storage at the expense of conservation storage. This would ultimately lead to reduced system reliability. For the Hetch Hetchy basin, an increase in total flows under both GCM downscaling approaches as a result of increasing precipitation is projected.

For the Arroyo Hondo watershed, the LOCA downscaled GCM projections suggest a decrease in total flows, resulting from significant temperature increases coupled with decreased precipitation. The BCCA projections also suggest a decrease in total flows, but to a lesser extent. This difference is primarily because LOCA downscaled GCMs project significantly less precipitation compared to the BCCA projections. GCM projections from both the downscaling approaches suggest peak winter flows shifting a month earlier.

Table 4: Summary of results from downscaled GCM climate simulations for the Arroyo Hondo watershed

Downscaling Approach	Model	Annual Precip (mm)	Annual Ave. Temp (C)	Annual Flow (MCM)	MAAF- 15 days (MCM)	MAAF- 60 days (MCM)
BCCA	access1	579	16.0	31.6	0.76	0.37
BCCA	canesm2	721	16.5	51.8	1.24	0.62
BCCA	ccsm4	606	15.6	34.6	0.79	0.39
BCCA	cesm1	676	15.8	44.0	0.96	0.51
BCCA	cnrm	710	15.7	45.7	1.14	0.55
BCCA	gfdl	625	16.4	34.9	0.68	0.37
BCCA	miroc5	541	15.7	27.8	0.56	0.30
LOCA	access1	535	16.2	26.0	0.57	0.28
LOCA	canesm2	623	16.8	36.3	0.78	0.40
LOCA	ccsm4	569	15.9	28.5	0.57	0.30
LOCA	cesm1	596	15.8	31.9	0.63	0.34
LOCA	cmcc	536	16.0	26.1	0.52	0.26
LOCA	cnrm	656	15.7	37.7	0.79	0.41
LOCA	gfdl	566	16.3	27.7	0.52	0.27
LOCA	hadgem2-cc	569	16.3	27.2	0.53	0.27
LOCA	hadgem2-es	525	16.6	24.7	0.49	0.24
LOCA	miroc5	511	15.8	24.2	0.46	0.25
observed		670	13	40.1	1.02	0.49

Table 4 presents a summary of the key climatic inputs and hydrologic outputs from the simulations runs for the Arroyo Hondo watershed. Results for each of the selected GCMs, and the associated downscaling approach are shown, along with the observed climate and hydrology for the watershed. The table shows that a higher mean annual average temperature than the observed is simulated by each of the GCMs, varying between 2.6° to 3.8° C more than the historic temperature. As noted in the literature review, there is comparatively little agreement between the GCMs on the direction of precipitation change. In general, precipitation projections indicate a decrease in precipitation over the East Bay watersheds, especially those obtained from the LOCA downscaling approach.

Results presented earlier suggest that hydrology in both the Upcountry and East Bay watersheds is more sensitive to changes in precipitation. The decreased precipitation, especially from the LOCA downscaling, translates into lower mean annual inflows into the Calaveras reservoir. Higher temperatures lead to higher evapotranspiration and lead to a reduction in mean annual flows. Results for two additional hydrologic variables, the mean annual average flow (MAAF) over 15 and 60 days are also shown here. This metric is important for reservoir operations from a flood control perspective. An increase in intensity and/or frequency of precipitation, as has been predicted by some for Northern California [*Neelin et al.*, 2013], would be expected to lead to higher average flows (MAAF-15 or MAAF-60) over shorter time periods. The changes in MAAF-15 and MAAF-60 under different climate futures are consistent with those for the mean annual flows, and do not indicate a drastic change in hydrology for the watershed.

A potentially important secondary effect of climate change, not included in this work, is changes in vegetation. There is evidence that warming in the western US is happening at a rate too fast for the local vegetation to adapt [*Brown et al.*, 2004]. The warming has also been linked to

increase forest fires and decreased forest cover [*MacDonald*, 2010]. Especially in the local watersheds with the ephemeral nature of streamflow and the relative importance of evapotranspiration in the water budget, changes in vegetation may influence water availability or even flood risks and would make for a valuable extension of this work.

5.6. Conclusion

California's water resources are tightly coupled with its climate. Changes in climate, projected to be amplified in the future, will have a significant impact on hydrology and water management. Given the varied climatology across the state, impacts of increased GHG emissions on climate and resultant hydrology will vary geographically and seasonally. In this study, we assess the impact of regionally and seasonally varying climate change on hydrology, using the water supply for San Francisco as a case study. To do so, we develop a spatially and temporally disaggregated stochastic weather generator and use it to drive hydrologic models developed for various watersheds that supply the bulk of San Francisco's water. We compare our vulnerability-based methodology with the scenario-based approach that uses downscaled GCM projections, and assess the effect of downscaling approach on hydrology.

Extrapolating observed trends in temperature for future climate, we find a minimal impact of spatially and temporally varying temperature changes on hydrology. Mean annual runoff in the snow dominated Upcountry watersheds is found to be more sensitive to precipitation changes, compared to temperature changes. For the local East Bay watersheds, precipitation changes are again observed to influence hydrology more than changes in temperature. Across both regions, higher temperatures lead to lower streamflow, especially in the summer. The ratio of flows between Upcountry and East Bay watersheds is found to be sensitive to both changes in

temperature and precipitation. For the Upcountry watersheds, GCM projections downscaled using two alternative approaches indicate a significant shifting of peak runoff towards the winter season, and suggest an overall increase in runoff due to projected increases in precipitation. For all the watersheds, the LOCA downscaled climate projected a smaller change in runoff compared to the BCCA downscaled climate.

While spatial and temporal changes in temperature were not found to meaningfully influence hydrology, a logical next step in this work would be to explore the effect of spatially varying precipitation changes across the watersheds. While no clear trends in precipitation are observed in the historical climate, GCM projections indicate different directions of precipitation changes for East Bay and Upcountry watersheds.

From a water management perspective, these results have key implications. The shift in peak flows in the Upcountry watersheds effectively translate into a loss of storage due to the snowpack reduction. As peak flows shift earlier increasing the threat of winter floods, flood storage may become a competing operational objective along with conservation storage. Change in ratios in flow between the Upcountry and East Bay watersheds in the future could alter the share of water the city receives from the respective watersheds, and may require SFPUC to reevaluate reservoir operation to maintain water supply reliability. Seasonal and geographic changes in hydroclimatology will likely occur. A better understanding of these changes and early identification of potential vulnerabilities can help water institutions be prepared to mitigate the effects of these changes.

CHAPTER 6

CONCLUSION

Improved water resources allocation can effectively mitigate the impacts of water scarcity on economic development (World Bank 2016). When developing models to inform water management, consideration of hydrology in isolation, as is often practiced, misses out important features of a region's water challenges and can present a misleading picture. To ensure optimal management of water resources, it is crucial to understand and to adequately represent the unique water use benefits derived by stakeholders into water resources modeling that informs decision-making processes. While representation of natural hydrologic processes in systems analysis has advanced considerably, human interaction with the natural system are significantly less understood. Human alterations of surface and groundwater hydrology have now been shown to even influence mesoscale hydro-meteorology. This dissertation presents methodologies to develop human-hydrologic models to inform surface water and groundwater management accounting for spatial and temporal heterogeneities using agent-based models of societal water use. The two-way feedbacks between human water management and hydrology are examined and the potential impact of climate change on management policies is evaluated.

Three central themes are emphasized in this dissertation. The first of these deals with the issue of spatial heterogeneity and equity; we see how management policies that ignore spatial variation in water use across a basin can give rise to extensive third party impacts, and become politically infeasible. The comparison between command-and-control and incentive-based groundwater management (Chapter 4) highlights the presence of these externalities. While groundwater markets are found to lead to increased economic benefits, the economic benefits are

unequally distribution it also results in creation of 'winners' and 'losers' across the system. A similar presence of spatial externalities is observed for transboundary surface water management in the Niger and Mekong River Basins. The coupled human-hydrologic modeling framework presented in Chapter 3 includes a parameter signifying level of cooperation between agents. When two agents are seen to negotiate a change in water management actions, the effects of these negotiations are experienced by riparian agents as well. These effects can be both negative and positive simultaneously for different agents. Third party impacts on the environment in terms of ecologic disturbances can also occur.

The effects of temporal variability on water management are explored in Chapter 4 and Chapter 5. In Chapter 4, climate change impacts on groundwater market dynamics are shown. Under different combinations of temperature and precipitation, the optimal groundwater market settings are seen to vary, highlighting the need for 'flexible' groundwater policies and proactive management. The analysis in Chapter 5 highlights how seasonally varying climate change can affect hydrology and water resource management for the city of San Francisco. Shifts in peak flow to earlier in the year would effectively translate to a loss of storage and require reconfiguration of reservoir operations. In addition, the spatial variation in the impact on hydrology could mean that the ratio of water supply from the different watersheds may change and affect system reliability.

The third key central theme in this dissertation has been that of feedbacks between human water use and the natural environment. The second chapter, focusing on development of a physically-based groundwater model for the Punjab province in Pakistan presented an example of groundwater management that does not incorporate human use feedbacks. While useful for understanding the spatial dynamics of groundwater use in Punjab, the scenario analysis using the groundwater model failed to capture the secondary impacts of management policies on

137

groundwater dynamics (e.g. how canal lining would affect surface water availability and demand for groundwater irrigation). Chapter 4 showed how incorporation of human use feedbacks enables a more realistic assessment of groundwater policy effectiveness by illustrating how farmers' groundwater pumping decisions change over time as they encounter the effects of past irrigation decisions. The importance of these feedbacks in surface water management are illustrated in Chapter 3 in the evolution of water use over time by heterogeneous agents representing transboundary countries.

This dissertation demonstrates the importance of accounting for spatial heterogeneity, temporal variability and usage of coupled human-nature models to aid water management. Some future research needs also emerge from this work. Human decisions are largely modeled in this work as deterministic, although some degree of stochasticity is introduced in Chapter 3. The use of Bayesian decision theory in addressing uncertainty of human decisions under stochasticity could be an exciting avenue of future research. Second, this work does not explicitly consider water management for extreme events (e.g. floods). For instance, making flood protection a part of the water management objective, along with incorporation of perceptions of flood risks would provide an interesting extension of this work.

APPENDIX A

SUPPLEMENTAL MATERIAL FOR CHAPTER 2

Data Collection

Land surface elevations were obtained from NASA's 90 m SRTM dataset. These elevations were compared to the point surface elevations provided in the SCARPs Monitoring Organization (SMO) dataset and adjusted using a simple linear regression.

Daily precipitation data for 60 stations was obtained from Pakistan Meteorological Department (PMD) and interpolated to estimate precipitation recharge across the entire model domain and aggregated on a seasonal level. The proportion of rainfall seeping into the aquifer is based on estimates from Ahmad and Chaudhry (1988) for the entire Punjab province. For quantifying evapotranspiration out of the aquifer, we used data from the Advanced Very High-Resolution Radiometer (AVHRR) dataset (Zhang & Kimball 2006) which provides monthly surface evapotranspiration data across the globe. The monthly data was aggregated into seasonal values across the model domain. The AVHRR dataset provides total surface evapotranspiration data, while the direct evaporation from the aquifer is a much smaller fraction of that. Based on estimates of evaporation from aquifer in water balance studies in the Indus, an adjustment was made to the data to correctly quantify evaporation (Ahmad and Kutcher 1992).

On a system-wide basis, recharge from rivers form a *relatively* small part of the overall aquifer flux. However, the recharge effects from the rivers are noticeable when considered on a point-basis for the regions along the river length. The River Package was used to simulate the interaction between groundwater and surface water across the model. For the River Package, three parameters are required: river stage, conductance, and the river bed elevation. River stage was obtained from NASA SRTM 90 m DEM data. No reliable time series of data for river stage across

our modeling domain are available, hence a constant river stage is used throughout the simulation period. While having a time-series for river stage would be preferred, the *relatively* small component of overall groundwater flux attributed to river recharge justifies ignoring seasonality in river flow. For the river bed elevation, based on knowledge of local conditions, we assume an average river depth of 3 meters. The conductance value for the river cells, which is a function of the hydraulic conductivity of the river bed and river width, was obtained by calibration to match the estimated river recharges provided in a water balance conducted by ACE-Halcrow (2001).

Monthly canal flow data on a Canal Command Area (CCA) level was obtained from WAPDA to simulate recharge from canal flows into the aquifer through the main canal channels. From a hydraulic perspective, while the head-dependent flux would better represent the seepage from the canals, the only available dataset for canal flows are from the Punjab Irrigation Department. Given these limitations, the most suitable way to represent seepage from the canals, is through the *Well* package. Canal seepage refers to the losses from the entire canal irrigation system, which includes both direct seepage from the canal and also irrigation return flows. For seepage from each canal, the seepage is distributed uniformly across the entire associated canal command area (CCA) (shown in Figure 48) both in space and time. We use seepage coefficients reported by Ahmad et al. (1990) for the seepage from the canals and the irrigation return flows.

MODFLOW Calibration

The hydraulic properties of the aquifer (hydraulic conductivity and specific yield) are calibrated on the district level, i.e. the hydraulic properties are thus divided in zones of uniform k/s_y. Given the variations in soil and aquifer characteristics over small areas, the ideal calibration scale for the aquifer characteristics in this model would be smaller. However, since there are approximately 200,000 active grid cells across the model domain, it was not computationally

feasible to perform the calibration on a grid cell basis. Therefore, the choice of spatial scale for the calibration was made as a compromise between calibrating on a fine spatial scale but also one that is computationally feasible. This calibration scale also allows us model at a spatial scale that provides meaningful information for policy makers.

The calibration is carried out using the genetic algorithm procedure (GA). The objective function for this GA minimizes the mean absolute error (MAE) between the observed and simulated heads across the model domain for each stress period in the calibration period. The calibration is performed by linking R statistical software and MODFLOW. R is used to generate the input files needed for MODFLOW and read output from the model to feed into the calibration routine. The calibration is initialized with a population size of 120 for each generation and the parameters are calibrated over 50 generations. In each generation, the error associated with each of the solutions relative to the calibration target is then calculated. The best performing solution in the population is retained, and each solution is then modified to form a new generation. The new generation is then used in the next iteration of the algorithm. Genetic algorithms have been shown to provide a practical alternative to trial-and-error and automated statistical calibration procedures (Madsen and Perry 2010).

The choice of eight (8) stress periods from April 1998 to March 2002 was primarily driven based on the availability of groundwater abstraction data. The only available reliable seasonal estimates across Punjab were obtained from an IWMI study for the 2001-2002 season. Based on these survey results and an assumption of constant water productivity, we back-calculate the groundwater abstractions in the previous four years. Due to the uncertainty associated with this approach, we limit our calibration to a four-year period.

Using the genetic algorithm, calibrated aquifer parameters for each district included in the model are obtained. Figure 51 and 52 show a comparison of the aquifer characteristics for the districts included in our model, with field observations from tests carried out across Punjab (Bennett et al 1967). Not all the districts that included in this model have field observations from the USGS studies. For the districts where a comparison was possible, a location is selected at random from each of the districts.

Model Validation Statistics

The calibrated model was then validated to evaluate the performance of the calibration. Using groundwater hydraulics in April 2002 as the starting heads, a model validation run over eight stress periods was performed. Inputs into the model for the validation period were obtained from historic time series data. Table 5 below shows summary statistics for the model validation run in terms of the residual, which is calculated as the difference between observed head and modeled head. The statistics suggest that the calibrated model performs satisfactorily on the whole. Figure 54 through Figure 59 show time series plots for observed groundwater heads compared to modeled heads from locations across the model domain. The calibrated model is able to capture temporal dynamics to a reasonable extent.

Table 6 shows the breakdown of the groundwater flux for the validation period and the comparison with results from ACE and Halcrow (2001). The groundwater balance shows the major components as seepage (leakage) from the irrigation system and groundwater abstraction. Precipitation infiltration and ET loss are around 10 NAF each. These components are within the same magnitude as previous study. Streamflow in the rivers across the model domain are augmented by the aquifer (3 MAF), primarily during the low flow season (October-April) and shows a larger disagreement compare to ACE and Halcrow (2001).

Scenario Analysis

The three forecast scenarios were selected and designed primarily because (i) these comprise the most significant components of the overall groundwater flux for which data is available (ii) forecasts of changes in these components over the long term have been found in the existing literature and (iii) they can be related directly to policy actions that can be taken.

For the precipitation scenario, the bounds were selected based on the estimates available in the existing literature. There exists huge uncertainty in the impact of climate change on precipitation across south Asia and how these changes will impact the South Asian monsoon. Depending on the climate model considered, these estimates predict both increases and decreases in precipitation across Pakistan. An earlier study on climate change impacts in semi-arid regions predicted annual average precipitation decrease of 5-25% for western India and Pakistan, depending on the climate model and emissions scenario considered (Ragab & Prudhomme 2002) . Another study considering the impact of climate change on the Asian Monsoon predicted a decrease of about 20-30% on annual average precipitation for much of the northern Punjab (Bae et al. 2015). On the other hand, estimates for increases in precipitation vary from increases of about 20% (Immerzeel et al. 2009) to 20-24% (Kripalani et al. 2007). To reflect this uncertainty in precipitation changes found in the literature, the future scenario analysis considers both an increase and decrease in precipitation.

The increase in groundwater abstractions across Pakistan, and Punjab in particular, is well documented (Qureshi et al. 2010). Concerns have been raised regarding the sustainability of this continuous upward trend in pumping to satisfy agricultural and domestic water demands (van Steenbergen & Gohar 2005). According to the Punjab government's statistics on major crop production data, an annual average increase in production of 1.1% was observed during the first

part decade of this century (GOP 2012). Assuming static water productivity levels, we develop bounds on our future scenario analysis for groundwater abstraction based on this historical increase rate. For the 23-year simulation period, we linearly increase groundwater pumping from status quo levels to 125% of current pumping levels as the upper bound. On the other hand, with the prospect of improved canal water supply, a reduction in groundwater abstraction is possible. Estimates for the increase in surface water availability through improved canal system efficiency vary significantly, so we assume a symmetric decrease as our lower bound for the future scenario. The purpose of this scenario analysis is to show the potential gains that a decrease in groundwater abstraction can bring for sustaining the Indus aquifer.

For the canal infrastructure scenario analysis, the range of variability in seepage from existing canal systems (PPSGDP 1998) is used to inform our system-wide canal leakage. The bounds on the scenario analysis represent the 'best' and 'worst' case development of the irrigation system, if all the canals were improved or deteriorated to the most extreme state existing in the system. Seepage coefficients directly from the main canal branches range from 0.1 to 0.5. Adding the return flow from irrigation, estimated at approximately 20% of total irrigation system losses (Yu et al 2012) into these means that we obtain a range of 0.3 (30%) to 0.7 (70%).

Table 5: Summary statistics for model validation from April 2002- March 2006

Absolute Residual Mean	4.43 m
Absolute Residual Standard Deviation	1.69 m
Scaled Absolute Residual Mean	2.8%
Root Mean Square Error	5.91 m

Table 6: Annual Average Groundwater Flux in million acre-feet (MAF) for the Validated Model (April 2002-Mar 2006), and a comparison with existing groundwater balance from ACE and Halcrow (2001)

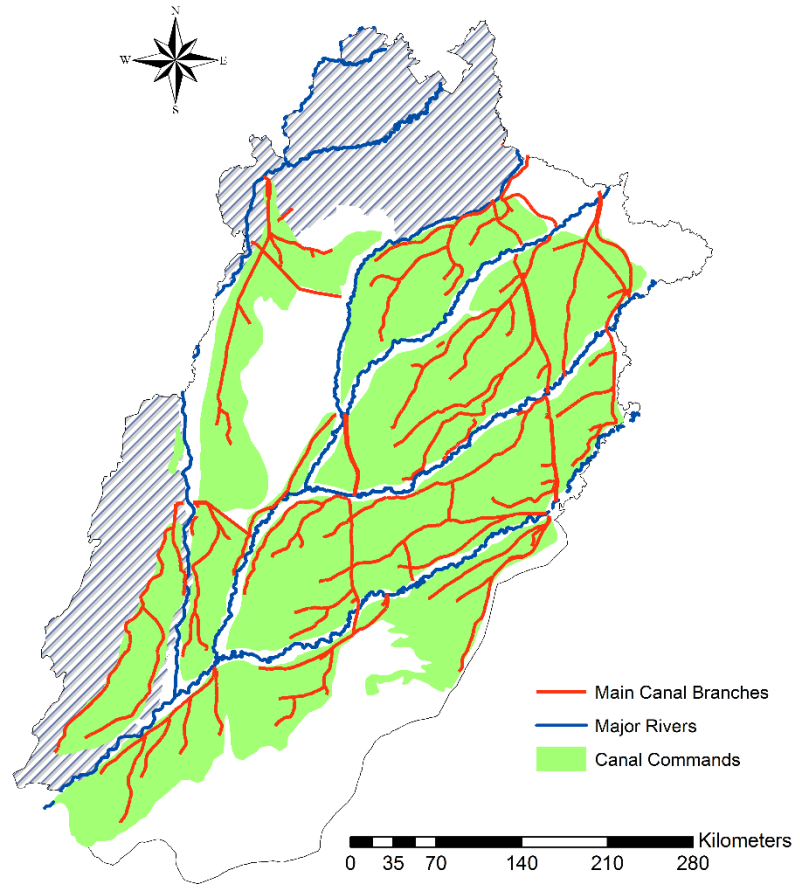|	Modeled Flux	ACE and Halcrow (2001)
Leakage from irrigation system	26.6	28.8
Groundwater Abstraction	35.2	34.0
River recharge	8.4	3.5
Baseflow to rivers	3.0	0
Precipitation Infiltration	9.5	9.9
Aquifer ET loss	9.0	8.75

Figure 48: Location of major rivers, canals and associated canal command areas across the model domain
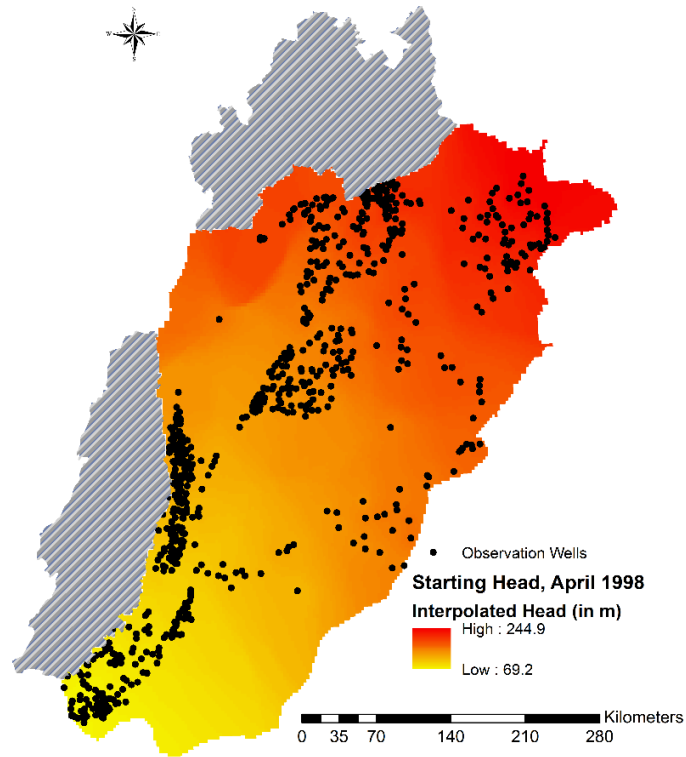
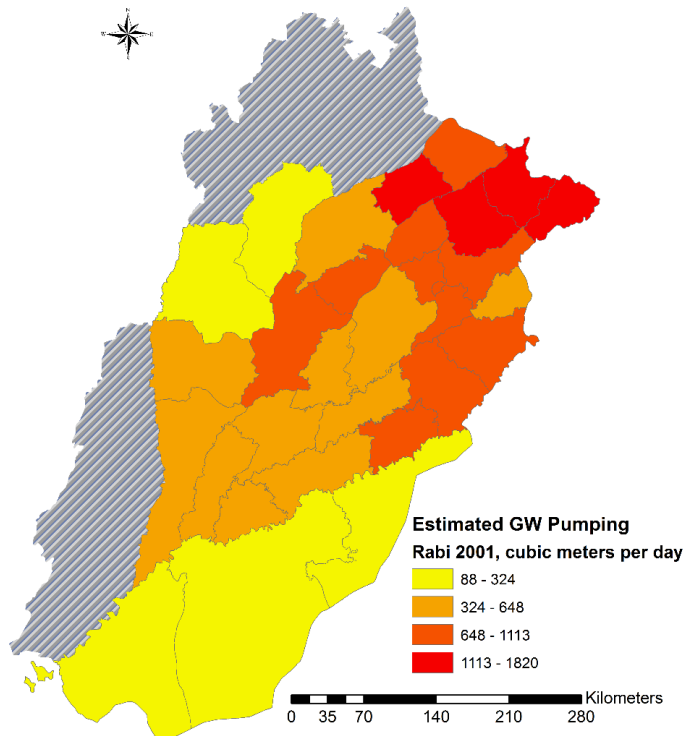Figure 49: Starting heads for beginning of MODFLOW calibration run

Figure 50: Estimated average groundwater abstraction across Punjab for Rabi 2001 season
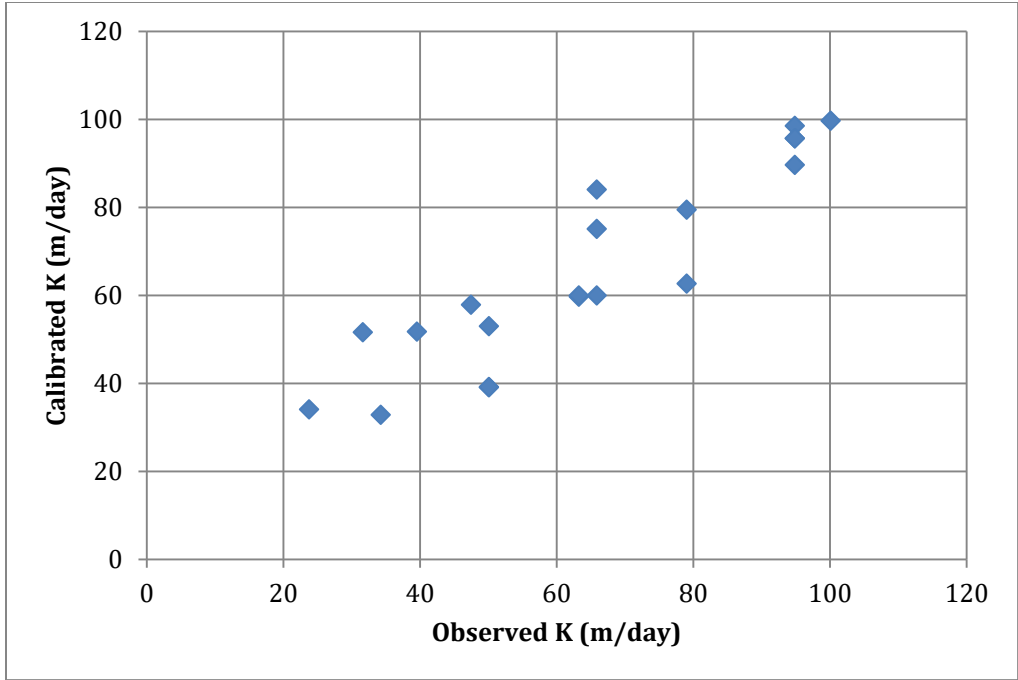
Figure 51: Comparison of calibrated and observed hydraulic conductivity (in meters/day) across model domain

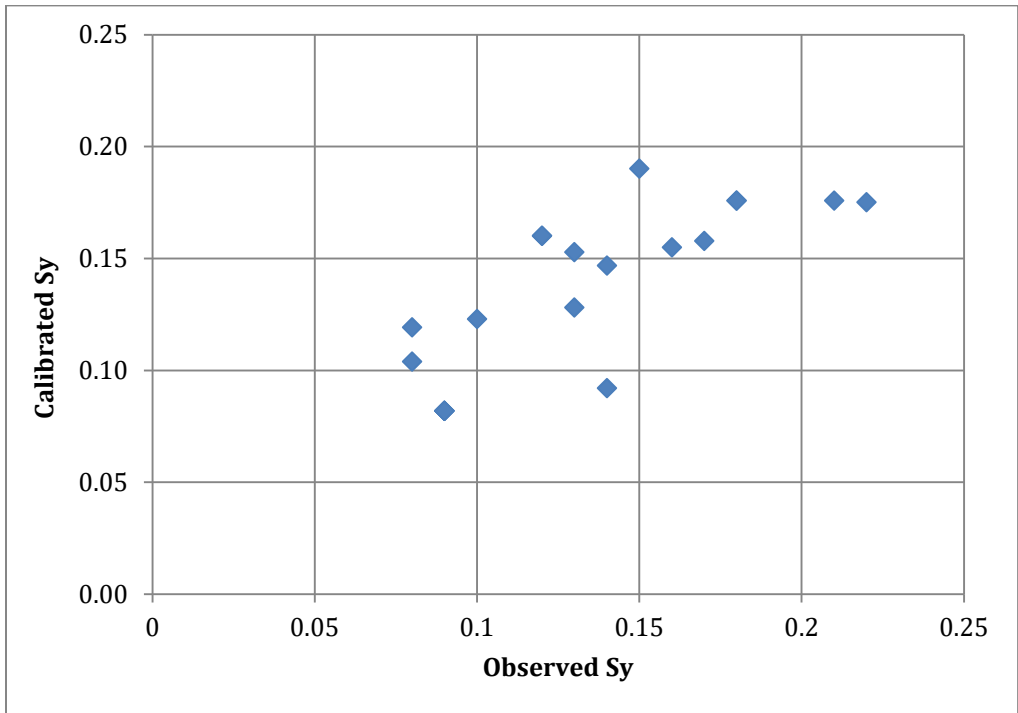Figure 52: Comparison of calibrated and observed specific yield across model domain
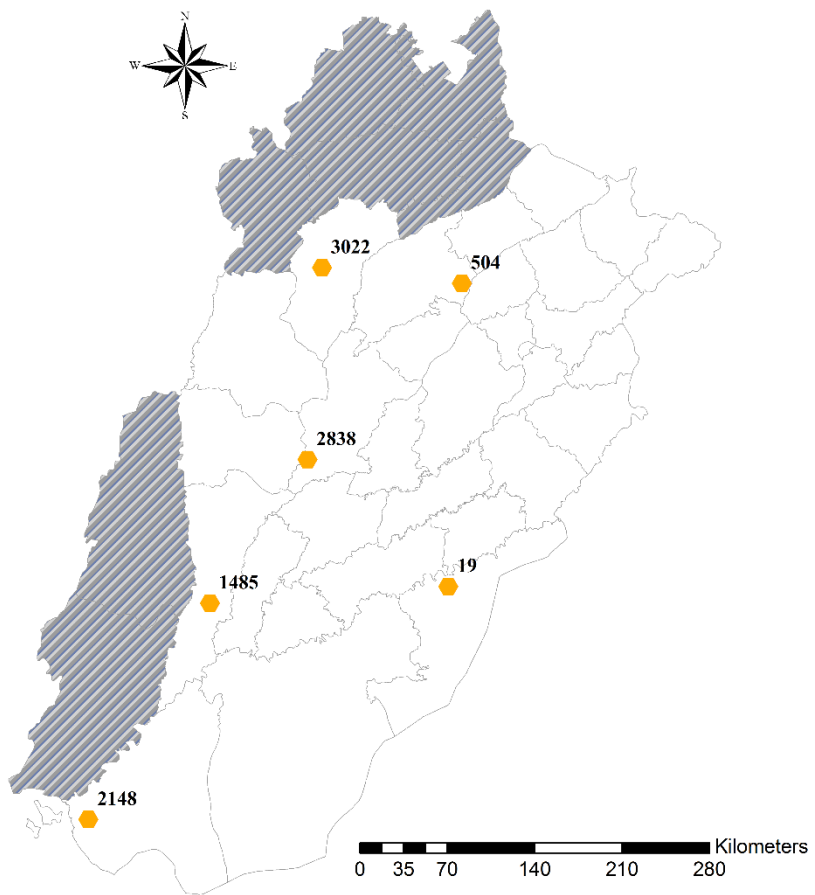
Figure 53: Map showing the location of sample wells for which model validation results are shown

Figure 54: Observed and modeled heads for model validation run (April 2002-March 2006) in Khushab district

Figure 55: Observed and modeled heads for model validation run (April 2002-March 2006) in Sargodha district

2838

Figure 56: Observed and modeled heads for model validation run (April 2002-March 2006) in Jhang district

19

Figure 57: Observed and modeled heads for model validation run (April 2002-March 2006) in Bahawalnagar district

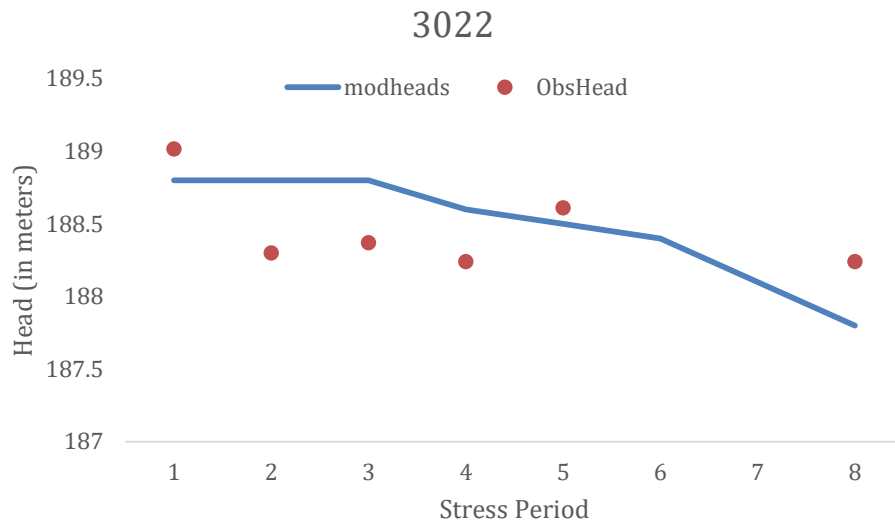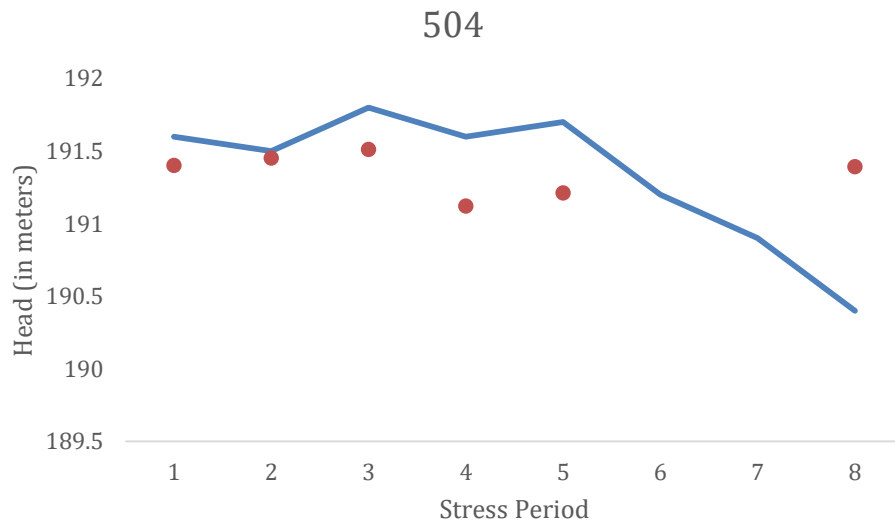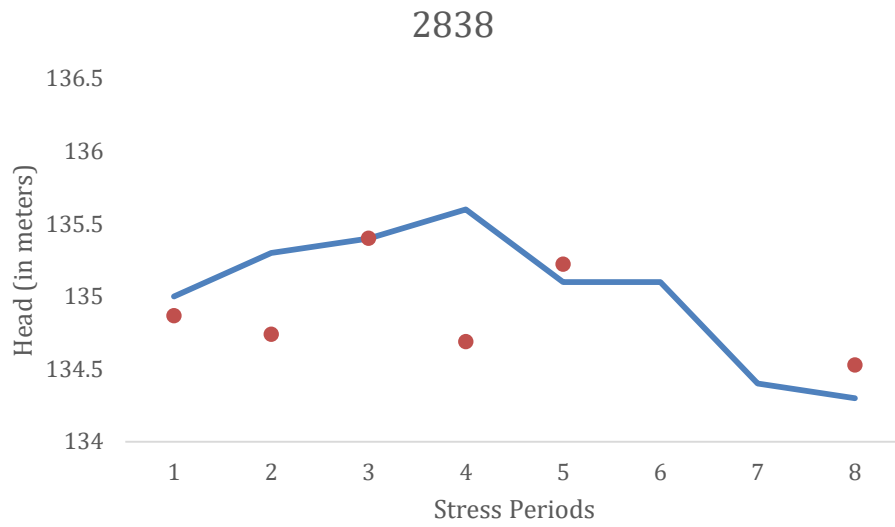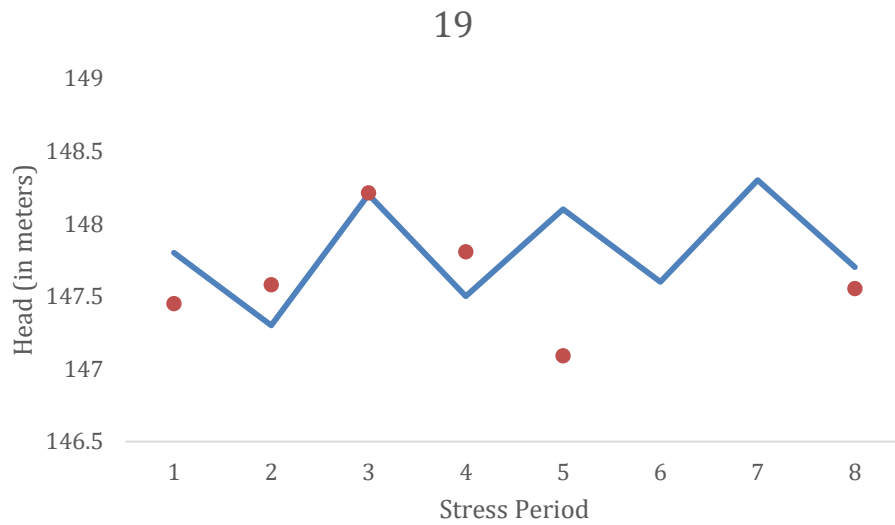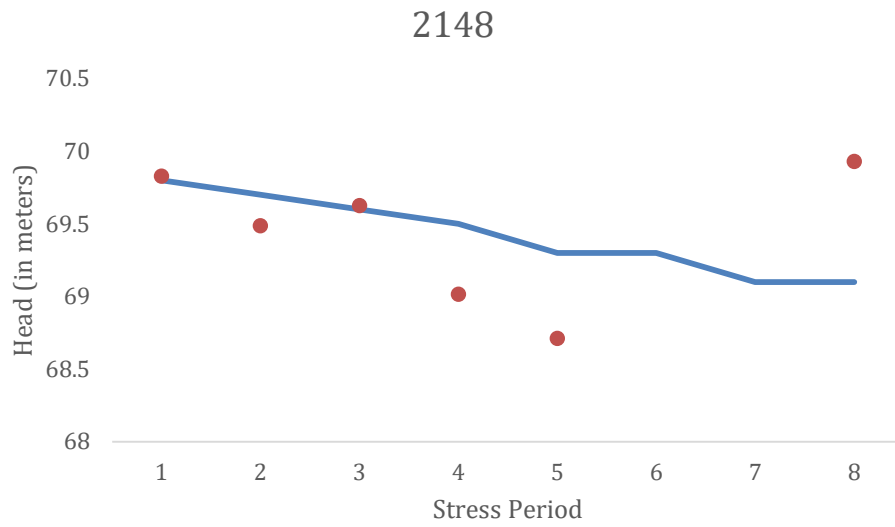Figure 58: Observed and modeled heads for model validation run (April 2002-March 2006) in Rahim Yar Khan district
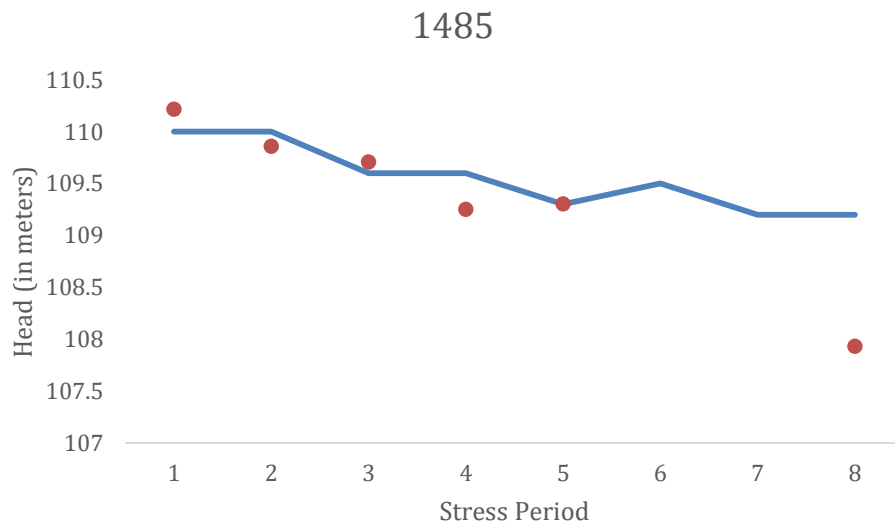

Figure 59: Observed and modeled heads for model validation run (April 2002-March 2006) in Muzzafargarh district

APPENDIX B

SUPPLEMENTAL MATERIAL FOR CHAPTER 3

SWAT model setup

The data used to set up the SWAT models for the two study river basins are shown in Table 7. SWAT is a semi-distributed model. In model setup, the Mekong River Basin is partitioned into 289 subbasins (Fig. 60(a)), and the Niger River Basin is divided into 178 subbasins (Fig. 60(b)). Hydrological response units (HRUs) were defined within subbasins to reflect the spatial variability of land use/land cover and soil. For this study, we defined crop HRUs for rainfed and irrigated upland crops and rice. The initial size of crop HRUs was estimated using cropping area data from International Food Policy Research Institute (IFPRI)'s SPAM database (You et al., 2014), which disaggregates national/sub-national crop production stations to a 5 arc minute grid.

The SWAT models contain customized modules to simulate storage and water surface variations of two major natural water impoundments: the Tonlé Sap in the Mekong River Basin and the Inner Niger Delta in the Niger River Basin. The storage variations of the Tonlé Sap and the Inner Niger Delta were modeled by following the approaches by Kirby et al. (2006) and Thompson et al.(2016), in which statistical relationships were developed to relate the outflow of the Tonlé Sap to streamflows at Kratie and outflow of the Inner Niger Delta at Diré to flows at Ké-Macina and Bénény Kégny. The water surface areas of the two water impoundments were further calculated using volume-surface relationship developed by Manley (2015) and Ogilvie (2017, personal communication).

Table 7: Data for SWAT model setup

Category	Data
Elevation	HydroSHEDS[1]
Land use/land cover	GLC2000[2] & SPAM 2005[3]
Soil	Soil Map of the World[4]
Precipitation	Mekong: APHRODITE[5] Niger: NCEP-CFSR[6] (monthly totals were corrected using monthly precipitation data in CRU TS v. 4.00[7])
Temperatures/solar radiation/relative humidity/wind speed	NCEP-CFSR

Sub-basin Delineation
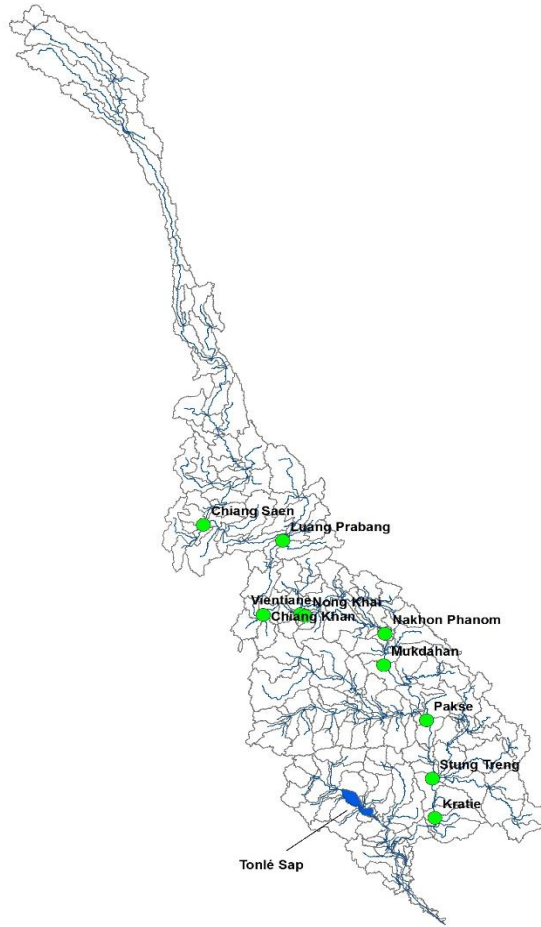
(a) **Mekong**   (b) **Niger**
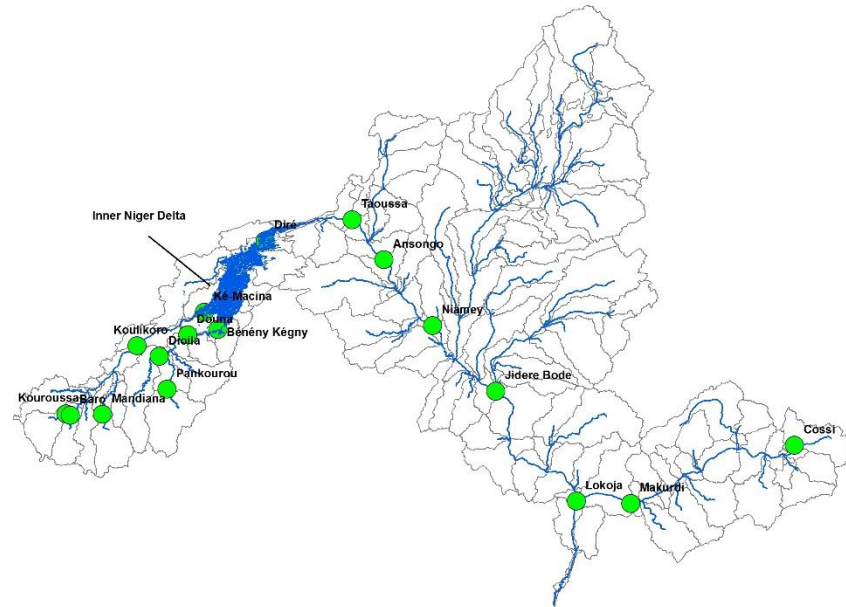
Figure 60: Watershed delineation schemes and locations of streamflow stations used in model calibration/validation

Model Calibration and Validation

The SWAT-Mekong model was calibrated and validated using daily streamflow data from 10 gauging stations, while for the Niger River basin, model calibration and validation was conducted on a monthly basis. The data were obtained from L'Institut de recherche pour le développement (IRD), Niger Basin Authority (NBA) and Global Runoff Data Centre (GRDC). The calibration/validation periods and the model fits achieved by the SWAT model in both case studies are shown in Figures 61 and 62, and Table 8.

Table 8: Nash–Sutcliffe model efficiency coefficient for the Mekong and Niger River Basins

Mekong

Station	Calibration (1983-1992)	Validation (1993-2007)
Chiang Saen	0.51	0.62
Luang Prabang	0.73	0.80
Chiang Khan	0.70	0.82
Vientiane	0.71	0.82
Nong Khai	0.74	0.82
Nakhon Phanom	0.80	0.84
Mukdahan	0.85	0.84
Pakse	0.82	0.85
Stung Treng	0.82	0.84
Kratie	0.83	0.85

Niger

Station	Calibration (1985-1994)	Validation (1995-2010)
Ansongo	0.88	0.50
Baro	0.80	0.33
Beneny Kegny	0.68	0.73
Cossi	0.81	0.08
Dioila	0.71	0.67
Dire	0.87	0.83
Douna	0.73	0.81
Jidere Bode	0.89	0.72
Koulikoro	0.92	0.72
Kouroussa	0.81	0.40
Ke Macina	0.88	0.66
Lokoja	0.86	0.72
Makurdi	0.81	0.87
Mandiana	0.65	0.42
Niamey	0.80	0.28
Pankourou	0.35	0.68
Taoussa	0.85	0.40
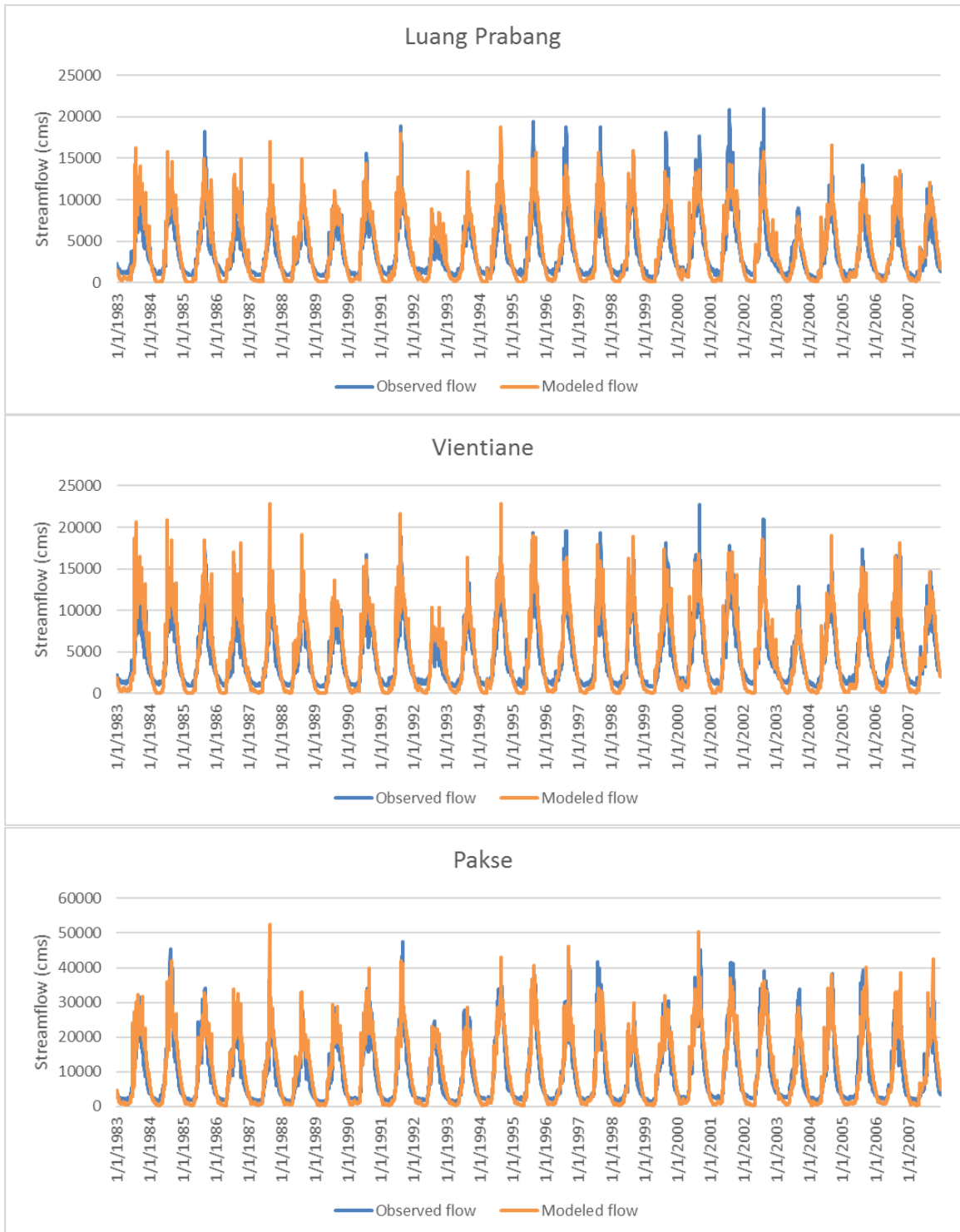
Figure 61: Simulated and observed streamflow at different locations along the Mekong River
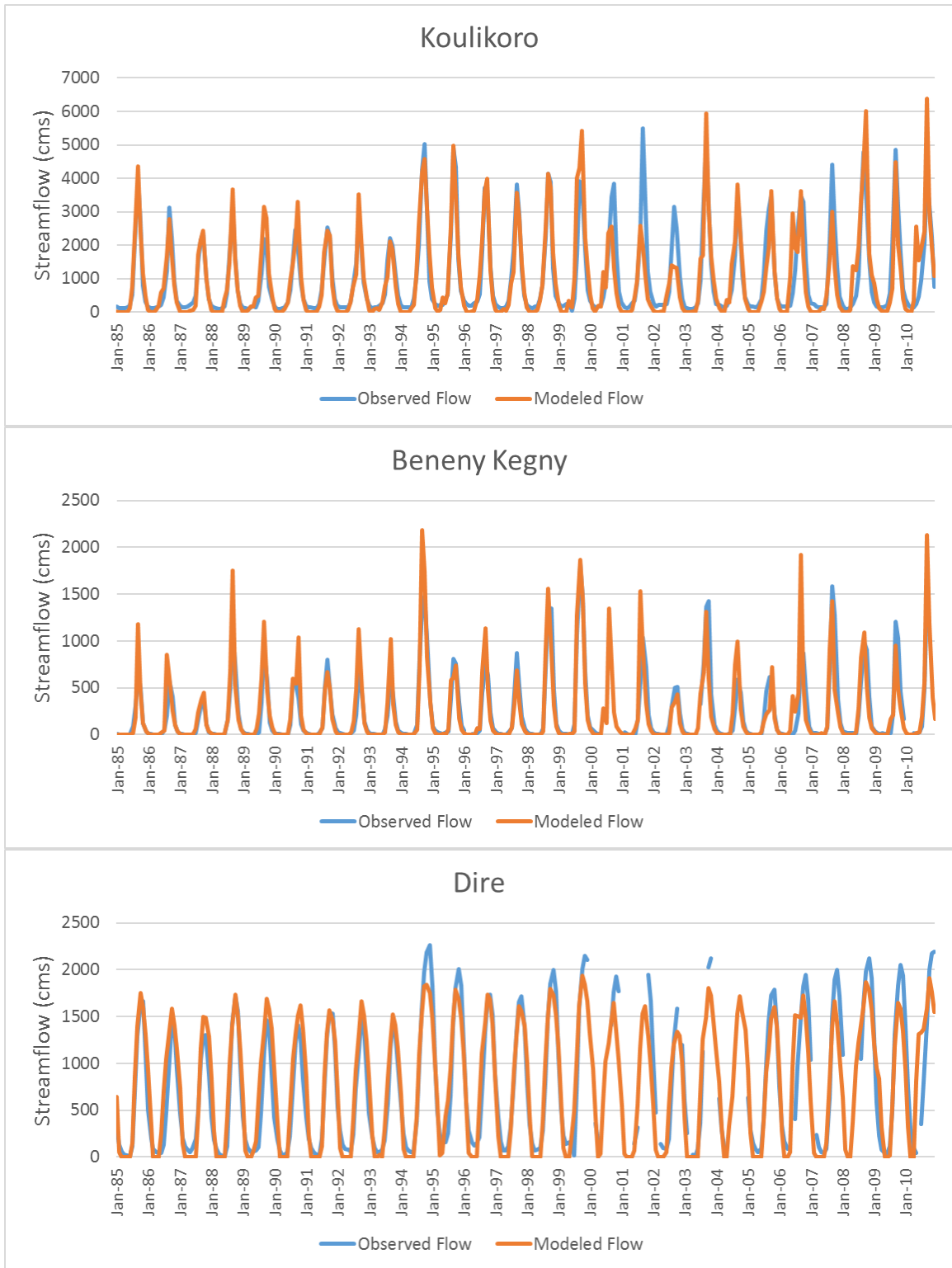
Figure 62: Simulated and observed streamflow at different locations along the Niger River
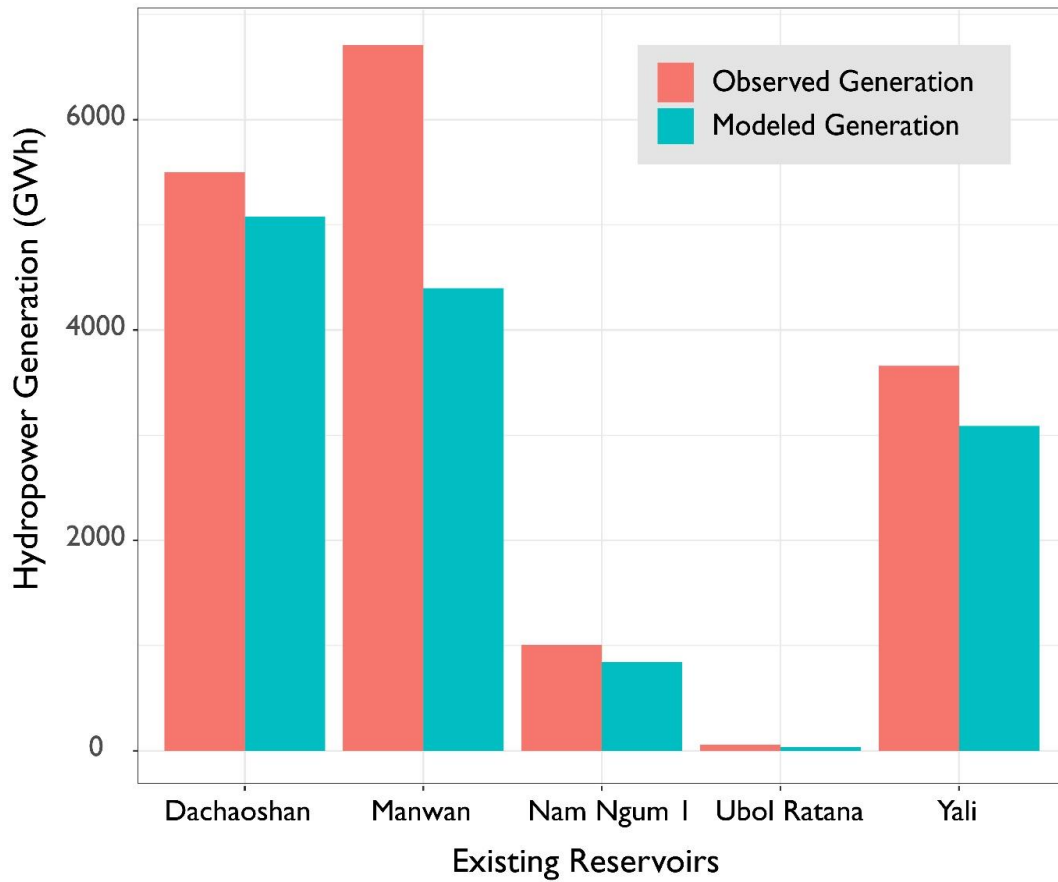
Figure 63: Comparison of simulated hydropower generated using the SWAT module under historic streamflow with observed generation in the Mekong River Basin

SUPPLEMENTAL MATERIAL FOR CHAPTER 5

Calibration results for the Alameda watersheds.
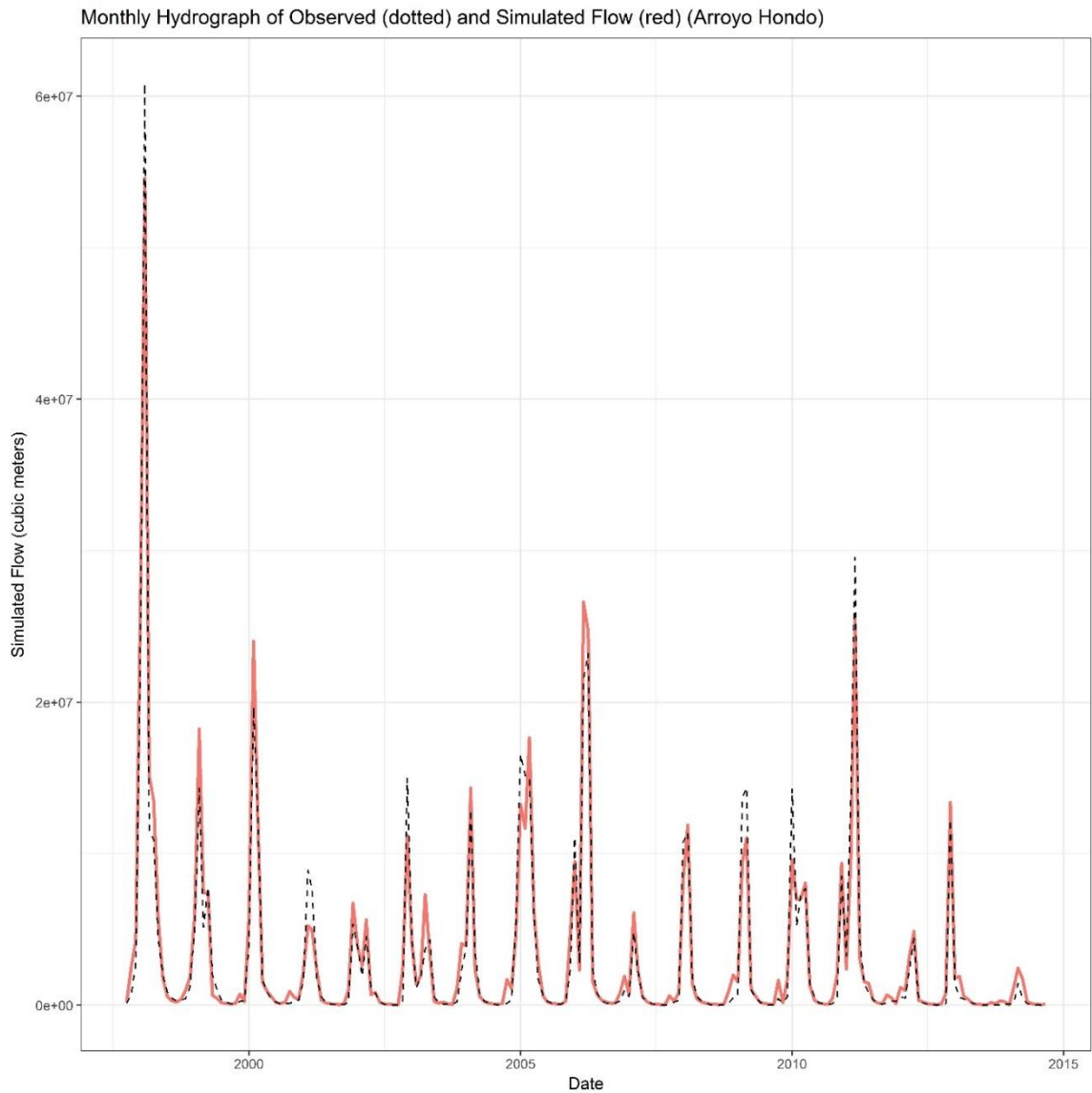
Figure 64: Monthly hydrograph of observed and simulated flow for the Arroyo Hondo watershed
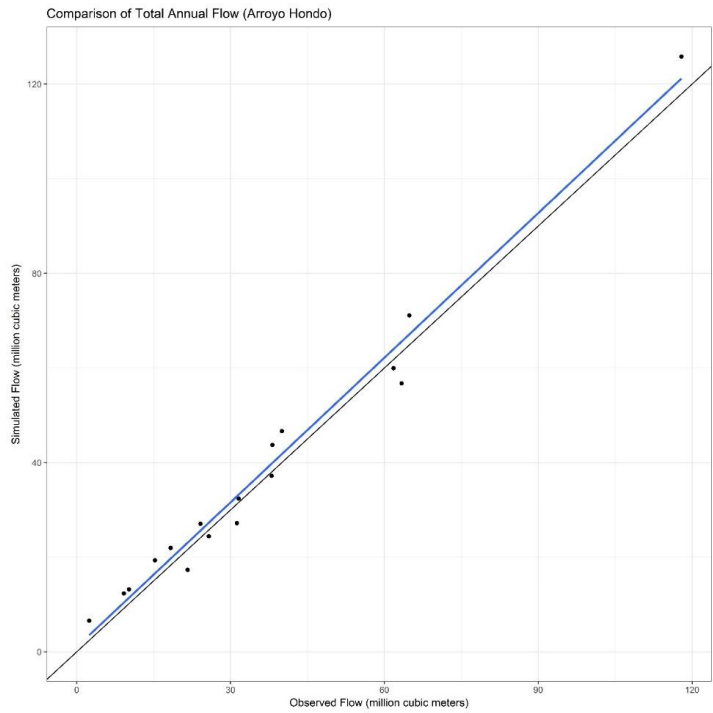
Figure 65: Comparison between the simulated and observed total annual flow for Arroyo Hondo watershed
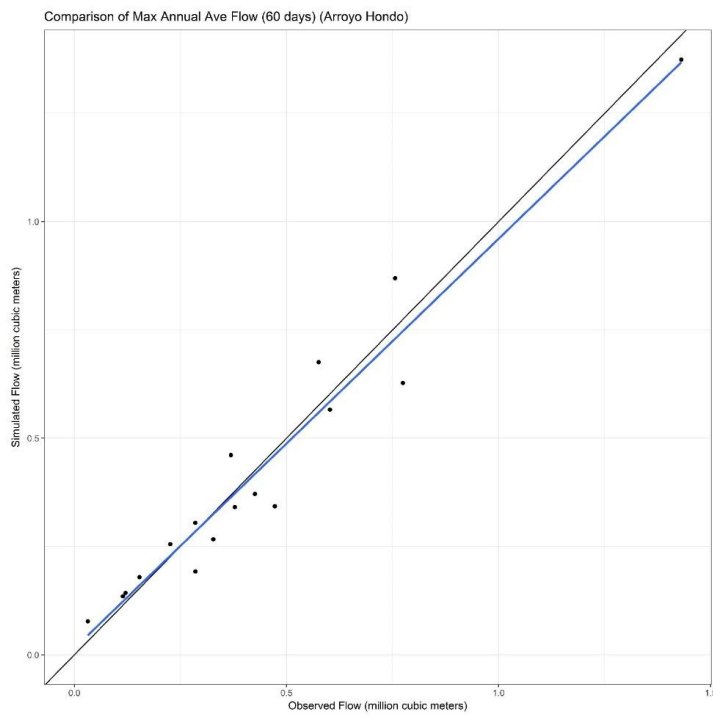
Figure 66: Comparison between the simulated and observed 60-day maximum annual average flow for the Arroyo Hondo watershed

162
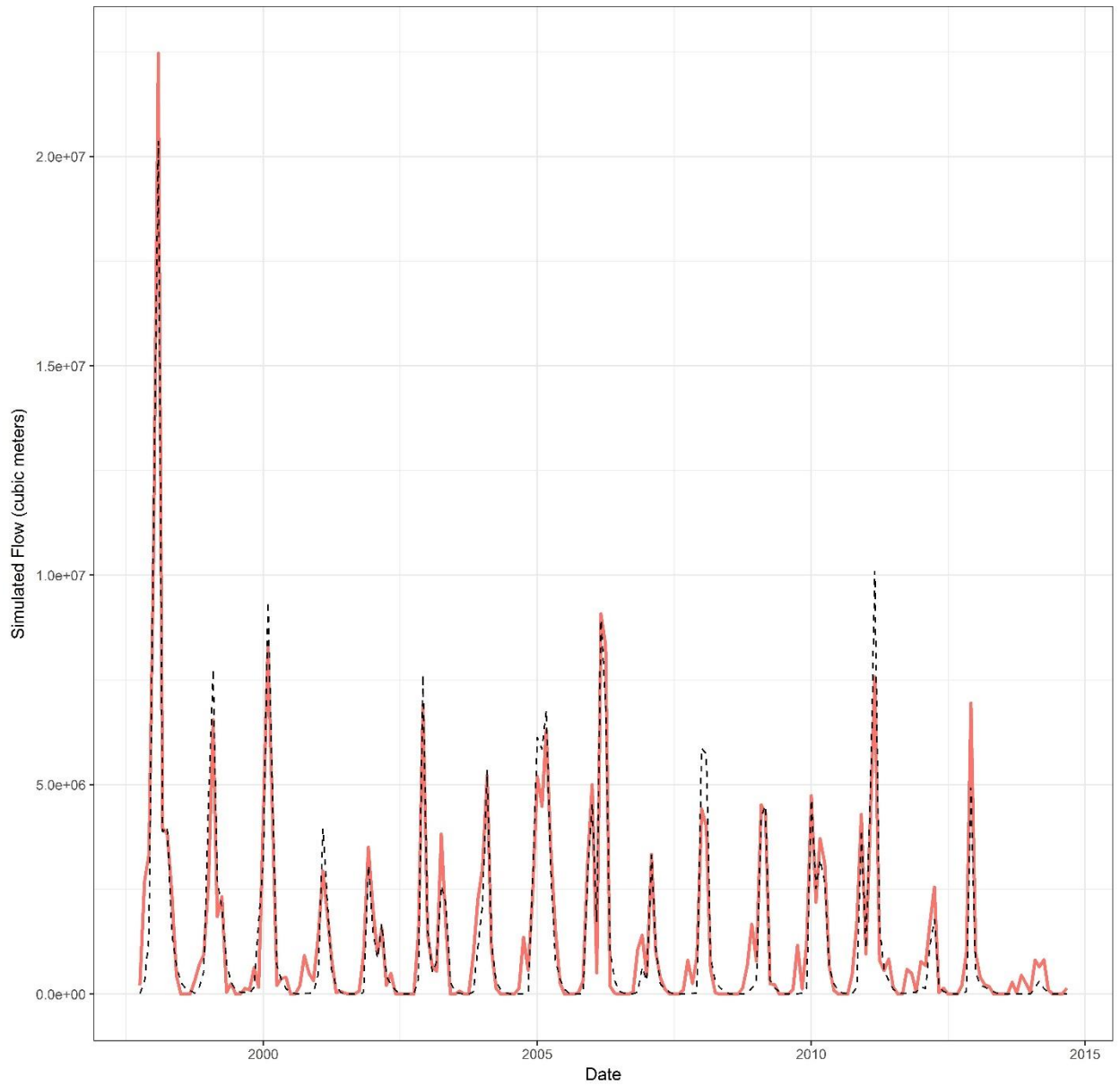
Figure 67: Monthly hydrograph of observed and simulated flow for the ACDD watershed
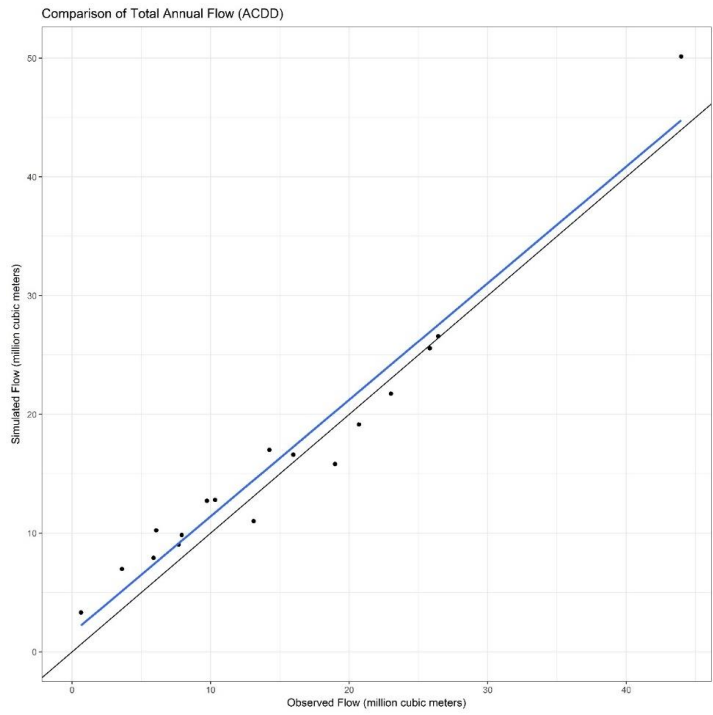
Figure 68: Comparison between the simulated and observed total annual flow for the
ACDD watershed
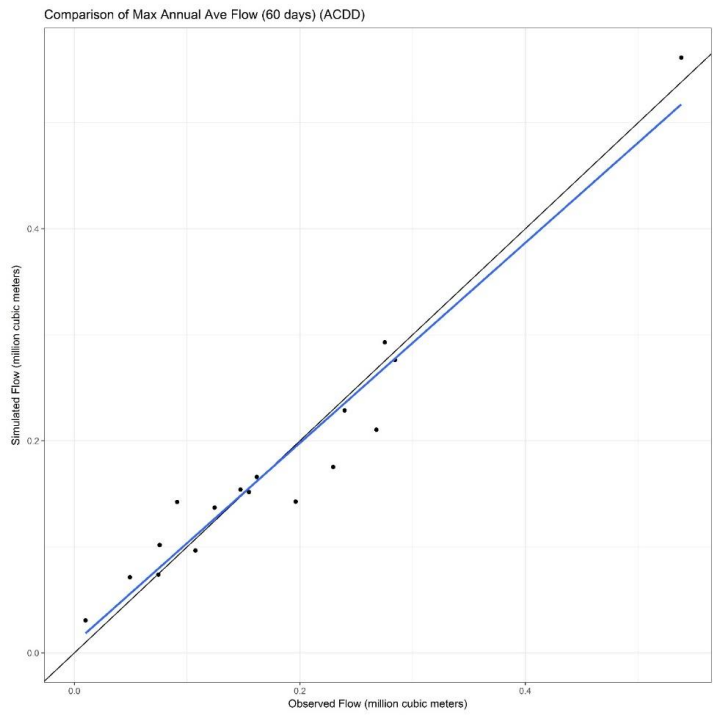
Figure 69: Comparison between the simulated and observed 60-day maximum annual
average flow for the ACDD watershed
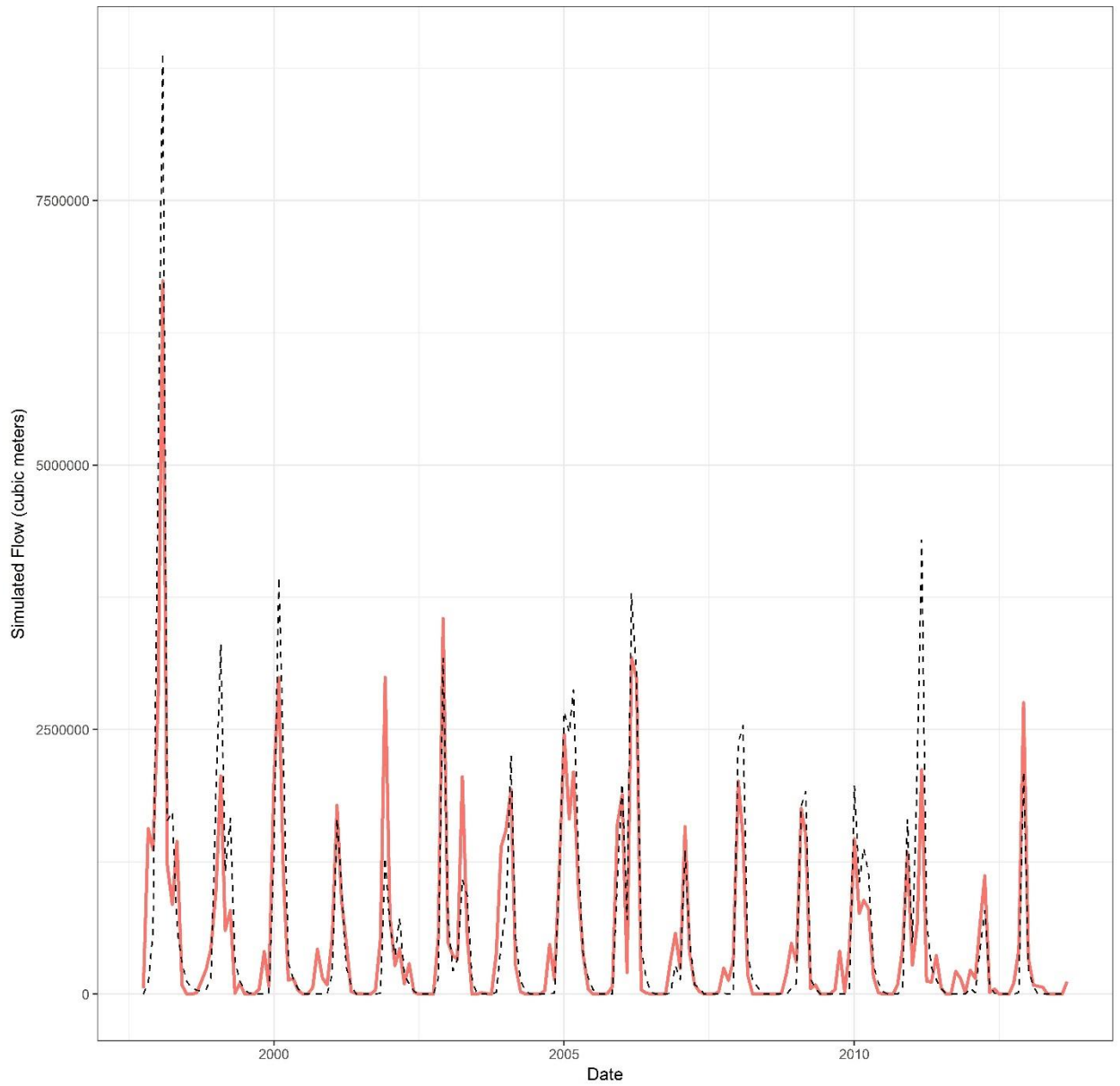
Figure 70: Monthly hydrograph of observed and simulated flow for the San Antonio watershed
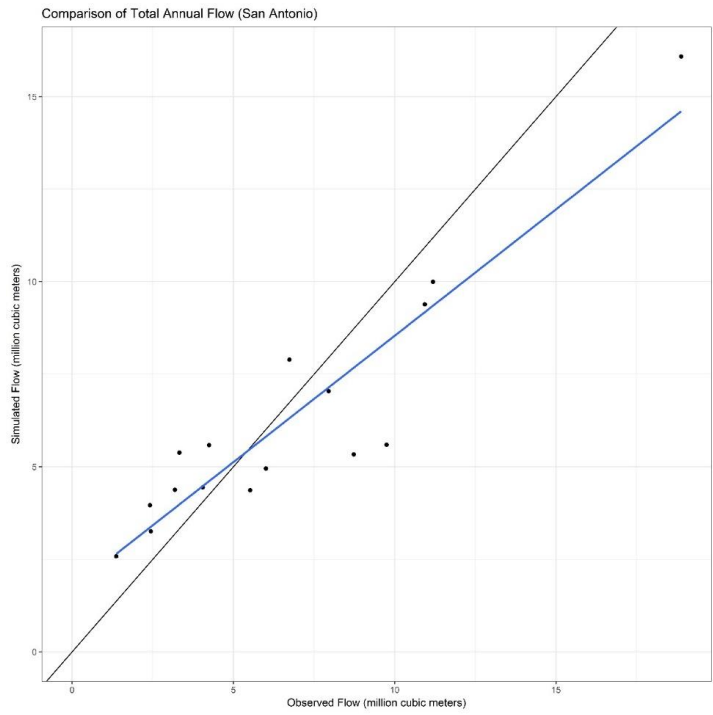
Figure 71: Comparison between the simulated and observed total annual flow for the San Antonio watershed
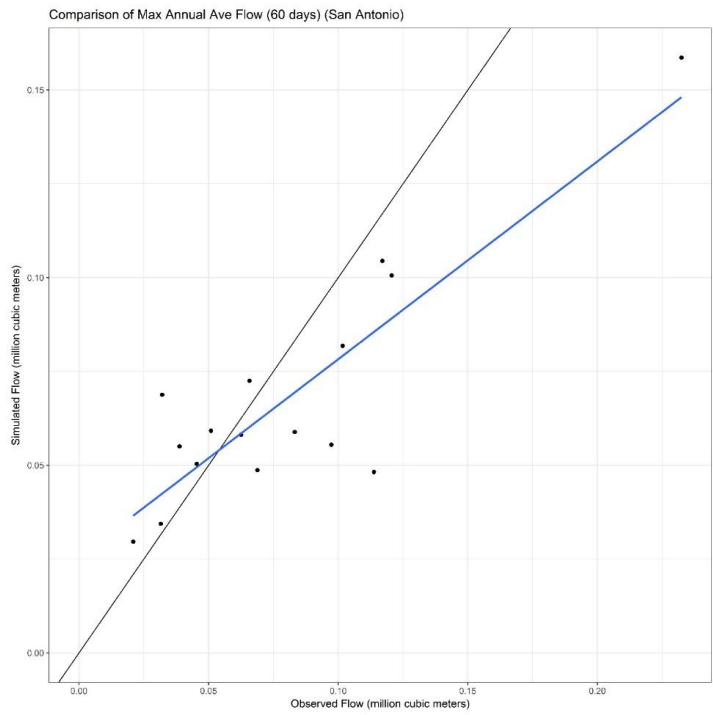
Figure 72: Comparison between the simulated and observed 60-day maximum annual average flow for the San Antonio watershed

BIBLIOGRAPHY

Abatzoglou, J. T., and R. Barbero (2014), Observed and projected changes in absolute temperature records across the contiguous United States, *Geophys. Res. Lett.*, *41*(18), 6501–6508, doi:10.1002/2014GL061441.

Abatzoglou, J. T., D. E. Rupp, and P. W. Mote (2014), Seasonal climate variability and change in the pacific northwest of the united states, *J. Clim.*, *27*(5), 2125–2142, doi:10.1175/JCLI-D-13-00218.1.

Aboubacar, A. (2007), *Niger River Basin Atlas*, Niger Basin Authority, Niamey.

Ahmad, M., and G. P. Kutcher (1992), *Irrigation Planning with Environmental Considerations*, Washington, DC.

Ahmad, Z., A. Ashraf, A. Fryar, and G. Akhter (2011), Composite use of numerical groundwater flow modeling and geoinformatics techniques for monitoring Indus Basin aquifer, Pakistan, *Environ. Monit. Assess.*, *173*(1–4), 447–457, doi:10.1007/s10661-010-1398-3.

Akhbari, M., and N. S. Grigg (2013), A Framework for an Agent-Based Model to Manage Water Resources Conflicts, *Water Resour. Manag.*, *27*(11), 4039–4052, doi:10.1007/s11269-013-0394-0.

Aladjem, D., and D. Sunding (2015), Marketing the Sustainable Groundwater Management Act: Applying Economics to Solve California's Groundwater Problems, *Nat. Resour. Environ.*, *30*(2), 1–4.

Allen, R. J., and R. Luptowitz (2017), El Niño-like teleconnection increases California precipitation in response to warming, *Nat. Commun.*, *8*(May), 16055, doi:10.1038/ncomms16055.

An, L. (2012), Modeling human decisions in coupled human and natural systems: Review of agent-based models, *Ecol. Modell.*, *229*, 25–36, doi:10.1016/j.ecolmodel.2011.07.010.

Asghar, M. N., S. . Prathapar, and M. S. Shafique (2002), Extracting relatively fresh groundwater from aquifers underlain by salty groundwater, *Agric. Water Manag.*, *52*, 119–137.

Bakker, K. (1999), The politics of hydropower: Developing the Mekong, *Polit. Geogr.*, *18*(2), 209–232, doi:10.1016/S0962-6298(98)00085-7.

Bandaragoda, D. J., and S. Rehman (1995), *Warabandi in Pakistan's Canal Irrigation Systems Widening Gap between Theory and Practice*, Lahore.

Barnett, T. P. et al. (2008), Human-Induced Changes United States, *Science (80-.).*, *319*(February), 1080–1084.

Baron, J., N. L. Poff, P. L. Angermeier, C. Dahm, P. H. Gleick, N. G. Hairston, R. B. Jackson, C. A. Johnston, B. D. Richter, and A. D. Steinman (2004), Sustaining healthy freshwater ecosystems, *Water Resour.*, (127), 25–58, doi:1092-8987.

Basharat, M., and A.-R. Tariq (2015), Groundwater modelling for need assessment of command scale conjunctive water use for addressing the exacerbating irrigation cost inequities in LBDC irrigation system, Punjab, Pakistan, *Sustain. Water Resour. Manag.*, (1), 41–55, doi:10.1007/s40899-015-0002-y.

Basharat, M., D. Hassan, A. Bajkani, and S. Sultan (2014), *Surface Water and Groundwater Nexus : Groundwater Management Options for Indus Basin Irrigation System*, Lahore.

Bauman, A., C. Goemans, J. Pritchett, and D. Thilmany (2015), Modeling imperfectly competitive water markets in the Western U.S., in *2015 AAEA Annual Meeting*, San Francisco, CA.

Beare, S., and A. Heaney (2002), Climate Change and Water Resources in the Murray Darling Basin , Australia: Impacts and Possible Adaptation, *2002 World Congr. Environ. Resour. Econ. Monterey, California, 24–27 June 2002*, 1–33.

Bennett, G., A. Rehman, I. A. Sheikh, and S. Ali (1967), *Analysis of Aquifer Tests in the Punjab Region West Pakistan*, Washington, DC.

Berger, T., R. Birner, J. Diaz, N. McCarthy, and H. Wittmer (2007), Capturing the complexity of water uses and water users within a multi-agent framework, *Integr. Assess. Water Resour. Glob. Chang. A North-South Anal.*, 129–148, doi:https://doi.org/10.1007/978-1-4020-5591-1_9.

Berglund, E. Z. (2015), Using Agent-Based Modeling for Water Resources Planning and Management, *J. Water Resour. Plan. Manag.*, *141*(11), 1–17, doi:10.1061/(ASCE)WR.1943-5452.0000544.

Bracken, C. (2016), Downscaled CMIP3 and CMIP5 Climate Projections- Addendum,

Bracmort, K. S., M. Arabi, J. R. Frankenberger, B. a Engel, and J. G. Arnold (2006), Modeling Long-Term Water Quality Impact of Structural BMPs, *Trans. Am. Soc. Agric. Biol. Eng.*, *49*(2), 367–374, doi:10.13031/2013.20411.

Brekke, L., B. L. Thrasher, E. P. Maurer, and T. Pruitt (2013), Downscaled CMIP3 and CMIP5 climate projections: Release of downscaled CMIP5 climate projections, comparison with preceding information, and summary of user needs, , (May), 104.

Brekke, L. D., N. L. Miller, K. E. Bashford, N. W. T. Quinn, and J. A. Dracup (2004), Climate Change Impacts Uncertainty for Water Resources in the San Joaquin River Basin, California, *J. Am. Water Resour. Assoc.*, *40*(1), 149–164, doi:10.1111/j.1752-1688.2004.tb01016.x.

Brill, T. C., and H. S. Burness (1994), Planning versus competitive rates of groundwater pumping, *Water Resour. Res.*, *30*(6), 1873–1880, doi:10.1029/94WR00535.

Brown, C., P. Rogers, and U. Lall (2006), Demand management of groundwater with monsoon forecasting, *Agric. Syst.*, *90*(1–3), 293–311, doi:10.1016/j.agsy.2006.01.003.

Brown, C., W. Werick, W. Leger, and D. Fay (2011), A Decision-Analytic Approach to Managing Climate Risks: Application to the Upper Great Lakes1, *JAWRA J. Am. Water Resour. Assoc.*, *47*(3), 524–534, doi:10.1111/j.1752-1688.2011.00552.x.

Brown, C., Y. Ghile, M. Laverty, and K. Li (2012), Decision scaling: Linking bottom-up vulnerability analysis with climate projections in the water sector, *Water Resour. Res.*, *48*(9), n/a-n/a, doi:10.1029/2011WR011212.

Brown, T. J., B. L. Hall, and A. L. Westerling (2004), The impacts of 21st century climate change on wildland fire danger in the western United States: an application perspective, *Clim. Change*, *62*(1–3), 365–388.

Brozovic, N., D. L. Sunding, and D. Zilberman (2010), On the spatial nature of the groundwater pumping externality, *Resour. Energy Econ.*, *32*(2), 154–164, doi:10.1016/j.reseneeco.2009.11.010.

Brozović, N., D. L. Sunding, and D. Zilberman (2010), On the spatial nature of the groundwater pumping externality, *Resour. Energy Econ.*, *32*(2), 154–164, doi:10.1016/j.reseneeco.2009.11.010.

CA DWR (2015a), *California Climate Science and Data - For Water Resources Management*, Sacramento, CA.

CA DWR (2015b), *Perspectives and Guidance for Climate Change Analysis*, Sacramento, CA.

Cayan, D. R. (2013), Future climate: Projected Future, in *Assessment of Climate Change in the Southwest United States: A Report Prepared for the National Climate Assessment*, pp. 101–125, Washington, DC.

Chandio, A. S., T. S. Lee, and M. S. Mirjat (2012), The extent of waterlogging in the lower Indus Basin (Pakistan) - A modeling study of groundwater levels, *J. Hydrol.*, *426–427*, 103–111, doi:10.1016/j.jhydrol.2012.01.017.

Cheema, M. J. M., W. W. Immerzeel, and W. G. M. Bastiaanssen (2014), Spatial quantification of groundwater abstraction in the Irrigated Indus Basin, *Groundwater*, *52*(1), 25–36, doi:10.1111/gwat.12027.

Ciou, S.-K., J.-T. Kuo, P.-H. Hsieh, and G.-H. Yu (2012), Optimization Model for BMP Placement in a Reservoir Watershed, *J. Irrig. Drain. Eng.*, *138*(8), 736–747, doi:https://doi.org/10.1061/(ASCE)IR.1943-4774.0000458.

Colby, B. G. (1990), Transactions Costs and Efficiency in Western Water Allocation, *Am. J. Agric. Econ.*, *72*(5), 1184–1192.

Crosbie, R. S., T. Pickett, F. S. Mpelasoka, G. Hodgson, S. P. Charles, and O. V. Barron (2013), An assessment of the climate change impacts on groundwater recharge at a continental scale using a probabilistic approach with an ensemble of GCMs, *Clim. Change*, *117*(1–2), 41–53, doi:10.1007/s10584-012-0558-6.

Daly, C., J. I. Smith, and K. V. Olson (2015), *Mapping atmospheric moisture climatologies across the conterminous United States*.

Dettinger, M. (2011), Climate change, atmospheric rivers, and floods in California - a multimodel analysis of storm frequency and magnitude changes, *J. Am. Water Resour. Assoc.*, *47*(3), 514–523, doi:10.1111/j.1752-1688.2011.00546.x.

Dettinger, M., and D. Cayan (2014), Drought and the California Delta—A Matter of Extremes, *San Fr. Estuary Watershed Sci.*, *12*(2), doi:10.15447/sfews.2014v12iss2art4.

Dettinger, M. D., and M. L. Anderson (2015), Storage in California's Reservois and Snowpack in this Time of Drought, *San Fr. Estuary Watershed Sci.*, *13*(2), 0–5, doi:10.15447/sfews.2015v13iss2art1.

Dettinger, M. D., D. R. Cayan, H. Diaz, and D. M. Meko (1998), North–South Precipitation Patterns in Western North America on Interannual-to-Decadal Timescales, *J. Clim.*, *11*, 3095–3111, doi:https://doi.org/10.1175/1520-0442(1998)011<3095:NSPPIW>2.0.CO;2.

Diffenbaugh, N. S., and M. Ashfaq (2010), Intensification of hot extremes in the United States, *Geophys. Res. Lett.*, *37*(15), 1–5, doi:10.1029/2010GL043888.

Dinar, A., and A. Wolf (1994), International markets for water and the potential for regional cooperation: Economic and..., *Econ. Dev. Cult. Change*, *43*(1), 43–66.

Döll, P. (2002), Impact of Climate Change and Variability on Irrigation Requirements: A Global Perspective, *Clim. Change*, *54*, 269–293, doi:10.1023/A:1016124032231.

Döll, P., and K. Fiedler (2008), Global-scale modeling of groundwater recharge, *Hydrol. Earth Syst. Sci.*, *12*(3), 863–885, doi:10.5194/hess-12-863-2008.

Feinerman, E., and K. C. Knapp (1983), Benefits from Groundwater Management: Magnitude, Sensitivity, and Distribution, *Am. J. Agric. Econ.*, *65*(4), 703–710, doi:10.2307/1240458.

Fischer, G., F. N. Tubiello, H. van Velthuizen, and D. A. Wiberg (2007), Climate change impacts on irrigation water requirements: Effects of mitigation, 1990-2080, *Technol. Forecast. Soc. Change*, *74*(7), 1083–1107, doi:10.1016/j.techfore.2006.05.021.

Fowler, H. J., S. Blenkinsop, and C. Tebaldi (2007), Linking climate change modelling to impacts studies: recent advances in downscaling techniques for hydrological modelling, *Int. J. Climatol.*, *27*(12), 1547–1578, doi:10.1002/joc.1556.

Garg, N. K., and a. Ali (2000), Groundwater management for Lower Indus Basin, *Agric. Water Manag.*, *42*(3), 273–290, doi:10.1016/S0378-3774(99)00043-8.

Garrick, D., and B. Aylward (2012), Transaction costs and institutional performance in market-based environmental water allocation, *Land Econ.*, *88*(1960), 536–560, doi:10.1353/lde.2012.0040.

Ghile, Y. B., M. Taner, C. Brown, J. G. Grijsen, and A. Talbi (2014), Bottom-up climate risk assessment of infrastructure investment in the Niger River Basin, *Clim. Change*, *122*(1–2), 97–110, doi:10.1007/s10584-013-1008-9.

Giacomoni, M. H., L. Kanta, and E. M. Zechman (2013), Complex Adaptive Systems Approach to Simulate the Sustainability of Water Resources and Urbanization, *J. Water Resour. Plan. Manag.*, *139*(5), 554–564, doi:10.1061/(ASCE)WR.1943-5452.0000302.

Gisser, M., and D. A. Sánchez (1980), Competition versus optimal control in groundwater pumping, *Water Resour. Res.*, *16*(4), 638–642, doi:10.1029/WR016i004p00638.

Giuliani, M., Y. Li, A. Castelletti, and C. Gandolfi (2016), A coupled human-natural systems analysis of irrigated agriculture under changing climate, *Water Resour. Res.*, *52*(9), 6928–6947, doi:10.1002/2016WR019363.

GOP (2014), *Punjab Development Statistics*, Lahore.

Gorelick, S. M., and C. Zheng (2015), Global change and the groundwater management challenge, *Water Resour. Res.*, *51*(5), 3031–3051, doi:10.1002/2014WR016825.

Green, T. R., M. Taniguchi, H. Kooi, J. J. Gurdak, D. M. Allen, K. M. Hiscock, H. Treidel, and A. Aureli (2011), Beneath the surface of global change: Impacts of climate change on groundwater, *J. Hydrol.*, *405*(3–4), 532–560, doi:10.1016/j.jhydrol.2011.05.002.

Groves, D. G., and E. Bloom (2013), *Robust Water-Management Strategies for the California Water Plan Update 2013 Proof-of-Concept Analysis*.

Harbaugh, A. W. (2005), *MODFLOW-2005 , The U . S . Geological Survey Modular Ground-Water Model — the Ground-Water Flow Process MODFLOW-2005*, Reston, Virginia.

Hassan, G. Z., and M. N. Bhutta (1996), A water balance model to estimate groundwater recharge in Rechna doab, Pakistan, *Irrig. Drain. Syst.*, *10*(4), 297–317, doi:10.1007/BF01104895.

Howe, C. W., C. S. Boggs, and P. Butler (1990), Transaction Costs as Determinants of Water Transfers, *Univ. Color. Law Rev.*, *61*(2), 393–405.

Hydrocomp (2012), *Sensitivity of Upper Tuolumne River Flow to Climate Change Scenarios*, San Francisco, CA.

Jewitt, G. (2002), Can Integrated Water Resources Management sustain the provision of ecosystem goods and services?, *Phys. Chem. Earth, Parts A/B/C*, *27*(11), 887–895, doi:10.1016/S1474-7065(02)00091-8.

Jiang, Q., and R. Q. Grafton (2012), Economic effects of climate change in the Murray-Darling Basin, Australia, *Agric. Syst.*, *110*, 10–16, doi:10.1016/j.agsy.2012.03.009.

Johnson, J., P. N. Johnson, E. Segarra, and D. Willis (2009), Water conservation policy alternatives for the Ogallala Aquifer in Texas, *Water Policy*, *11*(5), 537–552, doi:10.2166/wp.2009.202.

Karamouz, M., M. Taheriyoun, a Baghvand, H. Tavakolifar, and F. Emami (2010), Optimization of watershed control strategies for reservoir eutrophication management, *J. Irrig. Drain. Eng.*, *136*(12), 847–861, doi:10.1061/(ASCE)IR.1943-4774.0000261.

Katic, P. G., and R. Q. Grafton (2012), Economic and spatial modelling of groundwater extraction, *Hydrogeol. J.*, *20*(5), 831–834, doi:10.1007/s10040-011-0817-z.

Katz, R. W. (1977), Precipitation as a Chain-Dependent Process, *J. Appl. Meteorol.*, *16*(7), 671–676, doi:10.1175/1520-0450(1977)016<0671:PAACDP>2.0.CO;2.

Khair, S. M., S. Mushtaq, and K. Reardon-Smith (2014), Groundwater Governance in a Water-Starved Country: Public Policy, Farmers' Perceptions, and Drivers of Tubewell Adoption in Balochistan, Pakistan, *Groundwater*, *53*(4), 626–637, doi:10.1111/gwat.12250.

Khan, H. F., Y.-C. E. Yang, and C. Ringler (2017), *Heterogeneity in Riverine Ecosystem Service Perceptions : Insights for Water-decision Processes in Transboundary Rivers*, IFPRI Discussion Paper, Washington, DC.

Killam, D., A. Bui, S. LaDochy, P. Ramirez, J. Willis, and W. Patzert (2014), California Getting Wetter to the North, Drier to the South: Natural Variability or Climate Change?, *Climate*, *2*(3), 168–180, doi:10.3390/cli2030168.

Kite, G. (2001), Modelling the mekong: Hydrological simulation for environmental impact studies, *J. Hydrol.*, *253*(1–4), 1–13, doi:10.1016/S0022-1694(01)00396-1.

Knapp, K. C., and L. J. Olson (1995), The Economics of Conjunctive Groundwater Management with Stochastic Surface Supplies, *J. Environ. Econ. Manage.*, *28*(3), 340–356, doi:10.1006/jeem.1995.1022.

Knowles, N., and D. R. Cayan (2002), Potential effects of global warming on the Sacramento/San Joaquin watershed and the San Francisco estuary, *Geophys. Res. Lett.*, *29*(18), 38-1-38–4, doi:10.1029/2001GL014339.

Kocabas, V., and S. Dragicevic (2013), Bayesian networks and agent-based modeling approach for urban land-use and population density change: A BNAS model, *J. Geogr. Syst.*, *15*(4), 403–426, doi:10.1007/s10109-012-0171-2.

Koundouri, P. (2004), Current Issues in the Economics of Groundwater Resource Management, *J. Econ. Surverys*, *18*(5), 703–740, doi:10.1111/j.1467-6419.2004.00234.x.

Kripalani, R. H., J. H. Oh, A. Kulkarni, S. S. Sabade, and H. S. Chaudhari (2007), South Asian summer monsoon precipitation variability: Coupled climate model simulations and projections under IPCC AR4, *Theor. Appl. Climatol.*, *90*(3–4), 133–159, doi:10.1007/s00704-006-0282-0.

Kugelman, M., and R. M. Hathaway (2009), *Running on Empty: Pakistan's Water Crisis*, Woodrow Wilson International Center for Scholars, Washington, DC.

Lall, U., and A. Sharma (1996), A nearest neighbor bootstrap for resampling hydrologictime series, *Water Resour. Res.*, *32*(3), 679–693, doi:10.1029/95WR02966.

Lauri, H., H. De Moel, P. J. Ward, T. A. Rasanen, M. Keskinen, and M. Kummu (2012), Future changes in Mekong River hydrology: Impact of climate change and reservoir operation on discharge, *Hydrol. Earth Syst. Sci.*, *16*(12), 4603–4619, doi:10.5194/hess-16-4603-2012.

Lettenmaier, D. P., and D. P. Sheer (1991), Climatic Sensitivity of California Water Resources, *J. Water Resour. Plan. Manag.*, *117*(1), 108–125, doi:10.1061/(ASCE)0733-9496(1991)117:1(108).

Liu, J. et al. (2007), Complexity of Coupled Human and Natural Systems, *Science (80-.).*, *317*(5844), 1513–1516, doi:10.1126/science.1144004.

Loch, A., S. Wheeler, H. Bjornlund, S. Beecham, J. Edwards, A. Zuo, and M. Shanahan (2013), *The role of water markets in climate change adaptation*, Gold Coast.

Van Loon, A. F., E. Tijdeman, N. Wanders, H. A. J. Van Lanen, A. J. Teuling, and R. Uijlenhoet (2014), How climate seasonality modifies drought duration and deficit, *J. Geophys. Res.*, *119*(8), 4640–4656, doi:Doi 10.1002/2013jd020383.

Lund, J. R., and R. N. Palmer (1997), Water Resource System Modeling for Conflict Resolution, *Water Resour. Updat.*, *3*(Holling 1978), 70–82.

Lundy, L., and R. Wade (2011), Integrating sciences to sustain urban ecosystem services, *Prog. Phys. Geogr.*, *35*(5), 653–669, doi:10.1177/0309133311422464.

MacDonald, G. M. (2010), Water, climate change, and sustainability in the southwest, *Proc. Natl. Acad. Sci.*, *107*(50), 21256–21262, doi:10.1073/pnas.0909651107.

Mahmood, K., A. D. Rana, S. Tariq, S. Kanwal, R. Ali, and A. Haidar (2013), Groundwater Levels Susceptibility To Degradation in Lahore Metropolitan ., *Sci. Int.*, *25*(1), 123–126.

Marchlik, Z. (2014), The Effect of Climate Change on Water Markets in Colorado, University of Colorado, Boulder.

Maurer, E. P., L. Brekke, T. Pruitt, and P. B. Duffy (2007), Fine-resolution climate projections enhance regional climate change impact studies, *Eos, Trans. Am. Geophys. Union*, *88*(47), 504–504, doi:10.1029/2007EO470006.

Meko, D. M., C. A. Woodhouse, and R. Touchan (2014), *Klamath/San Joaquin/Sacramento Hydroclimatic Reconstructions from Tree Rings*.

Miller, N. L., K. E. Bashford, and E. Strem (2003), POTENTIAL IMPACTS OF CLIMATE CHANGE ON CALIFORNIA HYDROLOGY, *J. Am. Water Resour. Assoc.*, *39*(4), 771–784, doi:10.1111/j.1752-1688.2003.tb04404.x.

Mirza, G., and M. Latif (2012), Assessment of current agro-economic conditions in Indus Basin of Pakistan, in *International Conference on Water, Energy, Environment and Food Nexus*, Islamabad.

Mishra, S. K. (2013), Modeling water quantity and quality in an agricultural watershed in the midwestern US using SWAT : assessing implications due to an expansion in biofuel production and climate change, University of Iowa.

MRC (2002), *Annual Report*, Phnom Penh.

Mulligan, K. B., and D. P. Ahlfeld (2016), Model reduction for combined surface water/groundwater management formulations, *Environ. Model. Softw.*, *81*, 102–110, doi:10.1016/j.envsoft.2016.03.013.

Mulligan, K. B., C. Brown, Y.-C. E. C. E. Yang, and D. P. Ahlfeld (2014), Assessing groundwater policy with coupled economic-groundwater hydrologic modeling, *Water Resour. Res.*, *50*(3), 2257–2275, doi:10.1002/2013WR013666.

Murphy, J. J., a Dinar, R. E. Howitt, S. J. Rassenti, and V. L. Smith (2000), The Design of " Smart " Water Market Institutions Using Laboratory Experiments, *Environ. Resour. Econ.*, *17*(4), 375–394, doi:10.1023/A:1026598014870.

Neelin, J. D., B. Langenbrunner, J. E. Meyerson, A. Hall, and N. Berg (2013), California winter precipitation change under global warming in the coupled model intercomparison project phase 5 ensemble, *J. Clim.*, *26*(17), 6238–6256, doi:10.1175/JCLI-D-12-00514.1.

Nelson, R. L., and D. Perrone (2016), Local Groundwater Withdrawal Permitting Laws in the South-Western U.S.: California in Comparative Context, *Groundwater*, *54*(6), 747–753, doi:10.1111/gwat.12469.

Neuman, J. C. (2004), The Good, The Bad, and The Ugly: The First Ten Years of the Oregon Water Trust, *Neb. L. Rev.*, *83*(432), 432–484.

Ng, T. L., J. W. Eheart, X. Cai, and J. B. Braden (2011), An agent-based model of farmer decision-making and water quality impacts at the watershed scale under markets for carbon allowances and a second-generation biofuel crop, *Water Resour. Res.*, *47*(9), 1–17, doi:10.1029/2011WR010399.

Nigam, S., N. P. Thomas, A. Ruiz-Barradas, and S. J. Weaver (2017), Striking seasonality in the secular warming of the northern continents: Structure and mechanisms, *J. Clim.*, *30*(16), 6521–6541, doi:10.1175/JCLI-D-16-0757.1.

O'Mara, G. T., and J. H. Duloy (1984), Modeling efficient water allocation in a conjunctive use regime: The Indus Basin of Pakistan, *Water Resour. Res.*, *20*(11), 1489, doi:10.1029/WR020i011p01489.

O'Sullivan, D., T. Evans, S. Manson, S. Metcalf, A. Ligmann-Zielinska, and C. Bone (2016), Strategic directions for agent-based modeling: avoiding the YAAWN syndrome, *J. Land Use Sci.*, *11*(2), 177–187, doi:10.1080/1747423X.2015.1030463.

Ogilvie, A. et al. (2010), Water, agriculture and poverty in the Niger River basin, *Water Int.*, *35*(5), 594–622, doi:10.1080/02508060.2010.515545.

Van Oijen, M., D. R. Cameron, K. Butterbach-Bahl, N. Farahbakhshazad, P. E. Jansson, R. Kiese, K. H. Rahn, C. Werner, and J. B. Yeluripati (2011), A Bayesian framework for model calibration, comparison and analysis: Application to four models for the biogeochemistry of a Norway spruce forest, *Agric. For. Meteorol.*, *151*(12), 1609–1621, doi:10.1016/j.agrformet.2011.06.017.

Pagano, T. C., H. C. Hartmann, and S. Sorooshian (2002), Factors affecting seasonal forecast use in Arizona water management: A case study of the 1997-98 El Niño, *Clim. Res.*, *21*(3), 259–269, doi:10.3354/cr021259.

Palmer, M. A. et al. (2005), Standards for ecologically successful river restoration, *J. Appl. Ecol.*, *42*(2), 208–217, doi:10.1111/j.1365-2664.2005.01004.x.

Palmer, R. N., H. E. Cardwell, M. A. Lorie, and W. Werick (2013), Disciplined planning, structured participation, and collaborative modeling - applying shared vision planning to water resources, *J. Am. Water Resour. Assoc.*, *49*(3), 614–628, doi:10.1111/jawr.12067.

Parker, D. C., S. M. Manson, M. A. Janssen, M. J. Hoffmann, and P. Deadman (2003), Multi-agent systems for the simulation of land-use and land-cover change: A review, *Ann. Assoc. Am. Geogr.*, *93*(2), 314–337, doi:10.1111/1467-8306.9302004.

Petersen-Perlman, J. D., J. C. Veilleux, and A. T. Wolf (2017), International water conflict and cooperation: challenges and opportunities, *Water Int.*, *0*(0), 1–16, doi:10.1080/02508060.2017.1276041.

Pierce, D. W., D. R. Cayan, E. P. Maurer, J. T. Abatzoglou, and K. C. Hegewisch (2015), Improved Bias Correction Techniques for Hydrological Simulations of Climate Change, *J. Hydrometeorol.*, *16*(6), 2421–2442, doi:10.1175/JHM-D-14-0236.1.

PPSGDP (1998), *Guidelines for the modification of STWs and CTWs in PPSGDP. Technical Report No. 28*, Islamabad, Pakistan.

Qureshi, A. S., T. Shah, and M. Akhtar (2003), *The Groundwater Economy of Pakistan*, Lahore.

Qureshi, A. S., P. G. McCornick, a. Sarwar, and B. R. Sharma (2010), Challenges and Prospects of Sustainable Groundwater Management in the Indus Basin, Pakistan, *Water Resour. Manag.*, *24*(8), 1551–1569, doi:10.1007/s11269-009-9513-3.

Raffensperger, J. F., M. W. Milke, and E. G. Read (2009), A Deterministic Smart Market Model for Groundwater, *Oper. Res.*, *57*(6), 1333–1346, doi:10.1287/opre.1090.0730.

Ragab, R., and C. Prudhomme (2002), Climate Change and Water Resources Management in Arid and Semi-arid Regions: Prospective and Challenges for the 21st Century, *Biosyst. Eng.*, *81*(1), 3–34, doi:10.1006/bioe.2001.0013.

Ralph, F. M., and M. D. Dettinger (2011), Storms, floods, and the science of atmospheric rivers, *Eos (Washington. DC).*, *92*(32), 265–266, doi:10.1029/2011EO320001.

Reeves, H. W., and M. L. Zellner (2010), Linking MODFLOW with an agent-based land-use model to support decision making, *Ground Water*, *48*(5), 649–660, doi:10.1111/j.1745-6584.2010.00677.x.

Reilly, T. E., and A. W. Harbaugh (2004), *Guidelines for Evaluating Ground-Water Flow Models: U.S. Geological Survey Scientific Investigations Report 2004-5038*, Denver.

Republican River Compact Administration (2003), *Ground Water Model Documentation*.

Revelle, R., and P. Waggoner (1983), Effects of a Carbon Dioxide-Induced Climatic Change on Water Supplies in the Western United States, *Chang. Clim. Rep. Carbon Dioxide Assess. Comm.*, 419–432.

Rice, J. S., and R. E. Emanuel (2017), How are streamflow responses to the El Nino Southern Oscillation affected by watershed characteristics?, *Water Resour. Res.*, *53*(5), 4393–4406, doi:10.1002/2016WR020097.

Richey, A. S., B. F. Thomas, M.-H. Lo, J. T. Reager, J. S. Famiglietti, K. Voss, S. Swenson, and M. Rodell (2015), Quantifying renewable groundwater stress with GRACE, *Water Resour. Res.*, n/a-n/a, doi:10.1002/2015WR017349.

Richter, B., J. V Baumgartner, R. Wigington, and D. P. Braun (1997), How much water does a river need?, *Freshw. Biol.*, *37*(1), 231–249, doi:10.1046/j.1365-2427.1997.00153.x.

Richter, B. D., J. V Baumgartner, J. Powell, and D. P. Braun (1996), A Method for Assessing Hydrologic Alteration within Ecosystems, *Conserv. Biol.*, *10*(4), 1163–1174, doi:10.1046/j.1523-1739.1996.10041163.x.

Ringler, C. (2001), *Optimal Water Allocation in the Mekong River Basin*, Bonn.

Robinson, S., D. Mason-D'Croz, S. Islam, T. B. Sulser, R. Robertson, T. Zhu, A. Gueneau, G. Pitois, and M. Rosegrant (2015), *The International Model for Policy Analysis of Agricultural Commodities and Trade (IMPACT): model description for Version 3.*, IFPRI Discussion Paper, Washington, DC.

Rodell, M., and J. S. Famiglietti (2002), The potential for satellite-based monitoring of groundwater storage changes using GRACE: The High Plains aquifer, Central US, *J. Hydrol.*, *263*(1–4), 245–256, doi:10.1016/S0022-1694(02)00060-4.

Rupp, D. E., J. T. Abatzoglou, and P. W. Mote (2017), Projections of 21st century climate of the Columbia River Basin, *Clim. Dyn.*, *49*(5–6), 1783–1799, doi:10.1007/s00382-016-3418-7.

Scanlon, B. R., C. C. Faunt, L. Longuevergne, R. C. Reedy, W. M. Alley, V. L. McGuire, and P. B. McMahon (2012), Groundwater depletion and sustainability of irrigation in the US High Plains and Central Valley, *Proc. Natl. Acad. Sci.*, *109*(24), 9320–9325, doi:10.1073/pnas.1200311109.

SFPUC (2016), *2040 WaterMAP*, San Francisco, CA.

Shrestha, R. R., M. A. Schnorbus, A. T. Werner, and A. J. Berland (2012), Modelling spatial and temporal variability of hydrologic impacts of climate change in the Fraser River basin, British Columbia, Canada, *Hydrol. Process.*, *26*(12), 1841–1861, doi:10.1002/hyp.9283.

Sicke, W. S., J. R. Lund, J. Medellín-Azuara, and K. Madani (2013), Climate change adaptations for California's San Francisco Bay Area water supplies., *Br. J. Environ. Clim. Chang.*, *3*(3), 292–315, doi:10.9734/BJECC/2013/2708.

Silva, A. T., and M. M. Portela (2012), Disaggregation modelling of daily streamflows using a new approach of the method of fragments, *Hydrol. Sci. J.*, *57*(5), 942–955, doi:10.1080/02626667.2012.686695.

Simpson, I. R., T. A. Shaw, and R. Seager (2014), A Diagnosis of the Seasonally and Longitudinally Varying Midlatitude Circulation Response to Global Warming*, *J. Atmos. Sci.*, *71*(7), 2489–2515, doi:10.1175/JAS-D-13-0325.1.

Sivakumar, M., H. Das, and O. Brunini (2005), Impacts of present and future climate variability and change on agriculture and forestry in the arid and semi-arid tropics, *Clim. Change*, *70*, 31–72, doi:10.1007/s10584-005-5937-9.

Sivapalan, M., H. H. G. Savenije, and G. Blöschl (2012), Socio-hydrology: A new science of people and water, *Hydrol. Process.*, *26*(8), 1270–1276, doi:10.1002/hyp.8426.

Skurray, J. H., E. J. Roberts, and D. J. Pannell (2012), Hydrological challenges to groundwater trading: Lessons from south-west Western Australia, *J. Hydrol.*, *412–413*, 256–268, doi:10.1016/j.jhydrol.2011.05.034.

Sophocleous, M. (2005), Groundwater recharge and sustainability in the High Plains aquifer in Kansas, USA, *Hydrogeol. J.*, *13*(2), 351–365, doi:10.1007/s10040-004-0385-6.

van Steenbergen, F., and W. Oliemans (1996), Groundwater Resource Management in Pakistan, in *Groundwater Management: Sharing Responsibility For An Open Access Resource*.

Steinschneider, S., and C. Brown (2013), A semiparametric multivariate, multisite weather generator with low-frequency variability for use in climate risk assessments, *Water Resour. Res.*, *49*(11), 7205–7220, doi:10.1002/wrcr.20528.

Steinschneider, S., and U. Lall (2015), A hierarchical Bayesian regional model for nonstationary precipitation extremes in Northern California conditioned on tropical moisture exports, *Water Resour. Res.*, *51*(3), 1472–1492, doi:10.1002/2014WR016664.

Stone-Jovicich, S. (2015), Probing the interfaces between the social sciences and social-ecological resilience: Insights from integrative and hybrid perspectives in the social sciences, *Ecol. Soc.*, *20*(2), doi:10.5751/ES-07347-200225.

Strauch, M., J. E. F. W. Lima, M. Volk, C. Lorz, and F. Makeschin (2013), The impact of BMPs on simulated streamflow and sediment loads in a Central Brazilian catchment, , *127*, 1–18.

Sultan, T., A. Latif, A. Shakir, K. Kheder, and M. Rashid (2014), Comparison of Water Conveyance Losses in Unlined and Lined Watercourses in Developing Countries, *Tech. Journal, Univ. Eng. Technol. Taxila*, *19*(II), 23–27.

Sun, A. Y., R. Green, S. Swenson, and M. Rodell (2012), Toward calibration of regional groundwater models using GRACE data, *J. Hydrol.*, *422–423*, 1–9, doi:10.1016/j.jhydrol.2011.10.025.

Swain, D. L., D. E. Horton, D. Singh, and N. S. Diffenbaugh (2016), Trends in atmospheric patterns conducive to seasonal precipitation and temperature extremes in California, *Sci. Adv.*, *2*(4), e1501344–e1501344, doi:10.1126/sciadv.1501344.

Swarzenski, W. (1968), *Fresh and Saline Ground-Water Zones in the Punjab Region West Pakistan*, Washington, DC.

Taylor, R. et al. (2013), Ground water and climate change, *Nat. Clim. Chang.*, *3*(November), 1–8, doi:10.1038/NCLIMATE1744.

Tiezzi, S. (2016), Facing Mekong Drought, China to Release Water from Yunan Dam, *Dipl.*, 2–3. Available from: http://thediplomat.com/2016/03/facing-mekong-drought-china-to-release-water-from-yunnan-dam/

Treidel, H., J. L. Martin-bordes, and J. J. Gurdak (2012), *Climate Change Effects on Groundwater Resources: A Global Synthesis of Findings and Recommendations*, Taylor and Francis Group, London, UK.

Treydte, K. S., G. H. Schleser, G. Helle, D. C. Frank, M. Winiger, G. H. Haug, and J. Esper (2006), The twentieth century was the wettest period in northern Pakistan over the past millennium., *Nature*, *440*(7088), 1179–1182, doi:10.1038/nature04743.

Urban, F., J. Nordensvärd, D. Khatri, and Y. Wang (2013), An analysis of China's investment in the hydropower sector in the Greater Mekong Sub-Region, *Environ. Dev. Sustain.*, *15*(2), 301–324, doi:10.1007/s10668-012-9415-z.

Vano, J. (2015), Seasonal hydrologic responses to climate change in the Pacific Northwest, *Water Resour. ...*, *51*, 1959–1976, doi:10.1002/2014WR015909.Received.

Vanrheenen, N. T., A. W. Wood, R. N. Palmer, and D. P. Lettenmaier (2004), Potential implications of PCM climate change scenarios for Sacramento-San Joaquin River Basin hydrology and water resources, *Clim. Change*, *62*(1–3), 257–281, doi:10.1023/B:CLIM.0000013686.97342.55.

Vicuna, S., E. P. Maurer, B. Joyce, J. A. Dracup, and D. Purkey (2007), The Sensitivity of California Water Resources to Climate Change Scenarios1, *JAWRA J. Am. Water Resour. Assoc.*, *43*(2), 482–498, doi:10.1111/j.1752-1688.2007.00038.x.

Vicuna, S., J. A. Dracup, J. R. Lund, L. L. Dale, and E. P. Maurer (2010), Basin-scale water system operations with uncertain future climate conditions: Methodology and case studies, *Water Resour. Res.*, *46*(4), 1–19, doi:10.1029/2009WR007838.

Vogel, R. M., U. Lall, X. Cai, B. Rajagopalan, P. K. Weiskel, R. P. Hooper, and N. C. Matalas (2015), Hydrology: The interdisciplinary science of water, *Water Resour. Res.*, *51*(6), 4409–4430, doi:10.1002/2015WR017049.

Wang, Q. J. (1991), The genetic algorithm ans its applications to calibrating conceptual rainfall-runoff models, *Water Resour. Res.*, *27*(9), 2467–2471.

WAPDA (2013), Water and Power Challenges - Vision 2025 Perspectives,

Welcomme, R. L. (1986), The effects of the Sahelian drought on the fishery of the central delta of the Niger River, *Aquac. Res.*, *17*(2), 147–154.

Werner, A. T., M. A. Schnorbus, R. R. Shrestha, and H. D. Eckstrand (2013), Spatial and temporal change in the hydro-climatology of the Canadian portion of the Columbia river basin under multiple emissions scenarios, *Atmos. - Ocean*, *51*(4), 357–379, doi:10.1080/07055900.2013.821400.

Whateley, S., S. Steinschneider, and C. Brown (2016), Selecting Stochastic Climate Realizations to Efficiently Explore a Wide Range of Climate Risk to Water Resource Systems, *J. Water Resour. Plan. Manag.*, *142*(6), 1–7, doi:10.1061/(ASCE)WR.1943-5452.0000631.

Wheeler, S., A. Loch, A. Zuo, and H. Bjornlund (2013), Reviewing the adoption and impact of water markets in the Murray-Darling Basin, Australia, *J. Hydrol.*, *518*(PA), 28–41, doi:10.1016/j.jhydrol.2013.09.019.

Wilks, D. S. (1998), Multisite generalization of a daily stochastic precipitation generation model, *J. Hydrol.*, *210*(1–4), 178–191, doi:10.1016/S0022-1694(98)00186-3.

Willis, A. D., J. R. Lund, E. S. Townsley, and B. a. Faber (2011), Climate Change and Flood Operations in the Sacramento Basin, California, *San Fr. Estuary Watershed Sci.*, *9*(2), 1–18, doi:10.15447/sfews.2014v9iss2art3.

World Economic Forum (2016), *The Global Risks Report 2016*, Geneva.

Xiao, M., A. Koppa, Z. Mekonnen, B. R. Pagán, S. Zhan, Q. Cao, A. Aierken, H. Lee, and D. P. Lettenmaier (2017), How much groundwater did California's Central Valley lose during the 2012–2016 drought?, *Geophys. Res. Lett.*, *44*(10), 4872–4879, doi:10.1002/2017GL073333.

Xie, H., L. Longuevergne, C. Ringler, and B. R. Scanlon (2012), Calibration and evaluation of a semi-distributed watershed model of Sub-Saharan Africa using GRACE data, *Hydrol. Earth Syst. Sci.*, *16*(9), 3083–3099, doi:10.5194/hess-16-3083-2012.

Yang, Y.-C. E., X. Cai, and D. M. Stipanović (2009), A decentralized optimization algorithm for multiagent system-based watershed management, *Water Resour. Res.*, *45*(8), 1–18, doi:10.1029/2008WR007634.

Yang, Y.-C. E., C. M. Brown, W. H. Yu, and A. Savitsky (2013), An introduction to the IBMR, a hydro-economic model for climate change impact assessment in Pakistan's Indus River basin, *Water Int.*, *38*(5), 632–650, doi:10.1080/02508060.2013.830691.

Yang, Y. E., J. Zhao, and X. Cai (2012), Decentralized Optimization Method for Water Allocation Management in the Yellow River Basin, *J. Water Resour. Plan. Manag.*, *138*(4), 313–325, doi:10.1061/(ASCE)WR.1943-5452.0000199.

Young, R. K. (2016), *Smart Markets for Groundwater Trading in Western Nebraska : The Twin Platte*, Lincoln, Nebraska.

Yu, B., J. Tisdell, G. Podger, and I. Salbe (2003), A hydrologic and economic model for water trading and reallocation using linear programming techniques, in *International Congress on Modelling and Simulation*, pp. 965–970, Townsville.

Yu, W., Y.-C. E. Yang, A. Savitsky, D. Alford, J. Wescoat, D. Debowicz, S. Robinson, T. W. Bank, and S. A. Region (2012), *Climate Risks on Water and Food Security in the Indus Basin of Pakistan*, Washington, DC.

Zeff, H., G. Characklis, D. Kaczan, B. Murray, and K. Locklier (2016), *Benefits , Costs , and Distributional Impacts of a Groundwater Trading Program in the Diamond Valley , Nevada*.

Zhao, Q., and X. Cai (2017), WLE-ABM Web Interface User's Guide,

Zhu, T., M. W. Jenkins, and J. R. Lund (2005), Estimated Impacts of Climate Warming on California Water Availability Under Twelve Future Climate Scenarios, *J. Am. Water Resour. Assoc.*, *41*(5), 1027–1038, doi:10.1111/j.1752-1688.2005.tb03783.x.

Zhu, T., J. R. Lund, M. W. Jenkins, G. F. Marques, and R. S. Ritzema (2007), Climate change, urbanization, and optimal long-term floodplain protection, *Water Resour. Res.*, *43*(6), n/a-n/a, doi:10.1029/2004WR003516.